Dissertation

submitted to the
Combined Faculties for the Natural Sciences and for Mathematics
of the Ruperto-Carola University of Heidelberg, Germany
for the degree of
Doctor of Natural Sciences

presented by:
Paweł Gawliński
Diploma: Master of Biotechnology
born in Olsztyn, Poland
Oral examination:

Molecular characterization of the *Drosophila* mitotic inhibitor Frühstart

Referees: Prof. Dr. Herbert Steinbeisser
PD Dr. Jörg Großhans

Moim Rodzicom oraz
Prof. dr hab. Annie J. Podhajskiej dedykuję

Contents

Acknowledgements

This thesis was conducted at the Zentrum für Molekulare Biologie der Univerität Heidelberg (ZMBH) under the supervision of PD Dr. Jörg Großhans.

First of all, I would like to thank Dr. Jörg Großhans for giving me the opportunity to carry out this project in his group and for his supervision throughout my PhD years.

Furthermore, I would like to thank Prof. Herbert Steinbeisser for agreeing to be my first advisor and for offering me support and suggestions during my PhD.

I would like to thank Dr. Rainer Nikolai and PD Dr. Matthias Mayer for support in plasmon surface resonance experiments, Dr. Theis Stüven for support in nuclear export assay in permeabilized HeLa cells, Dr. Thomas Ruppert for mass-spectrometry support, Dr. Sławomir Bartoszewski and Dr. Robert Krzesz for constructive discussions and comments on my PhD thesis.

My thanks to all members of Dr. Jörg Großhans group, especially Christian Wenzl, Dr. Sławek Bartoszewski, Dr. Jochen Bogin, Yvonne Kußler-Schneider, Dr. Annely Haase, Dr. Fani Papagiannouli, Bhagirath Chaurasia, and my bench heiress Maria Polychronidou not only for their stimulating discussions about science, but also for making my time at the bench enjoyable.

Last but not least, I would like to express my gratitude to Dr n. med. Franciszka Maria Laskowska-Niewada for her great support and help not only during all my studies in Heidelberg but also for the times before.

Summary

The aim of this study was biochemical, molecular and genetic characterization of the *Drosophila* gene *frühstart*. Previous analysis revealed that Frühstart is a mitotic inhibitor that specifically counteracts protein phosphatase String and in this way delays mitosis in the ventral furrow cells to prevent an interference of mitotic events and morphogenetic movements during ventral furrow formation. Subsequent studies demonstrated that *frs* is also sufficient and partially required for pausing the rapid nuclear cycles after the last (13th) cleavage division during cellularisation process.

This study revealed several unknown physiological and biochemical features of Frs. Ectopic expression of Frs in later stages of *Drosophila* embryonic development, revealed that Frs can also inhibit normally occurring cell cycle and shortcut G2 with G1 phases by blocking M phase, what leads the cell cycle to endoreplication process. The endoreplication phenotype caused by Frs over-expression is consistent with the Cdk1 or CycA phenotype, when the physiological function of one of them is disrupted. To find a molecular link between mitotic Cdk1 and Frs, a set of Frs biochemical interactors was found and the interactions were analysed in a wide range of molecular techniques. It was shown that Frs interacts with two different sets of proteins: nucleoporins and cyclins.

Molecular analysis of the amino acid sequence of Frs revealed leucine rich region (putative NES) that is required for Frs-Nup50 complex formation, two main phosphorylation sites (T22 and T48) and a KxL motif that is essential for direct interaction with the hydrophobic patch of cyclins. The physiological meaning of these motifs was confirmed by *frs* ventral furrow rescue phenotype assay, which showed that the KxL motif that is required for proper Frs-Cyclins complex formation *in vitro* is also essential for Frs function in the embryo. Moreover, the rescue assay revealed that the two main phosphorylation sites of Frs appear to be partially required for proper Frs activity whereas the putative NES motif that is required for interaction with nucleoporins is not essential for Frs anti-mitotic activity *in vivo*.

The surface plasmon resonance data demonstrated a binding preference of Frs for mitotic cyclins and showed that Frs has much higher affinity for mitotic CycA compared to G1/S CycE. Moreover, no interaction with the Cdk subunit was observed in contrast to the members of two already established cyclin dependent kinase inhibitor families INK4 and CIP/KIP. This showed that the function of Frs is based on a new mechanism of Cdk inhibition.

In this work I demonstrated that blocking of the hydrophobic patch by Frs is sufficient to inhibit entry into mitosis 14 and that the hydrophobic patch plays an important role in cell cycle regulation during *Drosophila* mid-blastula transition.

Zusammenfassung

Das Ziel dieser Arbeit war die biochemische, molekulare und genetische Charakterisierung des *Drosophila* Gens *frühstart*. In früheren Studien konnte bereits gezeigt werden, daß Frs als mitotischer Inhibitor wirkt, der spezifisch der Funktion der Protein-Phosphatase String entgegenwirkt, dadurch die Mitosen in den Zellen der Ventralfurche verzögert und so diesen Zellen erlaubt, die für die Ventralfurchenbildung erforderlichen morphogenetischen Prozesse ohne Störungen durch mitotische Zellteilungen zu durchlaufen. Darüber hinaus wurde gezeigt, daß *frs* ausreichend und zum Teil notwendig ist, um die schnellen syncytialen Kernteilungen nach der 13. Teilung und während der nachfolgenden Zellularisierung auszusetzen.
Die vorliegende Arbeit beschreibt verschiedene weitergehende und bisher unbekannte physiologische und biochemische Eigenschaften von Frs. So wird gezeigt, daß durch die ektopische Expression von Frs in späteren embryonalen Entwicklungsstadien auch der reguläre Zellzyklus inhibiert werden kann, diese Inhibition durch Blockierung der M-Phase verursacht wird und der damit verbundene direkte Übergang von der G2 zur G1 Phase zu Endoreplikationen in den betroffenen Zellen führt. Dieser durch Frs-Überexpression verursachte Phänotyp ist konsistent mit den Phänotypen von Cdk1 und CycA Mutanten. Um eine molekulare Verbindung zwischen Cdk1 und Frs herstellen zu können, wurde in dieser Arbeit nach mit Frs interagierenden Faktoren gesucht, deren Interaktionen mit Hilfe vielfältiger biochemischer Methoden analysiert wurden. Frs interagiert hauptsächlich mit zwei verschiedenen Arten von Proteinen: Nukleoporinen und Cyclinen. Durch molekulare *in vitro* Analyse konnte gezeigt werden, daß die Aminosäuresequenz von Frs neben einer Leuzin-reichen Region (putatives NES), die für die Bildung des Frs-Nup50-Komplexes notwendig ist, zwei Haupt-Phosphorylierungsstellen (T22 and T48) und ein KxL-Motiv enthält, das essentiell für die direkte Interaktion von Frs mit dem hydrophoben Patch von Cyclinen ist. Die physiologische Funktion dieser Motive wurde in Rescue-Experimenten überprüft. So konnte gezeigt werden, daß das KxL-Motiv essentiell für die Frs-Funktion im Embryo ist. Die beiden Phosphorylierungsstellen tragen *in vivo* teilweise, das putative NES-Motiv hingegen überhaupt nicht zur antimitotischen Aktivität von Frs bei. Mit Hilfe von *surface-plasmon-resonance*-Analyse wurde zudem gezeigt, daß Frs bevorzugt an mitotische Cycline bindet und eine viel höhere Affinität für das mitotische Cyclin A als für das G1/S spezifische Cyclin E aufweist. Mit der gleichen Methode konnte keinerlei Interaktion von Frs mit der Cdk-Untereinheit nachgewiesen werden. Somit unterscheidet sich das Bindungsverhalten von Frs von dem bereits bekannter Mitglieder der Cyklin-abhängigen Kinase-Inhibitor-Familien INK4 und CIP/KIP, was darauf schließen läßt, daß die Funktion von Frs auf einem neuen Mechanismus der Cdk-Inhibierung basiert. Zusammenfassend bleibt festzustellen, daß die Bindung von Frs an den hydrophoben Patch ausreichend ist, um den Eintritt in Mitose 14 zu inhibieren und das der hydrophobe Patch somit eine wichtige Rolle in der Zellzyklusregulation während des *Drosophila*- Midblastula-Übergangs spielt.

Abbreviations

A	adenine (if DNA) or alanine (if protein)
aa	amino acid(s)
Ab	antibodies
Amp	ampicillin
Amp^R	ampicillin resistant
APS	ammonium peroxodisulphate
ATP	adenosine triphosphate
b	*bar* (*Drosophila* gene, genetic marker*)
bp	base pair(s)
BSA	bovine serum albumin
C	cytosine
ca	*claret* (*Drosophila* gene, genetic marker*)
cDNA	complementary DNA
Ci	Curie
cn	*cinnabar* (*Drosophila* gene, genetic marker*)
CSM	Complete Supplement Mixture (yeast medium)
CyO	*curly O (Drosophila gene, balancer and genetic marker*)*
DAPI	4',6'-Diamidino-2-phenylindole
DEPC	diethyl pyrocarbonate
ddH_2O	double distilled (deionized) water
Df	deficiency
dH_2O	distilled (deionized) water
DMSO	dimethyl sulfoxide
DNA	deoxyribonucleic acid
dNTP's	2'-deoxynucleotide triphosphahtes
DTT	1,4-dithiothreitol
e	*ebony* (*Drosophila* gene, genetic marker*)
E. coli	*Escherichia coli*
e.g.	for instance (exempli gratia)
EDTA	ethylenediaminetetraacetic acid
EGTA	ethyleneglycol-bis(β-aminoethyl)-N,N,N',N'-tetraacetic acid
emb	*embargoed* (*Drosophila* homolog of *crm1* gene)
et al.	and others
FACS	fluorescence-activated cell sorting
FCS	fetal calf serum
Frs	Frühstart protein
frs	*frühstart* gene
g	gram
GFP	green fluorescent protein
GSH	glutathione
GST	glutathione-S-transferase
h	hour(s)
HEPES	N-(2-Hydroxyethyl)piperazine-N'-(2-ethanesulfonic acid)
His	histidine
HS-	heat-shock
Ig	immunoglobulin
IPTG	isopropyl-ß-D-thiogalactopyranoside
k	kilo-
kbp	kilo base pairs

kDa	kilo Dalton
LiAc	lithium acetate
l	liter(s)
lacZ	β-Galactosidase
LB	Luria-Bertani medium
Leu	leucine
Ly	*lyra* (*Drosophila* gene, genetic marker*)
m	mili-
M	mol per liter or mouse (monoclonal antibodies)
μ	micro-
μl	micro liter(s)
MBT	mid-blastula transition
MCS	multiple cloning site
min	minute(s)
ml	milliliter(s)
MOPS	3-(N-Morpholino)-propanesulfonic acid
MS	mass spectrometry
Myc	protein tag
n	nano-
nt	nucleotide(s)
OD	optical density
ONPG	2-Nitrophenyl-β-galactopyranoside
ORF	open reading frame
P	P-element (*Drosophila* DNA transposable element)
p	pico- or plasmid if in front of the construct name
PAA	acrylamide/bisacrylamide (19:1) mix
PEG	polyethylene glycol
PBS	phosphate buffered saline
PBST	phosphate buffered saline + 2% Tween®20
PCR	Polymerase Chain Reaction
PMSF	phenylmethylsulphonylfluoride
R	rabbit (polyclonal antybodies)
Rb	Retinoblastoma protein
RNA	ribonucleic acid
RNase	RNA degrades protein
Roi	*rough eye* (*Drosophila* gene, genetic marker*)
rpm	revolutions per minute
RT	room temperature (~20^{o}C)
ry	*rosy* (*Drosophila* gene, genetic marker*)
SDS	sodiumdodecylsulphate
SDS-PAGE	SDS-polyacrylamide gel electrophoresis
se	*sepia* (*Drosophila* gene, genetic marker*)
sec	seconds
Sp	*sternopleural* (*Drosophila* gene, genetic marker*))
stg	*string* (*Drosophila* gene)
T	thymidine
TCA	Trichloroacetic acid
TEMED	N,N,N,N -tetramethyl-ethylenediamine
tev	cleavage site for Tev protease
TM3	tropomyosin 3 (*Drosophila* gene, balancer and genetic marker*)
TRIS	(hydroxymethyl)aminomethane hydrochloride

Trp	tryptophan
UAS	upstream activating sequence
Ura	uracil
o/n	overnight (~16 h)
rpm	revolutions per minute
U	unit(s)
UV	ultraviolet light
V	Volt
VF	ventral furrow
vol	volume
v/v	volume per volume
w	*white* (*Drosophila* gene, genetic marker*)
w/o	with no
wt	wild-type
w/v	weight per volume
X-Gal	5-bromo-4-chloro-3-indolyl-beta-D-galactopyranoside
YPD	yeast/peptone/dextrose medium
Y2H	yeast-two-hybrid system
ZZ	protein tag
°C	Celsius degree

* - All additional information about *Drosophila* genes used in this work as genetic markers like origins, cytological locations, phenotypes and references are precisely described in "The Genome of *Drosophila melanogaster*" Dan L. Lindsey, Georgianna G. Zimm, Academic Press, Inc. 1992.

Introduction

1. *Drosophila melanogaster* as a model organism

Drosophila melanogaster is one of many animal models widely used in genetic, molecular and biochemical studies, however this small fruit fly has contributed more than any other organism to understanding how particular genes determine body pattern formation. Already hundred years ago the fruit fly was established as an ideal model for genetic studies. The advantages of *Drosophila* as experimental organism are numerous. It is economic, easy to breed and rapid in its reproductive cycle. The adult fly has only 4mm size with space requirement of 1000 individuals per liter, a mature fertile female lays about 50 eggs per 24h and the generation time is only 14 days where the embryonic development occurs during first 24h. An additional advantage is the fact that flies have only four sequenced chromosomes (three main) that undergo recombination only in the female germ cells, are easy to mutagenize and screen for mutations. The small number of chromosomes allowed the development of several genetical instruments like balancer chromosomes with multiple inversions that prevent naturally occurring recombination, visible markers that allow the selection of expected progeny, and conditional lethal or sterile mutations making selection systems possible. These instruments have been and still are inestimable in the screens and genetic characterizations of the fly genes. Up to now about 20 000 *Drosophila* genes were determined, among which 5 000 were classified as essential for viability and less than 1000 as essential for fertility. In contrast to higher organisms, most of *Drosophila* genes code only one homolog of particular gene. In mammals as a result of gene duplication during millions of years of evolution the genomes contain two, three or even more homolog copies of one gene. Mutation of one gene homolog often does not expose its function because other homologues take over the activity. In *Drosophila* this occurrence, so call redundancy, is much less common and usually mutation of a gene in a straight line reveals its physiological function. Finally, it was found that nearly all *Drosophila* genes that were shown to be responsible for proper body pattern formation have close homologues on the protein and functional level in human and other mammals, for example homeoboxes. Due to this phenomenon, it was possible to progress rapidly in the vertebrate field by working in parallel with *Drosophila* and another simple organisms like mosquitoes or worms (Lawrence, P. A., 1992; Nüsslein-Volhard, 1995; Alberts et al., 2002).

2. The *Drosophila* egg as a model system

The small size of the *Drosophila* egg (about 0.5mm long and with a diameter of 0.15mm) makes it easy to handle in the laboratory. Collection of embryos, DNA transformation,

antibodies staining, cross sections and microscopy analysis do not raise any particular problems. After fertilization, the nucleus that is localized in the anterior-dorsal part of the embryo divides in 7 rapid synchronous rounds without cytokinesis that gives rise to a centrally localized syncytium. Subsequently, the majority of the nuclei migrates under the embryonic cell membrane forming a monolayer around the embryo and continues proliferation up to the moment when the 13th division is completed. These so called cleavage cell cycles give the syncytium that contains about 6000 nuclei. During cleavage cell cycles one full cell cycle round takes from 9 to 21 minutes and consists only of alternating M and S phases. Up to now, these are the fastest cell cycles identified among prokaryotes and eukaryotes. After the last (13^{th}) cleavage division the cell cycle enters a pause of about one hour that allows cellularisation to take place and to enclose the nuclei in the newly synthesized cell membrane. About 60 minutes later, during gastrulation, the cell cycle resumes and morphogenetic movements - for example ventral furrow formation - and mitosis proceed in a coordinated way. Monolayer syncytial blastoderm and cellular blastoderm embryos are used as quite simple models for studying biological phenomena like morphogen gradients, cell polarity, regulation of signaling during the cell cycle, cellularisation, morphogenetic movements and their coordination with most of the intracellular processes (Ashburner, M. 1989; Lawrence, P. A., 1992; Foe et al., 1993).

3. Cell cycle and its modifications during *Drosophila* development

The eukaryotic cell cycle is a cascade of events that occur between two subsequent cell divisions. Therefore, this is the process by which for example a fertilized mononuclear *Drosophila* egg becomes adult fly with blood cells, hairs, wings and complex internal organs. Several types of cell cycles exist, and are involved in cell differentiation during embryogenesis and morphogenesis as well as in the maintenance of stem cells in the adult fly (Figure 1). General cell cycle comprehends two main distinct phases. First, the interphase that is composed of G1 (Gap 1) phase, S (DNA synthesis) and G2 (Gap 2) phases, and second, the M phase (Mitosis) that consists of two closely tied processes, main mitosis where nuclear genetic material is equally distributed among the two daughter cells, and cytokinesis where the cytoplasm is dividing. Cells that have reached their final destination place in the tissue can stop proliferating and enter the so called G_Q (Gap and Quiescence) phase. Cells that reach the state of quiescence can stay permanently in this phase or only for a particular period of time if it is necessary, and then they can move back to the general cell cycle and start to proliferate again (Figure 1d).

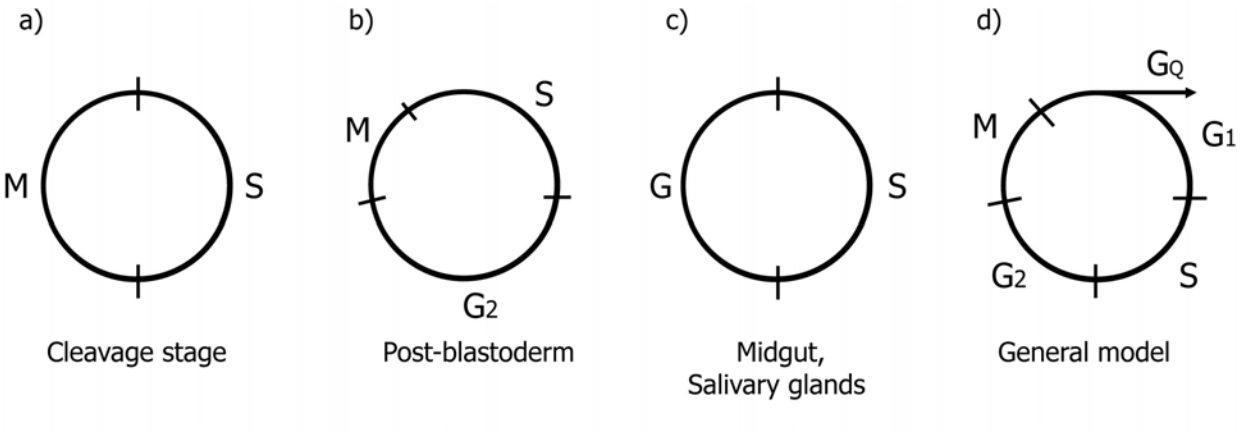

Figure 1. Different models of the cell cycle that take place during *Drosophila* development. **a**) Cell cycle with alternating only S and M phases characteristic for the first 13 divisions (cleavage stage) of early embryonic development. **b**) Postblastoderm divisions with M, S and G_2 phases that occur in 14-16 divisions. **c**) Endocycles that take place during central midgut and salivary glands development **d**) General model of eukaryotic cell cycle present in later stages of *Drosophila* development. Where M - is M phase (mitosis), G_Q - is G_Q phase (Gap and Quiescence), G_1 - is G_1 phase (Gap 1), S - is S phase (DNA synthesis and replication) and G_2 - is G_2 phase (Gap 2).

In the fertilized *Drosophila* embryo, the first 13 cell cycles contain only S and M alternating phases without cytokinesis determined by maternal components that are independent of zygotic transcription (Figure 1a). The interphase progressively extends during cycles 10 to 13 and G2 phase appears for the first time after S phase of 14th division (Figure1b), what allows the onset of zygotic genes expression and coordination of the cell cycle events with morphogenetic movements during gastrulation. Throughout postblastoderm cell cycles (divisions 14 to 16), G2 length is under developmental control, and groups of cells undergo mitosis in domains in response to patterning events (Lee and Orr-Weaver 2003). After the 16th mitotic division, epidermal cells exit mitosis and enter G_Q phase whereas the nervous system cells continue proliferation process according to S-G2-M pattern. The cells that during late embryogenesis differentiate into larval tissues enter S-G cycles (Figure 1c) that continue during larval stages. Groups of cells that proliferate into adult tissues during pupation stage like epithelial cells of wing imaginal discs use the classical cell cycle mode G1-S-G2-M (Figure 1d, Lee and Orr-Weaver 2003). In my project, I was interested in the regulation of cleavage stage cell cycle (Figure 1a, cycles from 1 to 13) especially transition from G2 into mitosis 14th where Frs anti-mitotic activity takes place.

The entry into mitosis depends on the phosphorylation state of Cdk1 (Cdc2) kinase and on the level of mitotic cyclins (Lee and Orr-Weaver 2003). During interphase, Cdk1 is cytoplasmic and inactivated through phosphorylation of its Thr14 and Tyr15 residues by Wee1 and Myt1 kinases. The main trigger into mitosis is protein phosphatase String (Cdc25) that dephosphorylates Cdk1 Thr14 and Tyr15 sites, thus resulting in restoration of its kinase activity. In the early prophase, activated Cdk1 enters and accumulates in the nucleus as a

complex with mitotic cyclins A (required) and B (not required) and pushes the cell cycle into mitosis (Lehner and O'Farrell, 1989; Yang et al., 1998; Pavletich et al., 1999).

Maternally contributed *string* during cleavage cell cycle is ubiquitously allocated in the embryo until the beginning of mitosis 13th when it gets degraded. All the mitoses following cellularisation (cycles 14 to 16) are zygotically controlled by transcription of *string*. The expression of *string* precedes exactly the mitotic pattern by a few minutes (Edgar and O'Farrell., 1989). *string* is necessary for mitosis, since *string* mutants remain in interphase 14 throughout embryonic development. Furthermore, *string* is sufficient, when uniformly over-expressed, to force all the cells into mitosis (Edgar and O'Farrell., 1989). There is however an exception to this rule - the ventral furrow region. Here, the gap between appearance of *string* RNA and mitosis is at least 20 minutes longer than in the other regions of the embryo, which allows the cells to invaginate before they start dividing. This cell type specific mitotic delay is dependent on transcription factor *snail* (the main trigger for mesoderm development and ventral furrow formation) and correlates with ventral furrow formation. Thus, its function may be to prevent an interference of mitosis and ventral furrow formation. Premature mitosis as induced by uniform over-expression of *string* inhibits morphogenetic movements like the ventral furrow formation. Recently, Großhans and Wieshaus, 2000 described two novel mitotic inhibitors, *tribbles* (*trbl*) and *frühstart* (*frs*) that counteract String specifically in the cells involved in ventral furrow formation during gastrulation. They proposed that Frs and Trbl form a link between morphogenetic movements and mitotic control (Großhans and Wieschaus, 2000; Großhans et al., 2003).

4. Synchronization of cell proliferation with morphogenetic movements in early *Drosophila* embryo as an example of switch in developmental programs

The early development of *Drosophila* embryo is characterized by alternating stages of cell proliferation and morphogenetic movements. Both processes depend on the rearrangement of the cytoskeleton. Parallel use of cytoskeleton components may presumably cause interference between these two processes especially during *Drosophila* early embryogenesis when development progresses very fast (Foe, 1989; Foe et al., 1993; Großhans and Wieschaus, 2000). During the first 2 hours the fertilized egg intensively divides in 13 synchronous rounds without cytokinesis and the so called syncytial blastoderm is formed. After the 13th division, the embryonic cell cycle enters about one hour pause at G2 of 14th division that allows the morphogenetic program to switch on. During this cell cycle pause, cellularisation and gastrulation take place. During gastrulation the cells elongate and morphogenetic movements

rearrange their position to one another (Leptin 1995; Großhans and Wieshaus 2000). The most prominent of these morphogenetic movements is formation of the ventral furrow as a consequence of ventral cells invagination and mesoderm anlage formation (Großhans and Wieshaus 2000). During gastrulation, the cell cycle starts again and subsequent morphogenetic movements take place. After gastrulation, the mitotic program proceeds in an asynchronous way separated in about 25 different embryonic domains, thus allowing cell proliferation and morphogenetic movements to proceed at the same time in different parts of the embryo (Großhans and Wieshaus 2000).

It is not clear yet how the transition between nuclear divisions and cellularisation is determined and the cell cycle is paused after exactly 13 divisions. It has been known since a long time, that the nucleocytoplasmic ratio is the initial determinant, since haploid embryos perform an extra division before the pause (Foe et al., 1993). An extra cleavage cycle is also observed in embryos injected with alpha-amanitin, an inhibitor of RNA polymerase II, which suggests that the nucleocytoplasmic ratio acts via zygotic gene or genes. Inhibition of zygotic gene expression does not disturb development prior to this point, which shows that the rapid nuclear divisions are solely controlled by factors supplied by the mother (Foe et al., 1993). Cell cycle progression of last three cleavage divisions (cycles 10-13) is controlled by maternal DNA repair checkpoint with protein kinases Grapes and Mei41 (Fogarty et al., 1997; Sibon et al., 1997, 1999; Yu et al., 2000). The *grapes* checkpoint delays mitosis during cycles 10-13, what allows zygotic expression to start, and is involved in establishing the pause after 13th division (Fogarty et al., 1997; Sibon et al., 1997). Großhans et al. 2003 reported *frühstart*, the only so far known zygotic gene that participates in the cleavage cell cycle pause and mitotic/morphogenetic switch observed during mid-blastula transition.

5. The role of *Drosophila* zygotic genes *frühstart* and *tribbles* in mid-blastula transition

So far, two genes that are required for the mitotic delay in the ventral furrow region (Figure 2) were identified in genetic screens for mutations that disrupt mesoderm invagination during gastrulation process - *tribbles* and *frühstart* (Müller et al., 1999; Seher and Leptin 2000).

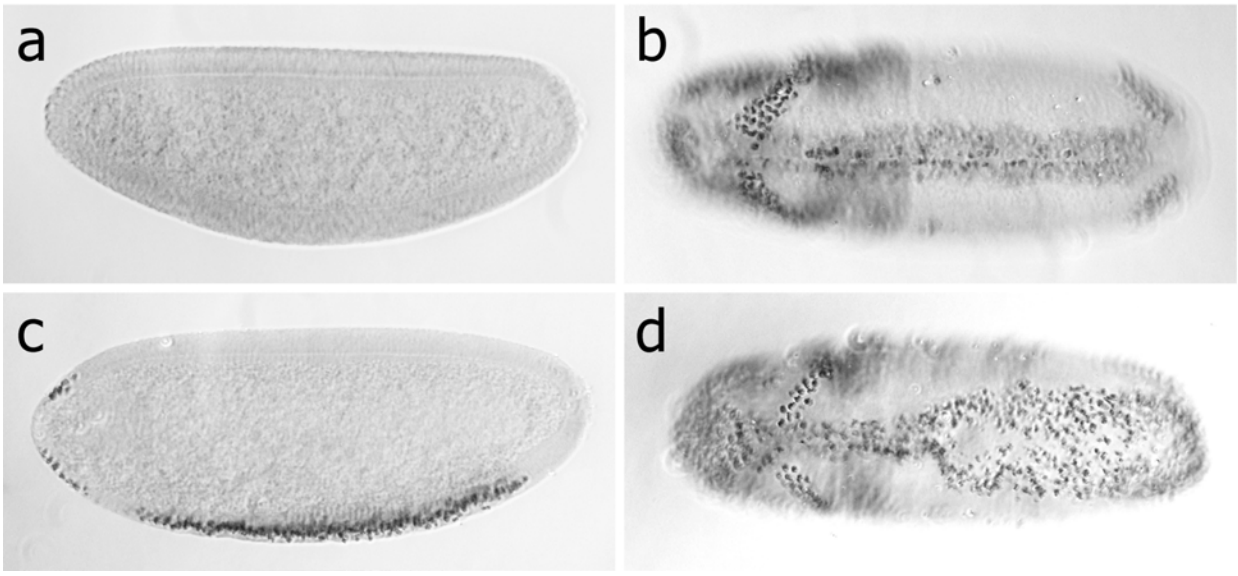

Figure 2. Frühstart ventral furrow phenotype. The pictures present wild-type *Drosophila melanogaster* embryos stage 6 (**a**) and stage 7 (**b**) and deficient for *frs* stage 6 (**c**) with premature mitosis in the ventral region and stage 7 (**d**) with open, not properly formed ventral furrow. All embryos were stained with anti-pHistone3 antibody (Materials and Methods).

Further analysis revealed that *tribbles* (*trbl*) and *frühstart* (*frs*) are uniformly expressed immediately after the last, 13th mitosis in the cleavage stage and reach a peak in the first half of cellularisation. When *frs* or *trbl* are expressed prematurely by RNA injection, the cell cycle stops already after 12 cycles (Großhans and Wieshaus, 2000; Großhans et al., 2003).

Trbl protein consists of 488 aa residues and belongs to the Snf1/Nim1/Hsl1 family of serine/threonine protein kinases. In yeast, the kinase Nim1 (*S. pombe)* and Hsl1 (*S.cerevisiae*) are positive regulators for the entry into mitosis. Based on sequence homology, it was found that related but uncharacterized proteins also exist in higher vertebrates (Großhans et al., 2000). Trbl has probably no kinase activity, because several of the invariant residues in the kinase consensus sequence are changed and the subdomains I to V are only weakly conserved. In addition, a mutation in the catalytic center does not affect *trbl* activity. In contrast to Nim1/Hsl1, Trbl is a negative regulator of mitosis. A possible model is that *trbl* behaves like a dominant-negative allele of a homologue of Nim1/Hsl1 with kinase activity and competes for substrates or effectors (Großhans and Wieschaus, 2000).

frs has a transcript of about 500 nucleotides and encodes a basic 90aa polypeptide that contains 19 basic residues and has an isoelectric point of 10 (Schulz and Miksch 1989). *frs* mRNA is uniformly expressed at the beginning of cell cycle 14th, reaches the peak during cellularisation and persists until the end of gastrulation. Moreover, *frs* RNA is detectable until the germ band extension stage in a group of presumable aminoserosa anlage cells (Großhans et al., 2003). In order to investigate the subcellular localization of Frs, specific antibodies were

applied for whole-mount stainings. Frs is uniformly distributed in the cytoplasm (Figure 3), despite its molecular weight that is far below the exclusion limit of the nuclear pores and its high content of basic amino acid residues (Großhans and Wieschaus, 2000).

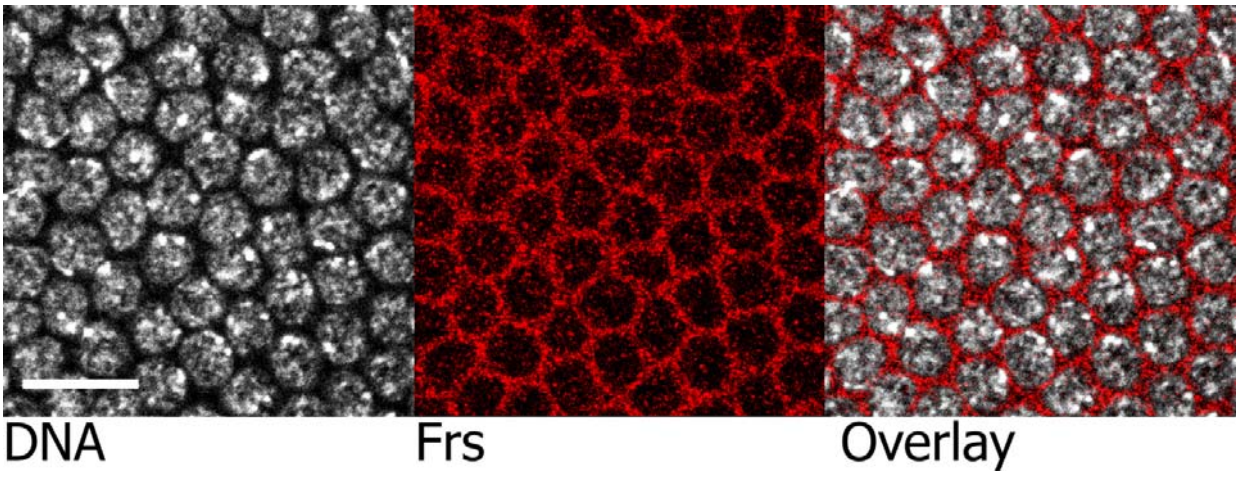

Figure 3. Polyclonal anti-Frs antibody staining of stage 5 (syncytial blastoderm) wild-type OrR embryo. DNA staining (white), Polyclonal anti-Frs antibodies (red). The scale bar represents 10µm.

The *frs* primary structure does not display homology to any of the known proteins or motifs and because of that it was very hard to predict a biochemical function of this polypeptide. It was already described by Großhans and Wieschaus, 2000 and Großhans et al., 2003 that *frs* has two functions in the early development of the embryo. They found that *frs* delays mitosis during mesoderm invagination and controls the cell cycle pause after exactly the 13th mitosis during mid-blastula transition (MBT). The timing of MBT depends on nucleocytoplasmic ratio and is shifted in diploid (after 13th division) and haploid (after 14th division) similar to the *frs* mutant embryo where an additional mitosis takes place. These observation together with the fact that onset of *frs* expression is also correlated with N/C ratio (in the haploid embryo *frs* expression peak takes place after the 14th division, not after the 13th like in the diploid) suggest that *frs* gene expression may be involved in linking the N/C with the pause of cleavage cycles (Großhans et al., 2003).

An additional interesting feature of *frs* gene is the fact that this mitotic inhibitor in contrast to other known cell cycle regulatory proteins is not crucial for cell cycle progression. This might suggest that *frs* is a kind of modulator or organizer of two biological processes, the cell cycle progression and morphogenetic movements, that take place in parallel during MBT (Großhans et al., 2003). *In vivo* data presented by Großhans et al., 2003 revealed that *frs* and *trbl* negatively control mitotic function of D-Cdc25 (*string* and *twine*) but the molecular explanation of this phenomenon still remains unclear.

6. Regulation of *Drosophila* cell cycle

A group of proteins known as cyclin dependent kinases (Cdks) plays the major role in cell cycle control machinery. The kinase activity of Cdks undergoes cyclical changes during the cell cycle, what directly leads to increasing and decreasing of the phosphorylation level of regulatory proteins that govern most biological processes like cell growth, replication, mitosis and cytokinesis (Sherr, 1994; Scherr et al., 1994; Nurse, 1994; King et al., 1994).

Cyclin dependent kinases

Cdks belong to the Serine/Threonine protein kinase family. In all eukaryotes (except yeasts), different Cdks are responsible for controlling the progress through the different phases of the cell cycle. When a specific Cdk is activated, the cell cycle enters the stage that is controlled by this particular Cdk. If a Cdk is not activated or activated and inhibited, the cell cycle stops (Morgan, 1997). The best characterized and described member of the Cdk family is Cdk2. The monomeric form of Cdk2 consists of a N-terminal lobe rich in β-sheet, a C-terminal lobe rich in α-helix, and a deep cleft at the junction of N lobe and C lobe that forms the catalytic center containing the ATP binding site (Pavletich, 1999). It was also found that Cdk2 has two fragments among its tertiary structure that do not match to the canonical kinase pattern (De Bond et al., 1993). The first one is an α-helix with PSTAIR unique sequence that was found only in the Cdks, and the second one a regulatory T-loop with activating phosphorylation site (Figure 4, Pavletich, 1999).

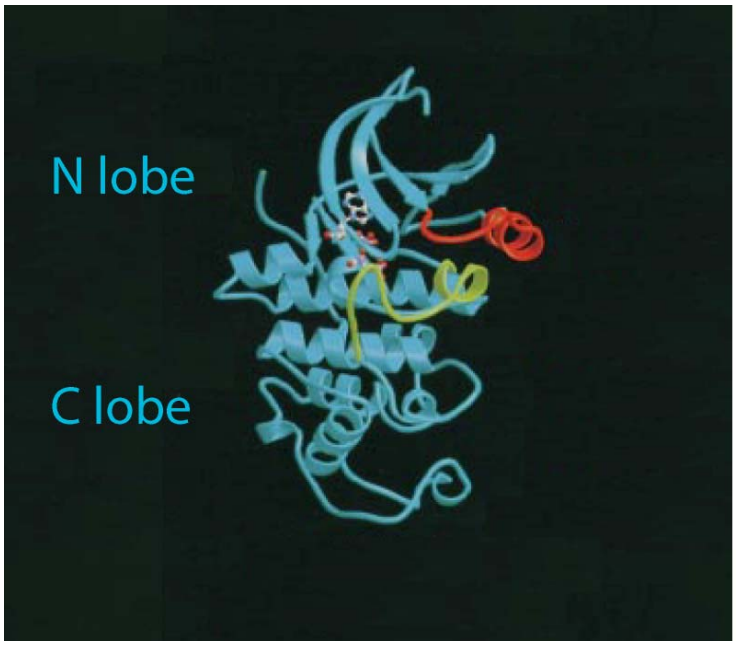

Figure 4. Crystal structure of monomeric, inactive form of Cdk2 protein. N and C lobes are marked in blue. PSTAIR helix is marked in red and T-loop in green (Adapted from Pavletich, 1999).

Crystallographic studies revealed, at least to some extent, the molecular mechanisms by which cyclin dependent kinases are regulated (Knighton et al., 1991; De Bondt et al., 1993; Brotherton et al., 1998; Russo et al., 1998; Pavletich et al., 1999). All Cdk regulatory events, like Cdk phosphorylation or binding of Cdk regulator proteins, cause conformational changes in the kinase catalytic cleft or in its direct neighborhood. This demonstrates the high internal elasticity of the structure of Cdks, which partially explains their aptitude to switching on/off as a reaction on multiple regulatory signals (Pavletich et al., 1999). In *Drosophila*, two Cdks are involved in cell cycle regulation, Cdk2 that is responsible for G1/S transition and Cdk1 that is responsible for entry into mitosis.

Mechanism of cell cycle activation

Newly synthesized, monomeric Cdk does not have kinase activity because of its not yet properly folded structure. For full kinase activation, several subsequent regulatory processes have to take place (Figure 6). A number of different groups of regulatory proteins that control the cyclical alterations of Cdks activity, have already been described. Proteins known as cyclins, play the most important and primary role in Cdks regulation. In *Drosophila melanogaster* there are six known cyclins that are involved in Cdk control during cell cycle progression. Cyclins A, B, B3 and J are involved in G2/M transition and mitosis, while only CycA is essential for proper cell proliferation, development and viability of the fly (Lehner and o'Farrell, 1989; Jacobs et al., 1998; Kolonin and Finley, 2000). CycE, CycD and CycC are involved in the G1/S transition and if mutated, *Drosophila* viability is not affected (Foe et al., 1993; Thomas et al., 1997; Edgar and Orr-Weaver, 2001, Emmerich et al., 2004). The structure of all cyclins in the main plan is similar. A destruction box sequence responsible for protein termination via ubiquitin ligases pathways is located in the N-terminal part of the protein and a motif of about 100aa, known as the cyclinbox, is found in the C-terminal part. The cyclinbox is required for Cyclin-Cdk complex formation and it contains a so called hydrophobic patch that is responsible for binding of the Cdk phosphorylation substrates as well as of some Cdks inhibitors (Polyak et al., 1994; Lacy et al., 2004; Loog 2005; Lowe et al., 2002). Cyclin binding to the non-activated form of Cdk induces conformational changes. The cyclin translocates Cdk PSTAIR helix deeper into the catalytic center and rotates it 90º. In parallel Cyclin-Cdk binding changes the position of the T-loop structure what leads to physical uncovering of the catalytic cleft and partial activation of the Cdk-Cyclin complex (Compare Figure 4 and figure 5, Pavletich, 1999, figure 6a and 6b).

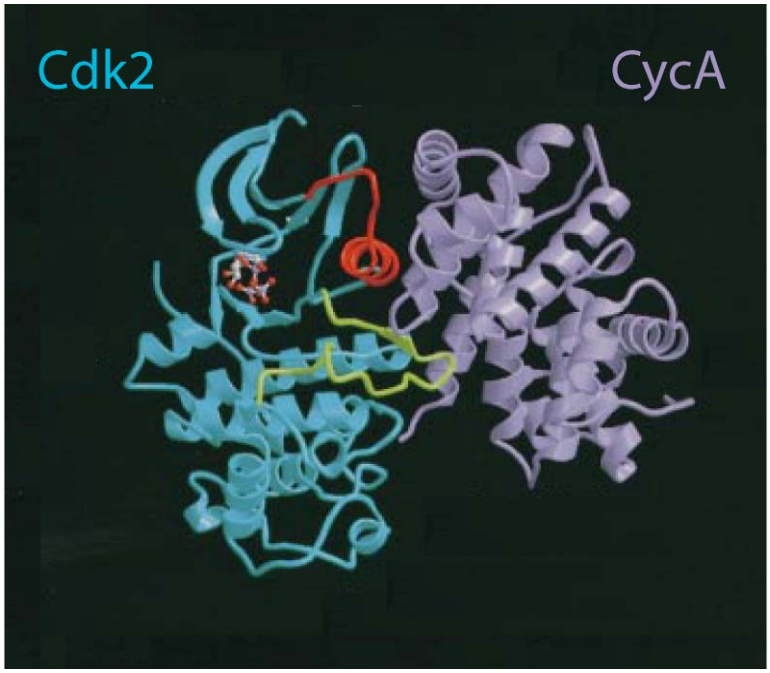

Figure 5. Crystal structure of Cdk2-CycA complex. The PSTAIR helix (in red) and T-loop motif (in green) change their conformation and partially uncover the catalytic center of Cdk (Adapted from Pavletich, 1999).

Subsequently, for full Cdk activation the T-loop motif has to be phosphorylated by CAK (Cyclin Activating Kinase) kinase (Russo et al., 1996; figure 6b and 6c). This phosphorylation causes successive conformational changes that complete the reorganization processes that take place in and around the Cdk catalytic center and makes Cdk-Cyclin complex fully active (Figure 6).

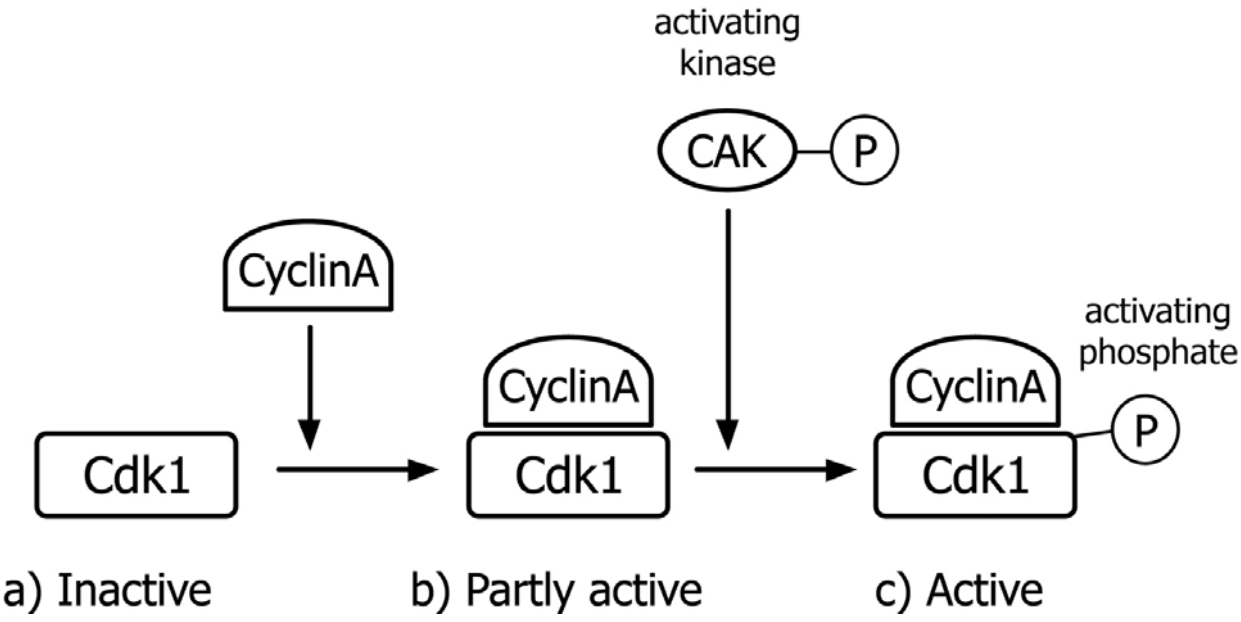

Figure 6. Scheme of Cdk activation process. Monomeric form of Cdk is inactive (**a**). Cyclin binding causes conformational changes that partially activate Cdk kinase activity (**a** and **b**). Full Cdk activation requires phosphorylation of Cdk by CAK kinase (**b** and **c**).

When a particular event of the cell cycle is coming to be completed, the Cdk that coordinates it has to be switched off. The cell inhibits previously activated Cdks, either via Cdk-Cyclin complex inhibitory phosphorylation or via protein inhibitors that physically bind to the Cdk-Cyclin complex and make it inactive.

Inactivation of Cdk-Cyclin complex kinase activity by protein phosphorylation

In *Drosophila*, Cdk1-CyclinA complex plays the main role in the entry into mitosis. During interphase, this complex is inactivated by phosphorylation of Cdk1 on Threonine 14 and Tyrosine 15 by the inhibitory kinases Wee1 and Myt1 (Russel and Nurse, 1987; Stumpff et al., 2004). Close to the end of G2 phase, protein phosphatase String (Cdc25) dephosphorylates T14 and Y15 of Cdk1 (Russel and Nurse, 1986; Millar and Russel, 1992) and in this way activates the Cdk1-CyclinA complex and pushes the cell cycle into mitosis (Edgar et al., 1994).

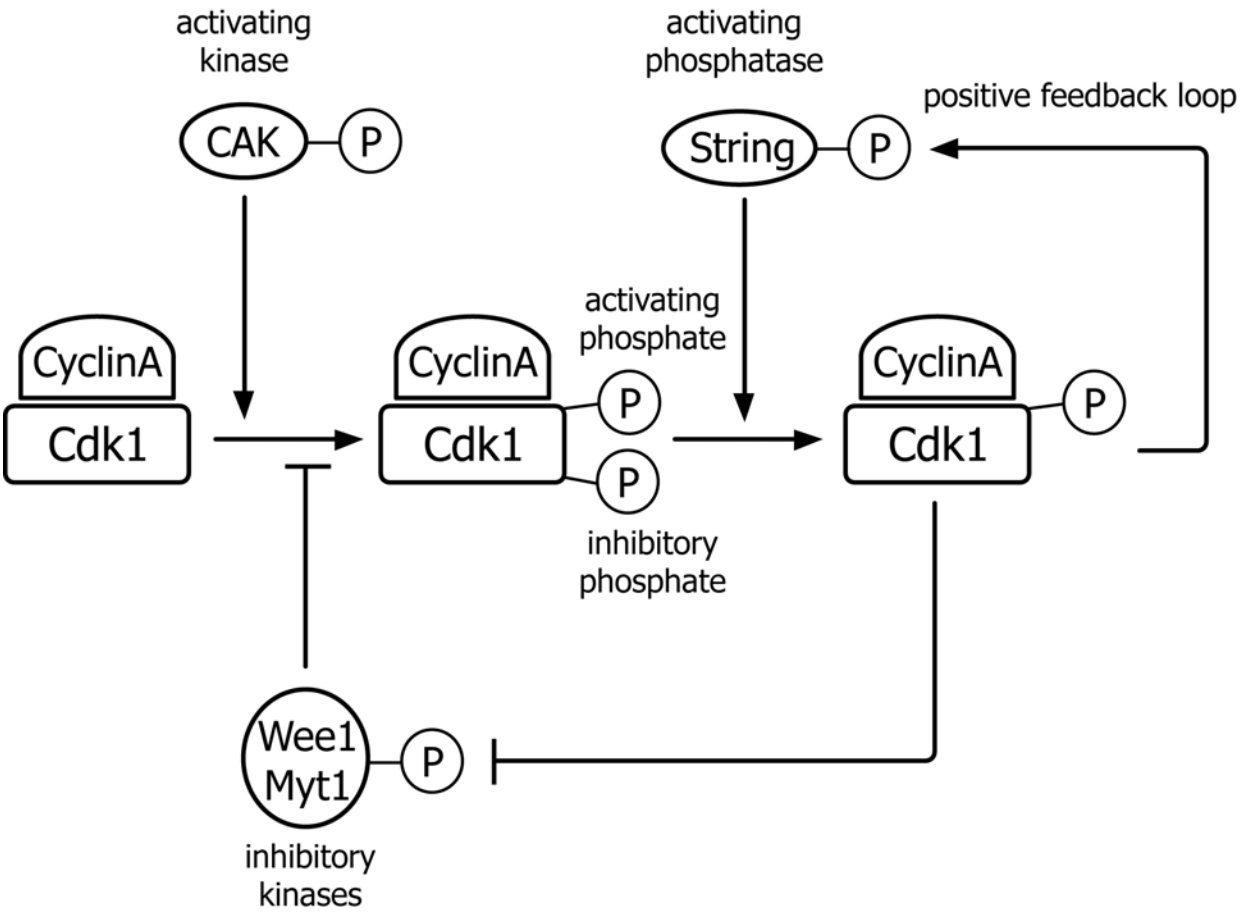

Figure 7. Scheme of Cdk1-CyclinA complex inhibition via Cdk1 phosphorylation by kinases Wee1/Myt1 and activation via Cdk1 dephosphorylation by protein phosphatase String.

Activated Cdk1-Cyclin complex multi-phosphorylates protein phosphatase String, thus enhancing its activity. In parallel, phosphorylation of inhibitory kinase Wee1 by Cdk1-Cyclin complex inhibits its kinase activity and makes the positive feedback loop (Figure 7). At the end of mitosis this auto-activating process is disrupted by downstream regulation of String and the cell cycle goes into G1 phase (Edgar and O'Farrel, 1989; Edgar and O'Farrel, 1990).

Inactivation of Cdk-Cyclin complex kinase activity by protein inhibition

The second known manner of Cdk-Cyclin complex inactivation is via protein inhibition. The Cdk-Cyclin protein inhibitors are classified in two families according to the differences in their inhibitory mechanisms - CIP/KIP and INK4. There is also a third group of inhibitors that do not belong to any of these families and have not been well characterized yet.

There are two well characterized G1/S Cdk-cyclin inhibitors that belong to the CIP/KIP family - p21 (Harper et al., 1995) and p27 with its *Drosophila* homolog Dacapo. Transient high level expression of Dacapo during the last (16th) zygotic cell division is required for arresting the cells in G1 phase of cycle 17 and for general exit from the cell cycle (Toyoshima and Hunter, 1994, Lane et al., 1996). CIP/KIP inhibitors block the Cdk-Cyclin kinase activity by binding to both complex subunits. The C-terminal end of G1/S inhibitor p27 binds to the catalytic cleft of Cdk2, whereas the N-terminus binds to the hydrophobic patch of CyclinE, resulting in inactivation of the complex. In addition, association of p27 with the Cdk-cyclin complex causes conformational changes of Cdk (Russo et al., 1996; Pavletich, 1999; Brown et al., 1999; Lacy et al., 2004). The function of the Cdk2 subunit is to phosphorylate (activate) via its catalytic center a set of substrates that are required for the cell cycle S phase. The cyclin hydrophobic patch is a docking site for some Cdk2 substrates (e.g. Rb, p53, E2F) that in order to be phosphorylated, they first have to bind and be recognized as proper substrates by the cyclin subunit (Adams et al., 1996; Adams et al., 1999; Lowe et al., 2002; Loog and Morgan, 2005). Furthermore, the hydrophobic patch is required for binding of CIP/KIP protein inhibitors like p21 and p27 to the Cdk-Cyclin complex (Lowe et al., 2002; Lacy et al., 2004). It was also found that CIP/KIP inhibitors are themselves substrates of Cdks. Phosphorylated form of p27 is downregulated (ubiquitylated) by SCF ubiquitin ligase. The ubiquitylated form of p27 is immediately exported into the cytoplasm and degraded by the proteasome (Alberts et al., 2002; Vlach et al., 1997; Müller et al., 2000).

Inactivation of Cdk-Cyclin complex kinase activity by INK4 proteins

The members of INK4 Cdks inhibitor family inactivate Cdk-Cyclin complex via binding to the Cdk subunit only. In contrast to CIP/KIP family, INK4 inhibitors like p16 and p19 do not bind directly to the catalytic cleft of Cdk but next to it. (Russo et al., 1998; Brotherton et al., 1998; Pavletich, 1999). Moreover, the INK4 and cyclin binding sites on the Cdk do not overlap each other. Binding of the p16 inhibitor causes allosteric changes in the Cdk catalytic cleft and its surrounding motifs and by this it prevents Cdk-Cyclin complex formation. p16 is also able to bind to the already formed Cdk-Cyclin complex and by this also shut down Cdk kinase activity even if this association does not lead to disruption of the Cdk-Cyclin complex (Russo et al., 1998; Pavletich, 1999).

Uncharacterized cell cycle protein inhibitors

The wide range of cell cycle studies revealed an additional, informal group of cell cycle inhibitors that have not been well characterized yet, at least on the molecular level. Several common features of these inhibitors might suggest that they share a common cell cycle regulatory mechanism. Members of this group are M/G1-S Sic1 (*Saccharomyces cerevisiae*), M/G1 Rum1 (*Shizosaccharomyces pombe*), mitotic Rux (*Drosophila melanogaster*) and also G2/M Frs (*Drosophila melanogaster*). *In vivo* studies revealed that Sic1, Rum1 and Rux are functional homologues and they can functionally replace each other (Sanchez-Diaz et al., 1998; Foley and Sprenger, 2001). What is striking is that these proteins almost do not share any sequence homology except for the RxL motif commonly used by Cdk substrates and some Cdk inhibitors to interact with Cdk-Cyclin complex via hydrophobic patch of the cyclin subunit (see above). More detailed molecular analysis revealed that Sic1 and Rux indeed bind directly to mitotic cyclins via this motif and specifically inhibit mitotic cyclin-Cdk complexes *in vitro* (Hodge and Mendenhall, 1999; Avedisov et al., 2000; Foley and Sprenger 2000). Negative control of mitotic cyclin-Cdk complexes by Sic1 and Rux *in vivo*, induced endocycles in proliferating epithelial cells of *Drosophila* wing imaginal discs (Foley at al., 1999; Thomas et al., 1997; Edgar and Orr-Weaver, 2001; Vidwans et al., 2002) what confirms their anti-mitotic specificity. There are additional common features within this group. All of these proteins are non-essential, as most likely they cooperate with other cell cycle regulatory mechanisms like cyclin proteolysis. Moreover, all of them are phosphorylated and subsequently degraded through the ubiquitin-dependent proteolytic pathway (Benito et al., 1997; Verma et al., 1997; Foley et al., 1999; Großhans and Wieschaus, 2000; Großhans et al., 2003; in the case of Frs, its phosphorylation is described in this work for the first time, while the significance of this

phosphorylation still remains not completely resolved). All the similarities described above suggest that these proteins might share a common molecular mechanism of inhibition of the cell cycle machinery but in order to reach a final conclusion, more detailed molecular analysis is required.

Cell cycle regulation via nucleocytoplasmic transport

The cell cycle progression is also regulated by nucleocytoplasmic trafficking of the proteins that are involved in cell cycle events. At the appropriate moment of the cell cycle, some of the cell cycle proteins must be imported into the nucleus while some others must be exported. The changes in the subcellular localisation of human Cdk1 during the cell cycle constitute a typical example. Close to the end of G2 phase, the protein phosphatase String (Cdc25) activates Cdk1-CyclinB1 complex that is accumulated in the cytoplasm during S and G2 phases. Activated Cdk1-CyclinB1 complex is transported into the nucleus during prophase by importin α/β heterodimers in NLS-dependent way (Pines and Hunter, 1994; Görlich et al., 1994; Görlich et al., 1995; Yang et al., 2006). When mitosis is close to its end Cdk1-CycB1 complex is exported back to the cytoplasm via NES-dependent Crm1 pathway (Toyoshima et al., 1998; Yang et al., 1998). Another example is p27 CIP/CIK inhibitor, which in order to be properly downregulated, must first be imported into the nucleus, get phosphorylated by Cdk2-CycE complex and be re-exported back to the cytoplasm in a Nup50 nucleoporin interaction dependent way where it is degraded in a ubiquitinylation dependent manner at the G1/S transition of the cell cycle (Müller et al., 2000). However, the detailed molecular mechanism of these processes, especially the initiating and terminating signals are unknown. Nuclear protein import requires a nuclear localization sequence (NLS) within the import substrate amino acid sequence. Experimental data revealed that NLS-containing substrates bind to importin-α which recruit importin-β to form a trimeric transport complex within the cytoplasm (Görlich et al., 1996; Weis et al., 1996; Fasken et al., 2000). Subsequently, the NLS-importin-α/importin-β complex directly binds to nucleoporins that are components of the nucleopore basket. Primarily, the import complex-nucleoporins interaction is stabilized by Ran-binding protein 1 (RanBP1)(Chi et al., 1996) and is likely stimulated by the interaction of Ran-GDP with pore components (Fasken et al., 2000). The mechanism that re-localizes the import complex from the cytoplasm to the nucleus through the nuclear pore is not completely understood up to now. In the nucleus, trimeric transport complex binds RanGTP, which dissociates the complex and disassembles the transported substrate (Rexach et al., 1995; Görlich et al., 1996; Fasken et al., 2000). Importins α and β complex subunits are afterward exported back to the cytoplasm

(Kutay, U., 1997). The primary mechanism by which substrates are imported into the nucleus is highly conserved, and components required for import have been identified in yeast (Matsusaka et al., 1998), plant (Ivasaki et al., 1998), *Drosophila* (Bhattacharya and Steward, 2002; Allemand et al., 2002) and animal cells (Nicolas et al., 1997)(Fasken et al., 2000).

In *Drosophila*, the nuclear export mechanism is driven by general export factor *embargoed* that is a functional and sequence homolog of human (71% identity) and yeast (*S. pombe* 49% identity) Crm1 protein (Collier et al., 2000). Embargoed (Emb) export factor requires two other proteins for its activity, small GTPase Ran and nuclear pore components (Görlich and Kutay, 1999) like e.g. Nup50, Nup88, Nup153, Nup214 and Nup358 (Askjaer et al., 1999; Smitherman et al., 2000; Guan et al., 2000; Roth et al. 2003; Bernad et al., 2004). Emb binds directly to the proteins that contain leucine-rich nuclear export signal (NES). A consensus sequence for leucine-rich NES has been defined by detailed functional analysis and amino acid sequence comparison of several proteins that contain NES (Bogerd et al., 1996). Nevertheless, this consensus does not provide a safe way of predicting Emb substrates from protein sequences alone. Not all sequence motifs that look like leucine-rich NES also function as such in their original protein context (Görlich and Kutay, 1999). Cargo-NES/Emb/RanGTP nuclear complex is exported from the nucleus by Emb-guided interactions with nucleoporins and the nuclear pore complex (Adachi and Yanagida, 1989; Stade et al., 1997; Fornerod et al., 1997; Fasken et al., 2000). In the cytoplasm, RanGTP is hydrolysed into RanGDP form what promotes dissociation of the export complex and recycling of Emb (Görlich and Kutay, 1999; Collier et al., 2000; Fasken et al., 2000).

Aim of the studies

The main goal of this project was to study the molecular mechanisms of regulation of mitosis in the context of embryonic development. Specifically, the unknown biochemical function of the zygotic gene *frühstart* (*frs*), which has been shown to inhibit mitosis and to coordinate cell shape changes and cell division in the early *Drosophila* embryo (Seher and Leptin 2000, Großhans and Wieschaus 2000, Großhans et al., 2003), was investigated.

Materials

1. Reagents

All standard chemicals were purchased from Sigma-Aldrich (Steinheim, Germany), AppliChem GmbH (Darmstadt, Germany), Serva (Heidelberg, Germany), Merck (Darmstadt, Germany) or Gibco BRL (Eggenstein, Germany) unless otherwise mentioned.

2. Radioactivity

- Redivue adenosine 5'-[γ-^{32}P] triphosphate, triethylammonium salt (6000Ci/mM, 10mCi/ml), Amersham Biosciences.
- Redivue L-[^{35}S] methionine (*in vitro* translation grade), (1000Ci/mmol, 15mCi/ml), Amersham Biosciences.

3. Antibiotics

- Ampicillin, stock (1000x): 100mg/ml, final concentration: 50-200µg/ml.
-Penicillin/Streptomycin solution, stock (100x): final concentration 50U penicillin G and 50µg streptomycin sulfate per 1ml of medium (1% of stock).

4. Enzymes

All enzymes were purchased from Fermentas (Lithuania) and Roche Diagnostics GmbH (Penzberg, Germany) and used according to the instructions delivered by the producers unless otherwise mentioned.

5. Peptides

- C16 Frs peptide - contains the last 16 C-terminal amino acids of Frühstart sequence (YEADKNFIKARKSLNF). Synthesized by Peptide Specialty Laboratories GmbH, Heidelberg.
- DmCdk1 peptide - contains the last 18 C-terminal amino acids of DmCdk1 sequence (CILEHPYFNGFQSGLVRN). Synthesized by SEQLAB Sequence Laboratories Goettingen GmbH.

6. Antibodies and immunochemicals

Primary antibodies

- R Ab Frs - J. Großhans (Großhans et al., 2003)
- R Ab DmNup50 - P. Gawliński (this work).

- R Ab DmCdk1 - P. Gawliński (this work, according to Knoblich et al., 1994).
- M Ab DmCdk1 PSTAIR - mouse IgG1 isotype, Sigma (Yamashita et al., 1991).
- R Ab DmCycA - gift from C. Lehner (Lehner et al., 1989).
- M Ab DmCycA - Developmental Studies Hybridoma Bank, University of Iowa.
- M Ab DmCycB - Developmental Studies Hybridoma Bank, University of Iowa.
- R Ab DmCycE - gift from C. Lehner (Knoblich et al., 1994).
- M Ab Anti-c-Myc - Roche.
- M Ab g-Tubulin - Sigma.
- M Ab a-Tubulin - Sigma.
- R Ab pHistone3 - Upstate.
- M Ab b-Gal - Boehringer.
- M Ab BrdU - Roche.
- M Ab Dlg - Developmental Studies Hybridoma Bank, University of Iowa.
- Sheep anti-Dig-AP - alkaline phosphatase, Fab fragments, Roche (preadsorbed on *Drosophila* wild-type embryos at 1:10).

Secondary antibodies

- Alexa 488, 546, 647 anti-mouse and anti-rabbit - Molecular probes.
- Horse peroxidase (POD) anti-mouse IgG (H+L) - Sigma.
- Horse peroxidase (POD) anti-rabbit IgG (H+L) - Sigma.
- Biotinylated anti-rabbit IgG (H+L) - Vector Laboratories, Inc., USA.
- Biotinylated anti-mouse IgG (H+L) - Vector Laboratories, Inc., USA.

Immunochemicals

- DAPI (4',6'-Diamidino-2-phenylindole) - Sigma.
- Alexa Fluor 488 phalloidin - Molecular probes.
- Hoechst 33342 - Sigma.

7. Buffers

- PBS (Phosphate Buffered Saline): 10mM Na_2HPO_4, 2mM KH_2PO_4 pH7.4, 137mM NaCl, 2.7mM KCl.
- PBST: Phosphate Buffered Saline with 0.2% Tween20.
- Error-prone PCR buffer: (10x) 100mM Tris-HCl pH8.3, 500mM KCl, 70mM $MgCl_2$.
- IP buffer: 50mM Hepes/NaOH pH7.5, 150mM NaCl, 0.5% TritonX-100, 10% glycerin.

- Kinase assay buffer: 80mM β-glycerophosphat pH7.2, 20mM EGTA, 15mM $MgCl_2$, 1mM DTT, 50μM ATP.
- SDS-PAGE sample buffer: 2x: 90mM Tris-HCl pH6.8, 6% SDS, 0.6% bromophenol blue, 20% glycerol, 6% β-mercaptoethanol.
- TE: 10mM Tris/HCl pH7.5, 1mM EDTA.
- Lithium acetate/TE buffer - 1 volume 10x TE pH7.5, 1 volume 1M lithium acetate, 8 volumes ddH_2O.
- Lithium acetate/TE/PEG buffer - 1 volume 10x TE pH7.5, 1 volume 1M lithium acetate, 8 volumes PEG 4000 (w/v).
- Yeast DNA extraction buffer: 10mM Tris/HCl pH8.0, 2% TritonX-100, 1% SDS, 100mM NaCl, 1mM EDTA.
- CNBr coupling buffer: 100mM $NaHCO_3$ pH8.3(NaOH), 300mM NaCl, 10mM $MgCl_2$.
- acetate buffer (CNBr sepharose blocker): 0.1mM Na-acetate pH4.0, 0.3M NaCl.
- Z-Buffer: 100mM Na-Phosphate pH7.0, 10mM KCl, 1mM $MgSO_4$, 50mM β-mercaptoethanol.
- *in vitro* transcription buffer 10x: 400mM Tris/HCl pH7.5, 60mM $MgCl_2$, 20mM spermidin.
- SPR buffer A: 10mM HEPES pH7.4, 150mM NaCl, 50μM EDTA, 0.005% Tween20.
- SPR buffer B: 50mM Tris pH8.0, 200mM NaCl, 3mM $CaCl_2$, 5mM $MgCl_2$, 10% glycerol, 1mM DTT, 0.005% Tween20.
- EQ buffer: 50mM Tris ph7.0, 200mM NaCl, 1mM EDTA.
- EL buffer: 100mM Tris pH8.0, 20mM NaCl, 1mM EDTA, 80mM DTT.
- *in vitro* nuclear export buffer - 20mM HEPES/KOH pH7.5, 110mM CH_3COOK, 5mM $(CH_3COO)_2Mg$, 0.5mM EGTA, 250mM sucrose.

8. Media

Bacterial media

- **LB**; per 1 liter: 10g Bactotrypton (Becton, Dickinson), 5g Yeast extract (Becton, Dickinson), 10g NaCl, 15g Bactoagar (Becton, Dickinson) if for plates.
- **SOB**; per 1 liter: 20g Bactotrypton (Becton, Dickinson), 5g Yeast extract (Becton, Dickinson), 500mg NaCl, 10mM Mg-sulfate, 2.5mM KCl.
- **SOC**; SOB supplemented with 20mM glucose (from a 1 M stock solution).

Yeast media

- **YPD** (complete medium); per 1 liter: 10g Yeast extract (Becton, Dickinson), 20g Peptone (Gibco), 20g Bactoagar (Becton, Dickinson), 900ml dH_2O, 20g glucose (in 100ml dH_2O autoclaved separately), for plates with one pellet of NaOH.

- **CS** (dropout medium, complemented synthetic medium); per 1 liter: 6.7g Yeast Nitrogen Base w/o Amino Acids (Base for classifying yeasts based on amino acid and carbohydrate requirements, Difco), 0.6g aa mix without His, Trp, Leu, Ura (CSM-HIS-LEU-TRP-URA, BIO 101), 20g Bactoagar (Becton, Dickinson), indicated below amounts of lacked amino acids/uracil if necessary, 900ml dH_2O.

amino acids/uracil:

- 20mg/l uracil (100x stock 2.4mg/ml)
- 20mg/l histidine (100x stock 2.4mg/ml)
- 60mg/l leucine (100x stock 7.2mg/ml)
- 40mg/l tryptophan (100x stock 5mg/ml)

- **Indicator plates medium** (to assay β-Gal activity); per 0.5l: 3.35g Yeast Nitrogen Base without Amino Acids (Base for classifying yeasts based on amino acid and carbohydrate requirements, Difco), 0.3g aa mix without His, Trp, Leu, Ura (CSM-HIS-LEU-TRP-URA, BIO 101), 10g Bactoagar (Becton, Dickinson), appropriate amounts of lacked amino acids/uracil (see CS medium above), one pellet of NaOH, 400ml dH_2O, 50ml 1M K-phosphate pH7.0, 10g sucrose, 50ml H_2O, after autoclave at 55°C 1ml X-Gal (20mg dissolved in 1ml DMF) was added.

Cell cultures media

- **DMEM**; Invitrogen/Gibco.
- **Schneider's *Drosophila* Medium**; Invitrogen/Gibco.

Fly food

20l of water was cooked 2h with 160g thread agar. After2h 500g fresh baker yeast, 200g soja bean meal and 440g molasses were added and cooked another 2h. After 2h cooking 1.6kg malt extract, 1.6kg corn meal and 125ml of propionic acid, mixed and filled the vials. The vials with

the food were left to cool down for 2h at room temperature and closed by stoppers. Food in the vials was stored at 19ºC for no longer than 2 months.

Apple-agar plates for *Drosophila* eggs collection

In 3l of hot (90ºC) water 70g of Agar was dissolved. In parallel 100g of sucrose was dissolved in 1l apple juice. Both mixtures were mixed in 90ºC pre-warmed water bath, cool down to about 60ºC and filled into Petri dishes. The apple-agar plates were stored at 4ºC.

9. Bacterial strains

- *E.coli* **DH5-α** F^-, ø80d*lacZ*ΔM15, Δ(*lacZYA-argF*)U169, *deo*R, *recA*1, *endA*1, *hsdR*17(r_K^-, m_K^+), *phoA*, *supE*44, λ–, *thi*-1, *gyrA*96, *relA*1.
- *E.coli* **BL21(DE)** B, F^- , *dcm, ompT, hsd*S($r_B^- m_B^-$), *gal* λ (DE3). Contains the T7 RNA polymerase gene under control of the *lacUV5* promoter. The polymerase gene is integrated into the bacterial chromosome from λ (DE3).

10. Yeast strains

- EGY48: Mat α, *his3, leu2::op(lexA)4LEU2, trp1, ura3-52*
- RFY206: Mat a, *his3, leu2, trp1, ura3-52*

11. Animal cell strains used in the cell cultures

- HeLa cells, Invitrogen.
- *Drosophila* Schneider 2 (S2) cells, Invitrogen.

12. Fly stocks

If not noted otherwise, used fly stocks are as described in Flybase (http://flybase.bio.indiana.edu/) and are either part of the Großhans Lab stock collection (j.grosshans@zmbh.uni-heidelberg.de) or were obtained from the Bloomington Stock Center (http://flystocks.bio.indiana.edu).

- w ; ΔKG7 e ca /ΔKG19 e ca. Deletions of the *frs* locus were produced by mobilization of the transposon KG(3)0224. *white* revertants were selected for lethality over Df(3L)BK10 and breakpoints mapped by PCR. The transheterozygotic combination of two excisions (KG7/KG19) delete *frs* and the two proximal genes *gdl* and *Eip71CD* (Großhans et al., 2003).
- w ; Nup214{w+}/CyO, GFP{w+} ; HS-Frs[5]{w+}.

- w ; emb[2] b cn/CyO, GFP{w+}.
- w ; emb[2] b cn/CyO, GFP{w+} ; HS-frs[5]{w+}.
- w ; P{w+, UAS-Cdk2c-Myc$_6$}[III.1] (Meyer et al. 2000).
- yw ; HS-frs#5. (III)
- w ; +/+ ; LyDf(3L)Bk10 e /TM3, Sb hb-lacZ{ry+}.
- w ; frs-ΔCDS-frs+{w+}[6] ; LyDf(3L)Bk10 e /TM3, Sb hb-lacZ{ry+}.
- w ; frs-ΔCDS-frs86ASA{w+}[4] ; LyDf(3L)Bk10 e /TM3, Sb hb-lacZ{ry+}.
- w ; frs-ΔCDS-frs11AxxA{w+}[18.3] ; LyDf(3L)Bk10 e /TM3, Sb hb-lacZ{ry+}.
- w ; frs-ΔCDS-frs22A48A{w+} ; LyDf(3L)Bk10 e /TM3, Sb hb-lacZ{ry+}.
- C(3) se.
- w ; paired-Gal4{w+}. (III)
- w ; patched-Gal4. (II)
- w ; patched-Gal4, UAS-frs[J]. (II)
- w, MS1096-Gal4 ; UAS-GFP. (X, II)
- w, MS1096{w+}/FM6, B ; UAS-frs[C]{w+}/SM6B, Roi. (II)
- w ; Sp/CyO ; GMR-Gal4, UAS[I]/TM3, hb-lacZ. (III)
- w ; p{UAS-GFP, w+}. (II)
- w ; UAS-string [4]. (III)
- yw ; UAS-frs[C]. (II)
- w ; UAS-frs[D]. (II)
- yw ; UAS-frs[H]. (II)
- yw ; UAS-frs[I]. (III)
- w ; UAS-CycA{w+}. (II)
- w ; UAS-CycB{w+}. (II)
- w ; UAS-CycB3{w+}. (II)
- w ; UAS-CycE{w+}. (III)

13. PCR primer sequences

Primers PG2-PG25 were synthesized by Invitrogen (Karlsruhe, Germany), primers PG49-P58 and JG68-JG214 were synthesized by MWG Biotech AG (Ebersberg, Germany). **Restriction sites** are marked as bold, underlined sequence means start or stop codon, letter **bold and underlined** means mutated nucleotide, letter in parenthesis means original nucleotide.

PG2 - CG **GAA TTC** AAT GCC AAG ATG CTG CAG A

PG7 - CGA CAA CCT TGA TTG GAG

PG8 - GCC TGA CTG GCT GAA ATC

PG11 - CG **GAATTC** ATG GCT GGC AAG CGA CAA C

PG12 - GCC **CTCGAG** CTA GGA GTT CGT TCT GGC GCT C

PG13 - GG **GAATTC** ACG GCA CAA GCT CGT TCT C

PG14 - GCC **CTCGAG** CTA GAG AGA GAA GGG CGT GGC

PG15 - GG **GAATTC** GCG GAG GAG GAA AAA GAA GA

PG16 - GCC **CTCGAG** CTA CTT GAT GTG CTC CTT GAT

PG17 - ACGC **GTCGAC** GCT GGC AAG CGA CAA GCC

PG18 - CG **GGATCC** CTT GAT GTG CTC CTT GAT CTT

PG25 - CG **GAATTC** ATG TAT TTC CGG GAG AGC GAG AA

PG49 - CCG **CTCGAG** CTA AGT GTC TCT ATT GTA CTT TTC C

PG55 - CCG **GAA TTC** ATG ATT AAC ATG CGG ACG CC

PG56 - CCG **CTC GAG** TCA GGG ATT GCT TCT ACT GC

PG57 - CTG AAA ATC GTG GAA **G(A)**CC CCA AAG GAG CAG C

PG58 - G CTG CTC CTT TGG GG**C(T)** TTC CAC GAT TTT CAG

JG68 - ACA **CTC GAG** TCA GCC CAT GTC CAC ATC C

JG70 - GG **GAA TTC** AGT AGC AAA TCA GCA ACG TCA

JG71 - GG **CTC GAG** AAG GCG CGG AAA GTA AAA TGT

JG95 - GG **GAA TTC** ATG TCG TCG ACC AAT GAA ACC

JG96 - GG **GGA TCC** ATG TCG TCG ACC AAT GAA ACC

JG100 - GG **CCATG GG**A TCG TCG ACC AAT GAA ACC AAC

JG107 - GTA ATA CGA CTC ACT ATA G

JG116 - GG **CCA TGG** GA TCG TCG ACC AAT GAA ACC AAC

JG117 - GG **GGA TCC** GAA GTT CAG AGA TTT GCG AGC

JG141 - GG **AGA TCT** AAT AAC TGC TAG GCT GGC TGA

JG147 - GG **AGA TCT** ATA **GCT AGC** TCA TAA TAC GAA CCG ATG TAA TC

JG182 - GA **AGA TCT** ATG TCG TCG ACC AAT GAA ACC

JG183 - GC **TCT AGA** TTA GAA GTT CAG AGA TTT GCG AG

JG185 - TTC ATC AAG GCT CGC **GC(AA)**A TCT **GC(TT)**G AAC TTC TAA TCA TAA

JG186 - TTA TGA TTA GAA GTT C**GC(AA)** AGA T**GC(TT)** GCG AGC CTT GAT GAA

JG196 - GAA ACC AAC CAA GTG **GC(CT)**G CAG CGC **GC(CT)**G AAC AGC CTG AAA ATC

JG197 - GAT TTT CAG GCT GTT C**(AG)GC** GCG CTG C**(AG)GC** CAC TTG GTT GGT TTC

JG209 - ATT AGC CAC AAT **GC(AT)**G CGC TCC ATC **GC(CT)**T ATT GAT **GC(TG)**G CTG GTT GAG GTT

JG210 - CTC CTC AAC CAG C**GC(CA)** ATC AAT A**GC(AG)** GAT GGA GCG C**GC(AT)** ATT GTG GCT AAT

JG211 - TCC CTG GTA CCA GCC **G(A)**CC CCC AGC AGC TCA GGA

JG212 - TCC TGA GCT GCT GGG GG**C(T)** GGC TGG CAT CAG GGA

JG213 - GCG **CC ATG G**AT ATC AGC GTG GGC ACT G

JG214 - GG **AGA TCT** TTA AAA CTT ATA AAA CAA ATT CAC G

14. Constructs

DNA was amplified by vent DNA polymerase (New England Biolabs) with primers introducing suitable restriction sites. The purified and digested PCR products were cloned into specified plasmids and sequenced. Site-directed mutations were produced by inverse PCR with appropriate oligonucleotides and Pfu DNA polymerase (Stratagene). Mutagenised clones were selected by DpnI (Roche) digest. The region of interest of the mutagenised plasmids was sequenced and recloned into a new plasmid.

Table 1. List of constructs used in this study.

Construct	Primer pair	UTR	cloning scheme
pCS2-frs	JG70(EcoRI)/JG71(XhoI)	5'-3'	PCR with P1 DS08110, cloned into pCS2 EcoRI/XhoI (Großhans et al. 2003).
pCS2-frs86ASA	JG185/JG186	-	Mutagenesis of pCS-frs. Großhans J.
pCS2-frs11AxxA	JG196/JG197	-	Mutagenesis of pCS-frs. Großhans J.
pCS2-frs48A	JG211/JG212	-	Mutagenesis of pCS-frs. Großhans J.
pFus-frs	JG100/unknown	3'	PCR with pCS2-frs cloned into pFus NcoI/XhoI. Großhans J.
pMCS1-His_{10}-GFP-frs	-	3'	frs NcoI/XhoI cleaved from pFus-frs and cloned into pMCS-His_{10}-GFP NcoI/SalI. Gawliński P.
pMK26/ACTSV40BS-frs-GFP	-	-	frs-GFP HindIII/XbaI cleaved from pCS2-frs-GFP and cloned into pMK26 HindIII/EcoRV. Gawliński P.
pCS2-frs-GFP	-	5'-3'	GFP SpeI/NheI (PCR Lecuit T.) into pCS2-frs SpeI. Großhans J.
pCS2-nup50	-	-	pJG4-5-nup50 EcoRI cloned into pCS2 EcoRI/SAP. Gawliński P.
pLex-frs	JG95(EcoRI)/JG71(XhoI)	3'	PCR with pCS-frs cloned into pEG202 EcoRI/XhoI. Großhans J.
pLex-frs86ASA	JG95(EcoRI)/JG71(XhoI)	3'	PCR with pCS-frs86ASA cloned into pEG202 EcoRI/XhoI. Großhans J.
pLex-frs11AxxA	JG95(EcoRI)/JG71(XhoI)	3'	PCR with pCS-frs11AxxA cloned into pEG202 EcoRI/XhoI. Großhans J.
pLex-trblΔ124	PG2(EcoRI)/JG68(XhoI)	-	PCR with pCS-trbl cloned into pEG202 EcoRI/XhoI. Gawliński P.
pJG4-5-nup50	-	-	Found in frs Y2H ovarian screen. Contains additional EcoRI site at the C-terminus behind ORF. Gawliński P.
pJG4-5-nup50/ IABM (1-246)	PG11(EcoRI)/PG12(XhoI)	-	PCR with pJG4-5-nup50 cloned into pJG4-5 EcoRI/XhoI. Gawliński P.
pJG4-5-nup50/FG repeats (251-423)	PG13(EcoRI)/PG14(XhoI)	-	PCR with pJG4-5-nup50 cloned into pJG4-5 EcoRI/XhoI. Gawliński P
pJG4-5-nup50/ IABM+FG (1-423)	PG11(EcoRI)/PG14(XhoI)	-	PCR with pJG4-5-nup50 cloned into pJG4-5 EcoRI/XhoI. Gawliński P.
pJG4-5-nup50/ RanBD (436-564)	PG15(EcoRI)/PG16(XhoI)	-	PCR with pJG4-5-nup50 cloned into pJG4-5 EcoRI/XhoI. Gawliński P.
pQE80-ZZ-tev-frs-His_6	JG116(NcoI+ATG G)/JG117(BamHI)	-	PCR with pCS-frs cloned into pQE80-ZZ-tev-His_6 NcoI/BamHI. Großhans J.
pQE30-frs	JG96(BamHI)/JG71(XhoI)	3’	PCR with pCS-frs as BamHI/XhoI cloned into pQE30 BamHI/SalI. Gawliński P.
pQE80-His_{10}-ZZ-tev-frs	-	3’	frs BamHI/HindIII cleaved from pQE30-frs and cloned into pQE80-His_{10}-ZZ BamHI/HindIII. Großhans J.
pQE80-ZZ-tev-	PG17(SalI)/PG18(BamHI)	-	PCR with pJG4-5-nup50 cloned into pQE80-His_{10}-

nup50-His_6			ZZ-tev SalI/BamHI. Gawliński P.
pGEX-frs	JG95(EcoRI)/JG71(XhoI)	3'	PCR with pCS-frs cloned into pGEX4T-1 EcoRI/XhoI. Großhans J.
pGEX-frsASA	JG95(EcoRI)/JG71(XhoI)	3'	PCR with pCS-frsASA cloned into pGEX4T-1 EcoRI/XhoI. Großhans J.
pGEX-frs11AxxA	JG95(EcoRI)/JG71(XhoI)	3'	PCR with pCS-frs11AxxA cloned into pGEX4T-1 EcoRI/XhoI. Großhans J.
pGEX-frs48A	JG95(EcoRI)/JG71(XhoI)	3'	PCR with pCS-frs48A cloned into pGEX4T-1 EcoRI/XhoI. Großhans J.
pGEX-frs22A48A	PG57/PG58	3'	Site directed mutagenesis of pGEX-frs48A. Gawliński P.
pQE-CycAΔN170	JG213(NcoI)/JG214 (BglII)	-	PCR with pSP64 HA-CycA cloned into pQE80N60 NcoI/BglII. Großhans J.
pCS2-CycA(210-440)	PG25(EcoRI)/PG49(XhoI)	-	PCR with pSP64 HA-CycA cloned into pCS2 EcoRI/XhoI. Gawliński P.
pGEX-thrombin-tev-CycAΔN170	-	-	CycAΔN170 NcoI/BglII from pQE-CycAΔN170 cloned into pGEX4T-1-thrombin-tev NcoI/BamHI. Gawliński P.
pGEX-thrombin-tev-CycEΔN300	PG55(EcoRI)/PG56(XhoI)	-	PCR with pSP64- CycE cloned into pGEX4T-1-thrombin-tev EcoRI/XhoI. Gawliński P.
pSP-CycA-AAA	JG209/JG210	-	Mutagenesis of pSP64-CycA, M235L239W242 to AAA. Großhans J.
pBKS-frsΔCDS	JG141(BglII)/JG147(BglII, NheI)	5'-3'	Inverse PCR with pBKS-frs-3'HSP70. Genomic fragment of frs without the coding sequence. Großhans J.
pBKS-frsΔCDS-frs^+	JG182(BglII)/JG183(XbaI)	5'-3'	PCR with pCS-frs cloned as BglII/XbaI into pBKS-frsΔCDS BglII/NheI. Großhans J.
pBKS-frsΔCDS -frs86ASA	JG107/JG182(BglII)	5'-3'	PCR with pCS-frs86ASA XbaI/BglII and cloned into pBKS-frsΔCDS BglII/NheI. Großhans J.
pBKS-frsΔCDS -frs11AxxA	JG182(BglII)/JG183(XbaI)	5'-3'	PCR with pCS-frs11AxxA BglII/XbaI and cloned into pBKS-frsΔCDS BglII/NheI. Großhans J.
pBKS-frsΔCDS -frs22A48A	JG182(BglII)/JG183(XbaI)	5'-3'	PCR with pGST-frs22A48A BglII/XbaI and cloned into pBKS-frsΔCDS BglII/NheI. Gawliński P.
pCasper-HS-frs	-	5'	frs (cDNA) as EcoRI/XhoI from pCS-frs into pCasper-HS EcoRI/XhoI. Großhans J.
pCasper-frs^+	-	5'-3'	Cloned from pBKS-frsΔCDS+frs^+ XbaI/XhoI into pCasper4 XhoI/XbaI. Großhans J.
pCasper-frs86ASA	-	5'-3'	Cloned from pBKS-frsΔCDS-frs86ASA XhoI/XbaI into pCasper4 XhoI/XhoI. Großhans J.
pCasper-frs11AxxA	-	5'-3'	Cloned from pBKS-frsΔCDS-frs11AxxA XbaI/XhoI into pCasper4 XbaI/XhoI. Großhans J.
pCasper-frs22A48A	-	5'-3'	Cloned from pBKS-frsΔCDS-frs22A48A XbaI/XhoI into pCasper4 XbaI/XhoI. Gawliński P.

Table 2. List of provided constructs.

Construct	**Origin**
pLex-pelle	Großhans et al., Nature 372: 563-566 (1994).
pCS-pelle	Großhans et al., Mech Dev. 81: 127-38 (1999).
pLex-dynein light chain	Schnorrer et al., Nat Cell Biol. 2: 185-90 (2000).
pLex-exuperantia	Großhans J. (unpublished data).
pLex-cactus	Großhans et al., Nature 372: 563-566 (1994).
pJG4-5-dorsal	Großhans et al., Nature 372: 563-566 (1994).
pBKS-frs-3'HSP70	Großhans et al., Dev Cell 5: 285-294 (2003).
pCS-frs	Großhans et al., Dev Cell 5: 285-294 (2003).
LaminDmO His_6-L(1-179)	Stuurman. FEBS Lett. 401: 171-174 (1997).
pQE-His_{10}-ZZ-huCdk2 CAK	Görlich D. (unpublished data).

pSP64 HA-CycA	Kaspar et al., Curr Biol. 11: 685-690 (2001).
pMK033 CycA(1-170)	Kaspar et al., Curr Biol. 11: 685-690 (2001).
pTS004 CycA(171-491)	Kaspar et al., Curr Biol. 11: 685-690 (2001).
pSP64 HA-CycB	Foley et al., Curr Biol. 11: 151-160 (2001).
pNB40 CycB3	Lehner C. (unpublished data).
pSP-CycE	Sprenger F. (unpublished data).
pSP64 Cdk1	Sprenger F. (unpublished data).
pGEX-huRb(379-928)	Kaelin et al. Cell 64: 521-532 (1991).
pQE-His_{10}-ZZ-huCycA1	Görlich D. (unpublished data).
pQE-His_{10}-ZZ-huCycB1	Görlich D. (unpublished data).

15. Chromatography

- Glutathione Sepharose 4B (Pharmacia Biotech).
- HisTrap HP affinity columns (Amersham).
- IgG Sepharose 6 Fast Flow (Pharmacia Biotech).
- ProteinA Sepharose CL-4B (Pharmacia Biotech).
- CNBr activated Sepharose 4B (Amersham Pharmacia Biotech).
- Superdex200 10/300GL (Pharmacia Biotech).
- Thiopropyl-activated Sepharose 6B (Sigma)

16. Kits for the molecular biology

- TNT SP6 Coupled Reticulocyte Lysate System (Promega, USA).
- VECTASTAIN Elite PK-6100 ABC kit (Vector Laboratories, Inc., USA).
- DAB substrate kit for peroxidase (Vector Laboratories, Inc., USA).
- ECL plus Western Blotting Detection System (Amersham Biosciences).
- QIAGEN Plasmid Midi Kit (QIAGEN GmbH, Germany).
- Effectene Transfection Reagent kit (QIAGEN GmbH, Germany).

17. Equipment

Microscopy:	Leica, Zeiss, Olympus.
PCR:	PTC-200 Peltier Thermal Cycler (MJ Research)
Western blot:	Trans-blot SD Semi-Dry Transfer Cell (BIO-RAD)
Radiography materials:	Kodak X-OMAT AR film, XAR-5, size 13x18 cm
	Fuji Medical X-Ray film, size 13x18 cm
	Imaging plate BAS-MS 2040 (Fujifilm)
Radiography registrator:	FUJIFILM FLA-3000. Image Reader V1.8E program.
Sonicator:	Cell Disruptor B15 Sonifier, BRANSON
Micro fluidizer	EmulsiFlex-C5, Avestin (Ottawa, Canada)

Agarose gel registrator:	Raytest IDA (Image Documentation & Analysis)
Video copy processor:	Mitsubishi P91
Electroporator:	Gene Pulser™, BIO-RAD
Protein purifier	Ächta prime, Amersham Pharmacia Biotech
Protein condensator	Vivaspin500 (10 kDa MWCO), Vivascience Satorius.
Glass needle maker	Marishige PN-30 (Japan).
Incubators:	Kuener Switzerland ISF-1-W
	Kuener Switzerland ISF-1-V

Methods

1. Standard methods in molecular biology

All standard methods of molecular biology that are not described in detail in this chapter were done according to Sambrook et al. 1998.

2. Isolation of DNA from yeast cells

Saturated overnight yeast culture was collected in 1.5 ml tube and dissolved in the extraction buffer (Materials). Lysate was extracted with phenol/chloroform/i-Amylalcohol (25:24:1) solution in the presence of glass beads (about 20µg/reaction, 0.45-0.5mm, B. Braun Melsungen AG, autoclaved) on the vortex. After centrifugation (10min, 13000rpm) the aqueous phase was transferred to a new tube with 100% ethanol and precipitated 30min at -20ºC. Centrifuged white DNA pellet was washed with 70% ethanol, dried with speed-vac and dissolved in 1x TE buffer (Materials).

3. Polymerase Chain Reaction (PCR)

For the molecular cloning the amplification reactions were done using Vent DNA Polymerase (New England Biolabs) or Pfu DNA polymerase (Stratagene). For standard PCR reaction the following reagents were mixed in a thin-wall PCR tubes: 50-200ng template, 0.4µM forward and reverse primers, 50µM dNTP (each), 10x standard PCR buffer (polymerase dependent), 1-2 units (per 50µl of the reaction) Vent or Pfu polymerase. The PCR reactions were done using the following conditions:

Step 1 (initial denaturation): 94°C for 2min
Step 2 (denaturation): 94°C for 30sec
Step 3 (annealing): 50-60°C for 1min
Step 4 (elongation): 72°C for 1min per kb to be amplified
Step 5: repetition of steps 2-4 for 20-35 times
Step 6 (final elongation): 72°C for 5-10min

4. Error-prone Polymerase Chain Reaction

To generate the library of *frühstart* mutants, the error-prone PCR was done. PCR reaction was performed in the presence of special error-prone PCR buffer.

1x reaction mix:

- 10x Error-prone PCR buffer (Materials)
- 10% DMSO (for GC rich template regions)
- 0.3mM $MnCl_2$
- 100pM of each primer (JG95 and JG71)
- 10ng template (pCS2-*frs* for 0.1ml reaction volume)
- 25mM dNTP's mix
- 5u *Taq* DNA Polymerase (for 0.1ml reaction volume)
- ddH_20

To prevent over-representation of a single mutation in all clones of the library the PCR reaction mix was split into four aliquots (100µl was split into 4 PCR tubes - 25µl each).

PCR program:

Step 1 (denaturation): 94°C for 30sec
Step 2 (annealing): 56°C for 1min
Step 3 (elongation): 72°C for 40sec
Step 4: repetition of steps 1-3 for 30 times
Step 5 (final elongation): 72°C for 5min

5. DNA sequencing

All DNA sequencing was done in cooperation with Sequence Laboratories Göttingen GmbH, Hannah-Vogt-Strasse 1, D-37085 Göttingen, Germany. Tel.:0551-3700010, Fax:0551-3700012, e-mail: Bio-Service@SEQLAB.de, web page: http://www.SEQLAB.de. Sequencing samples were prepared according to the company instructions.

6. 2-Nitrophenyl-β-galactopyranoside (ONPG) test

From saturated overnight yeast cultures in CS glucose (-His, +Leu, -Trp, -Ura) medium, the fresh cultures were inoculated in CS galactose (-His, +Leu, -Trp, -Ura) medium to OD_{600}=0.15-0.3 density. When the cultures reached OD_{600}=0.5-0.7 the cells were briefly centrifuged and 1ml of Z-Buffer (Materials) added. 800µl of the yeast cells suspensions were transformed into new vials. To each of the vials one drop of 0.1% SDS and two drops of chloroform were added. To open the cells all vials were 30sec vortex. Next step was 10 min preincubation at 30ºC. After preincubation time to all of the vials 200µl of 2-Nitrophenyl-beta-galactopyranoside (4mg/ml in

Z-Buffer) were added. After few seconds or minutes (time depends from the interaction between tested proteins. The color appears if the interaction takes place, important is also how the interaction is strong, if stronger, the yellow color is more intensive) the reaction mixtures become yellow. To stop the reactions 0.5ml of 1M Na_2CO_3 were added, then reaction mixtures were centrifuged and supernatants measured at OD_{420}. The β-galactosidase activity was calculated from the pattern:

$$n = 1000 \cdot \frac{A_{420}}{OD_{600} \cdot t \cdot Volume}$$

Where:

n – units of ONPG activity

A_{420} – Absorption of the yellow reaction product at wavelength 420

OD_{600} – optical density of the measured yeast culture

t – reaction time

Volume – volume of measured sample

For each investigated protein pair the experiment was repeated three times and the results were summarized and averaged.

7. Protein expression and purification

GST and GST-frs expression was induced for 4h, 0.1mM IPTG, 37°C. GST proteins were isolated by chromatography of the cleared, ultra-centrifuged lysate (PBS, 150mM NaCl and 1mM DTT) with 1ml GSH Sepharose columns (Amersham) and eluted with 50mM Tris/HCl pH8.0, 50mM NaCl, 1mM DTT, 10mM glutathione. GST-Rb protein expression was induced for 6h at 18°C and purified as the other GST proteins. Purification and thrombin cleavage of GST-thrombin-tev-CycA ΔN170 and GST-tev-CycE ΔN300 proteins are precisely described in the Surface Plasmon Resonance part of the Methods chapter. Two-steps purification of His_{10}-GFP-Frs protein is described in detail in the *In vitro* GFP-Frs nuclear export assay in permeabilized HeLa cells part of the methods chapter. His-tagged proteins were expressed by 0.1M IPTG for 4h, 37°C, purified from the cleared lysate (20mM Na-phosphate pH8.0, 500mM NaCl, 20mM imidazol) by chromatography with Ni-NTA sepharose (Amersham) and eluted with 20mM Na-phosphate pH8.0, 500mM NaCl, 250mM imidazol. The His_{10}-ZZ-huCdk2 protein was expressed from a bicistronic plasmid with CAK kinase for 6h at 18°C, 0.1mM

IPTG. Protein concentrations were determined by Bradford assay (Sigma). Proteins were stored in 10% gycerol at -70°C.

8. Antibody staining of embryos and tissues

Dechorionated embryos by bleach (50-100%), dissected guts or larval and pupal discs were fixed with 4% formaldehyde 30min on the shaker (100-200rpm). Subsequently fixed embryos and tissues were briefly washed 3x with PBST and 1x with PBST 5min on the rotating wheel. After washing, the embryos and tissues were blocked in PBST with 5% BSA 1h on the rotating wheel, then washed once with PBST and incubated 2h at room temperature or overnight at 4ºC with primary antibodies. After incubation with the primary antibodies the embryos and tissues were washed with PBST 3x briefly and 4x 15min on the rotating wheel and incubated with secondary antibodies for 2h at room temperature or overnight at 4ºC. After subsequent washing procedure (3x briefly and 4x 15min with PBST) and optional immunochemicals staining (Phalloidin and DAPI) samples were mounted in Aquapolymount (Polyscience) and analysed by a confocal microscopy.

The following concentrations of antibodies and immunochemicals were used in the results and appendix sections of this work: primary antibodies - 1µg/ml Frs, 0.1µg/ml Nup50, 0.2µg/ml γ-tubulin, 0.5µg/ml pHistone3, 4µg/ml BrdU, 0.2µg/ml β-galactosidase, 0.5µg/ml Dlg, 4µg/ml of secondary antibodies labelled with Alexa dyes, 0.2 µg/ml DAPI, 6nM phalloidin coupled with Alexa dyes (Molecular Probes).

9. Estimation of the Frühstart concentration in the embryo

To estimate Frs concentration in the embryo three different amounts of recombinant His_{10}-ZZ-Frs (0.1, 1 and 10ng) protein and total extract from precisely staged wild-type embryos (20, 50, and 100 embryos at mid-cellularisation stage) were compared. As a negative control total extract of 20 embryos deficient for *frs* (w;ΔKG7 e ca/ΔKG19 e ca) was used. Embryos were collected from apple-juice agar plates under the binocular to estimate the right stage of them. To about 200 properly staged embryos SDS-PAGE sample buffer (Materials) was added to reach ~10 embryo/µl concentration. The samples were analysed by 12% SDS-PAGE electrophoresis and western blot with Frühstart polyclonal antibodies (1:2000) under standard conditions.

10. Yeast-Two-Hybrid *frühstart* ovarian library screen

All yeast procedures and experiments were done according to Russell L. Finley Jr. and Roger Brent "Gene Probes – A practical Approach" 1995, unless otherwise mentioned. Y2H *frs* ovarian screen was made in EGY48 yeast strain (Materials).

cDNA library *ovoIb* from ovarian RNA used in the screen was kindly provided by Dr. Jörg Großhans. The RNA was extracted from ovaries of *Drosophila melanogaster* (OregonR) wild-type flies and isolated by extraction with guanidinium thiocyanate, followed by CsCl ultracentrifugation and fractionation with OligodT cellulose (Großhans et al. 1999). The cDNAs with EcoRI and XhoI sites at their ends were ligated into linearised vector pJG4-5 (containing LexA activating domain and TRP1 rescue gene). The complexity of this library is about 4mln clones with about 0.9mg /ml DNA concentration.

The yeast strain EGY48 was first transformed with two plasmids, pSH18-34 (containing LexA binding place fused with LacZ, and URA3 rescue gene) and pLex-*frs* (containing fragment of LexA protein responsible for binding to the promoter region of β-galactosidase fused with full-length *frühstart,* and HIS3 rescue gene). Such transformed EGY48/18-34/Lex-*frs* strain was grown in 50 ml of the CS glucose (-His, +Leu, +Trp, -Ura) medium at 30ºC on a shaker at 200rpm until OD_{600} reached 0.6 (start OD_{600}=0.2 inoculated always from a fresh saturated overnight culture), then spin 2000rpm 3min, dissolved in 25ml sterile ddH_2O and centrifuged again. Pellet was dissolved in 1ml 100mM Lithium acetate/TE buffer (Materials), transferred into 1.5ml tube, centrifuged again and dissolved in 60µl 100mM Lithium acetate/TE buffer. Dissolved cells suspension was split into five tubes (10µl/transformation). To such prepared yeast cells fallowing ingredients were carefully added:

- 300µl Lithium acetate/TE/PEG buffer
- 50µl career Salmon sperm ss-DNA (stock 2mg/ml, Stratagene)
- 1µl ovarian pJG5-5 library DNA (stock 1mg/ml)

Subsequently the transformation mixtures were incubated in a water bath 30min at 30ºC and heat shocked in the other water bath 15min at 42ºC. After heat shock from a random vial as a control 35µl of the transformation mixture was taken and separately plated on the CS glucose (-His, +Leu, -Trp, -Ura) agar plate to test a transformation efficiency of the experiment that usually was about 8x 10^5 transformants per one vial (what gave in all five transformation reactions about 4x 10^6 transformants). Because in the yeast cells Lex-*frs* (bait) fusion protein is constitutively expressed whereas expression of the library clones (preys) from the pJG4-5 vectors is induced by galactose, the rest of the transformation mixtures were plated on the CS galactose (-His, -Leu, -Trp, -Ura) medium plates. The transformation plates were incubated at

30ºC for 4-6 days. After recovering time, all positive (growing) clones were transferred into a new CS galactose (-His, -Leu, -Trp, -Ura) plate and named by numbers.

To retest achieved clones for Frs interaction a LacZ (β-Gal activity) assay was done. All positive clones found in the screen were put on the CS glucose (-His, +Leu, -Trp, -Ura) plates and after 4-5 days transferred (by the stamp covered with a sterile velvet) on four indicator plates:

- CS glucose + **X-Gal** (-His, +Leu, -Trp, -Ura) – LacZ activity test
- CS galactose + **X-Gal** (-His, +Leu, -Trp, -Ura) – LacZ activity test
- CS glucose (-His, **-Leu**, -Trp, -Ura) – minus leucine growing test
- CS galactose (-His, **-Leu**, -Trp, -Ura) – minus leucine growing test

β-Gal assay reconfirm Frs-interacting clones found in the screen and uncovered four false positive (e.g. growing on the CS galactose -Leu plate but no LacZ activation was observed) that were removed from the clone collection. All positive clones found in Y2H ovarian library screen were amplified from total yeast DNA extract by PCR and sequenced. All PCR fragments were amplified from pJG4-5 vector by vent polymerase (NEB) and two primers, PG8 (sense) and PG7 (anti-sense).

11. Yeast-Two-Hybrid *frühstart** mutants library screen

To generate *frs** mutants library the coding sequence of *frs* (pCS2-*frs*) was amplified by error-prone PCR with Taq polymerase and cloned into pEG202 as EcoRI/XhoI. Error-prone PCR resulted in more than one mutation per 500bp. Full-length Nup50 (pJG4-5, EcoRI/XhoI) and CyclinEΔN319 (pJG4-5 EcoR/XhoI) were used as baits proteins. The *frs** library was transformed into EGY48/pSH18-34 strain and all clones were plated into CS glucose -His, +Leu, +Trp, -Ura plates and numbered. In parallel RFY206/pSH18-34 strain was transformed with pJG4-5-Nup50 and pJG4-5-CyclinEΔN319 separately and uniformly plated on the CS glucose +His, +Leu, -Trp, -Ura plates. By the stamp covered with a sterile velvet EGY48 *frs** clones were transferred from the master plates into RFY206/pSH18-34/pJGNup50 and RFY206 CyclinEΔN319 plates and subsequently on the YPD plates for 2 days 30ºC for mating. All diploid clones were tested for LEU2 and lacZ reporter genes activation on the CS galactose -His, -Leu, -Trp, -Ura plates. The *frs** clones that interact with Nup50 and do not interact with CyclinEΔN319 and the clones that interact with CyclinEΔN319 and do not interact with Nup50 were further analysed. The *frs** clones of interest were amplified by PCR and sequenced by JG95 (sense) and JG71 (anti-sense) primers.

12. *In situ* hybridization of *nup50* gene

To synthesize anti-sense RNA of *nup50* the pCS2-*nup50* construct was linearised by HindIII under standard conditions. The labeling mixture was prepared as fallowing:

- 1µl DNA (linearised 1µg)
- 2µl 10x NTP+Dig labelling mix
- 2µl 10x transcription buffer
- 2µl RNA polymerase (40U of SP6)
- 1µl RNase inhibitor (20U)
- 12µl ddDEPC water

Labeling mixtures were incubated 2h at 37°C, and subsequently 15min at 37°C with 2µl DNaseI (RNase free). RNA reaction mixture was precipitated with 1:10 volume of 3M Natrium acetate and 2.5 volume of 100% ethanol at -20°C at least for 30min, then pellet (10min, 13000rpm), washed once with 70% ethanol (DEPC) and dry. Dry pellet was dissolved in 20µl DEPC water and store -20°C. The RNA concentration reached 1mg/ml. 2µl of such prepared probe (2µg) was mixed with 1µl of tRNA (50mg/ml) and 20µl DEPC water, boiled 4min at 100°C and rapidly cooled down in ice water. 200µl of hybridization solution was added to the reaction mixture. The wild-type embryos were dechorionated in 50% bleach, fixed for 30min in heptain/4% formaldehyde in PBS and pop in methanol. Fixed embryos were transferred in PBST, rinsed 3x and washed 2x 5min. Washed embryos were incubated 10min in 1:1 hybridization solution/PBST, then 10min in hybridization solution at room temperature. In the next step the embryos were pre-hybridized in hybridization solution for 1h at 57°C. After 1h incubation appropriate anti-sense probes were added to the embryos and over night incubation at 57°C followed. Such once used probe can be reused several times. After over night incubation the embryos were rinsed 3x with pre-warmed hybridization solution, and then washed 3x30min in hybridization solution at 57°C. In the next steps the embryos were washed: 10min 4:1 hybridization solution/PBST at 57°C, 10min 3:2 hybridization solution/PBST at 57°C, 10min 2:3 hybridization solution/PBST at 57°C, 10min 1:4 hybridization solution/PBST at room temperature. To reduce the background and block unspecific epitopes the embryos were washed 2x20min in PBST with 1% BSA at room temperature and washed 1x with PBST in the end. To such prepared embryos a digoxigenin antibody coupled with alkaline phosphatase (Boehringer, Fab fragments) at 1:2000 in PBST were added and incubated for about 2h at room temperature (optionally overnight at 4°C). After incubation time the embryos were rinsed 3x with PBST and washed 4x 15min in PBST. Then the embryos were washed 3x

5min with AP buffer. The reaction was initiated by adding to 1ml of AP buffer 4.5µl NBT (Nitro-blue tetrazolium chloride, 50mg/ml) and 3.5µl BCIP (5-bromo-4-chloro-3'-indolyphosphate p-toluidine salt, 50mg/ml). The incubation time may vary from few minutes to 3h or even over night and the reaction should be kept in the darkness. To stop the developing reaction the embryos were rinsed 4x with PBST, washed 1x 1:1 ethanol/PBST and washed 1x10min with 100% ethanol. Finally the embryos were rinsed 1x 1:1 ethanol/PBST, washed 1x with PBST 10min and mounted in aquapolymount.

digoxigenin antibody: (stored at 4°C) *a*-Dig-AP (alkaline phosphatase, Fab fragments, Roche 1093274): preadsorbed on wt embryos at 1:10, stored at 4°C with 0.02% Natrium azide (NaN_3).

NTP+Dig labelling mix (10x) Dig-11-UTP: 10mM solution (25 µl, Roche #1209256) -10mM ATP, 10mM GTP, 10mM CTP, 6.5mM UTP, 3.5mM Dig-11-UTP, pH7.5.

transcription buffer (10x) for SP6, T3, T7 RNA polymerase, store at -20°C: 400mM Tris-HCl, pH 8.0, 60mM MgCl2, 100mM DTT, 20mM spermidine, 100mM NaCl.

DEPC treatment: 2ml diethyl pyrocarbonate per 1 l of water/solution incubated at 37°C overnight and autoclaved.

NBT/BCIP: NBT (nitro-blue tetrazolium, Sigma), 75 mg/ml in 70% DMF, BCIP (5-bromo-4-chloro-3'-indolyphosphate p-toluidine salt, Sigma), 50 mg/ml in DM, stored at -20°C.

Hybridization solution: stored at -20°C (else formamide hydrolyses): 25% formamide, 5x SSC, 50µg/ml heparin, 0.2% Tween, 100µg/ml tRNA, DEPC water.

AP buffer (AP buffer forms a precipitate after some time): 100mM Tris pH9.5, 100mM NaCl, 50mM MgCl2, 0.2% Tween, ddDEPC water.

13. Polyclonal antibodies against DmNup50 protein

To raise polyclonal antibodies against *Drosophila melanogaster* Nup50 a full-length ZZ-Nup50-His_6 fusion protein was used. ZZ-Nup50-His_6 was *E. coli* expressed and purified under native conditions. A rabbit was injected four times, each time with 550µg of the protein. Before first injection preimmune serum was taken as a negative control. Injection mixture was prepared as following:

First injection:

- 550µl of ZZ-Nup50-His_6 (1mg/ml=0.55mg)
- 550µl of Freund's adjuvants incomplete
- 30µg dipeptide N-muramyl-alanyl-isoglutamin (Sigma)

Each next injection:

- 550µl of ZZ-Nup50-His_6 (1mg/ml=0.55mg)
- 550µl of Freund's adjuvants complete
- 30µg dipeptide N-muramyl-alanyl-isoglutamin (Sigma)

Between one and another injection were always 4 weeks break for immunoresponse of the rabbit. Before each next injection a blood sample was taken and immunoresponse was tested by western blot analysis with embryonic total protein extract (0-4h wild-type collection). The antibodies were additionally affinity purified from the serum with CNBr-activated Sepharose 4 B (Amersham, Pharmacia Biotech). 6mg ZZ-Nup50-His_6 protein was dissolved in coupling buffer (Materials). 1ml of CNBr-activated Sepharose was activated by 15min 1mM HCl incubation, washed with 100ml 1mM HCl, subsequently washed with coupling buffer (50ml), mixed with ZZ-Nup50-His_6 protein and incubated at 4ºC degrees over-night. CNBr sepharose beads coupled with ZZ-Nup50-His_6 were blocked by 2h RT incubation with acetate buffer pH4.0 (Materials), loaded onto the column and washed with 5 cycles of low (acetate) and high (coupling) pH buffers. Before use, the column was equilibrated with 5 volumes of PBS. The 5ml of serum was ultra-centrifuged 30min, 40k at 4ºC degrees and loaded on the column (0.2ml/min). The column was washed with 20 volumes of PBS+0.3M NaCl and the antibodies were eluted with 4M $MgCl_2$ pH3.5. Collected fractions were immediately neutralized with 1M Na-phosphate pH.8.0 and dialyzed with PBS. The protein concentration was measured with A=280 (1mg/ml=1.36) and reached 1mg/ml. The activity of the antibodies was tested in *Drosophila* embryo staining (Ab concentration 1:10000) and western blot analysis (Ab concentration 1:40000).

14. Polyclonal antibodies against C-terminus of DmCdk1 protein

Polyclonal antibodies against peptide corresponding to the C-termini of the *Drosophila* cdc2 (cdk1) kinase (CILEHPYFNGFQSGLVRN) were done with Imject Maleimide Activated Keyhole Limpet Hemocyanin (PIERCE Biotechnology). The peptide was synthesized at Peptide Specialty Laboratories GmbH, Heidelberg (www.peptid.de) and delivered in

powder form. 10mg peptide was hardly dissolved in the 0.7ml of PBS and 0.9ml of DMSO that gives 60% DMSO final concentration. Dissolved peptide ended with $CONH_2$ group (CILEHPYFNGFQSGLVRN- $CONH_2$) was covalently coupled with KLH protein by cross-linking cysteine residues with Sulfo-SMCC linker. The injection mixture with KLH conjugate was prepared as following:

First injection:

- 250µl of KLH-peptide (4mg/ml=1mg)
- 250µl of Freund's adjuvants incomplete
- 30µg dipeptide N-muramyl-alanyl-isoglutamin (Sigma)

Second, third and fourth injections:

- 250µl of KLH-prptide (4mg/ml=1mg)
- 250µl of Freund's adjuvants complete
- 30µg dipeptide N-muramyl-alanyl-isoglutamin (Sigma)

Between injections there always was a 4 weeks break for immunoresponse of the rabbit. Before each next injection a sample of the blood was taken and immunoresponse was tested by western blot analysis with embryonic total protein extract (0-4h wild-type collection). The antibodies were not affinity purified and were used in all experiments as a plain serum. Similarly raised antibodies were already published by Knoblich et al. 1994.

15. Immunoprecipitation of Frs from embryonic lysate

To immunoprecipitate Frs protein complex from *Drosophila* embryonic extract polyclonal antibodies against DmCycA were used. The embryos were staged (0-4h), heat-shocked (1h 37ºC) and collected from HS-frs#5 and *frs* deficient flies (w ; ΔKG7 e ca /ΔKG19 e ca). Dechorionated embryos (1min in 100% Chlorix) were weighted, frozen in liquid nitrogen and stored at -80°C. The 1000 embryos/reaction were homogenized with several strokes in a Dounce homogenizer in 1ml IP buffer (Materials) at 4ºC. Homogenized embryos were centrifuged for 10min at 13000rpm speed and the supernatant extracted with 1,1,2-Trichlorotrifluoroethane (1:1) to remove lipids. To extracted supernatant 10µl of R Ab DmCycA serum was added. Total embryonic protein extract with the antibodies was incubated for 2h at 4ºC on the rotating wheel and then 60µl of ProteinA Sepharose CL-4B was added and the mixture was incubated for another 1h at 4ºC. After incubation the beads were washed three

times with IP buffer and suspended in 40µl SDS-PAGE sample buffer. The beads coupled with immunoprecipitated complexes were divided in four equal parts and separated in 12% SDS PAGE gel. After semi-dry western blot analysis the nitrocellulose stripes were incubated with the primary antibodies (M Ab CycA 1:200, M Ab Cdk1 PSTAIR 1:50 000 and R Ab Frs 1:2500 separately. M α-Tubulin 1:50 000 antibody was used as a beads washing control) overnight at 4ºC. After incubation with the primary antibodies, the nitrocellulose stripes were incubated with the secondary peroxidase (POD) anti-Mouse and anti-Rabbit antibodies (Sigma, 1:500 each) for 2h at room temperature, washed and developed by ECL plus Western Blotting Detection System (Amersham Biosciences).

16. *In vitro* binding test with TNT Coupled Reticulocyte Lysate System expressed proteins

To test protein-protein interactions the following constructs were *in vitro* expressed in TNT Coupled Reticulate Lysate System kit (Promega): SP64-HA-*CycA*, CS2-*CycA AAA*, MK033-*CycA*(1-170), TS004-*CycA*(171-491), CS2-*CycA*(210-440), SP64-HA-*CycB*, NB40-*CycB3*, SP64-*CycE*, SP64-*Cdk1*), CS2-*nup50*, CS2-*pll*, NB His_{10}-*ZZ*-hu*CycA1*, NB-His_{10}-*ZZ*-hu*CycB1*. The proteins were expressed according to the protocols delivered by the manufacturer (www.promega.com) and stored at -80ºC. A few examples of such expressed and labeled by [^{35}S]methionine (Materials) proteins are presented below (Figure 1).

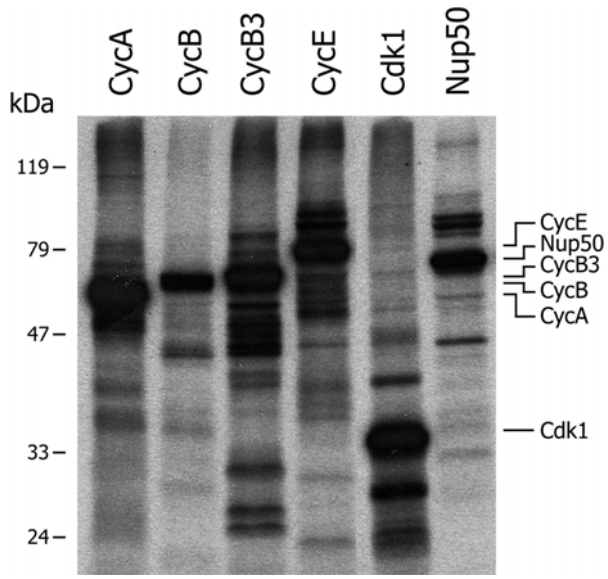

Figure 8. SDS-PAGE gel with an example *Drosophila* proteins expressed with TNT Couplet Reticulocyte Lysate and used in *in vitro* binding assays (in all cases 2µl of the lysate were loaded and autoradiography).

All *in vitro* binding assays with TNT Reticulocyte expressed proteins were performed in PBST buffer (Materials) + 150mM NaCl and 1mM DTT. GST, GST-frs, GST-frs86ASA, GST-

frs48A, GST-frs22A48A and His_{10}-ZZ-huCdk2 fusion proteins were used as baits. Bait proteins were expressed in *E.coli* BL21, the cultures were centrifuged, the pellet was suspended in binding buffer (see above) in the presence of 1mM PMSF and frozen at -20ºC. Each pellet containing the expressed bait protein (20µl per reaction) was suspended in 1ml of binding buffer, sonicated four times (30sec burst, 1min break) and centrifuged. The supernatant was transferred into new tube containing Glutathione Sepharose 4B beads slurry (20µl per reaction) or IgG Sepharose (20µl per reaction) and incubated 1h 4ºC on a rotating wheel. After incubation time the Sepharose beads were centrifuged and washed 4 times with binding buffer. The beads were divided into new tubes (about 10µl coupled beads per reaction) and suspended in 500µl of the binding buffer. 2µl of TNT expressed protein was added to the tubes and incubation of 2h at 4ºC on a rotating wheel followed. After incubation, the beads were washed four times with binding buffer, dissolved in 15µl of SDS-PAGE sample buffer and 50% (15µl) of it loaded on a gel. Unbound fractions were precipitated with 10% trichloroacetic acid (TCA) 30min on ice and centrifuged for 10min at 13000rpm. The pellets were washed with 100% ethanol, dried, dissolved in 15µl of SDS-PAGE sample buffer and loaded on 12% SDS PAGE gel together with the bound fractions. After SDS PAGE analysis the gel was stained with coomassie, dried and autoradiography was performed.

17. Surface plasmon resonance (SPR)

A standard amine coupling procedure via N-Hydroxysuccinimide (NHS) and N-ethyl-N´-(3-diethylaminopropyl)carbodiimide (EDC) was used to immobilized 200 response units (RU) of *E.coli* purified His_{10}-ZZ-frs on the surface of one flow cell of a CM5 sensor chip. 1000RU correspond to a change of about 1ng/mm^2 in surface protein concentration. A reference flow cell was generated by treatment with the same coupling reagents but without protein immobilization. GST-thrombin-tev-CycA(171-491) and GST-thrombin-tev-CycE(300-709) proteins were expressed in *E.coli* BL21 (6h at 18°C with 0.1mM IPTG), the cultures were centrifuged and the pellets were suspended in binding buffer (PBST) + 150mM NaCl and 1mM DTT in the presence of 1mM PMSF and frozen -20ºC. 1ml of such prepared cultures was sonicated four times (30sec. burst, 1min break) in 2ml tube and centrifuged for 10min at 13000 rpm. The supernatant was transferred into a new 1.5ml tube containing 200µl Glutathione Sepharose 4B beads slurry and incubated 1h 4ºC on a rotating wheel. The GST beads were subsequently washed 4 times with binding buffer. The beads were divided into 4 new 1.5ml tubes (50µl beads/reaction) and suspended in 90µl of the SPR buffer B (Materials). 10U of thrombin protease from bovine plasma (SERVA Electrophoresis GmbH) were added in each

tube and 4h incubation at 4ºC on a rotating wheel followed. After incubation, the cleaved proteins were blocked by 1mM PMSF (10min at 4ºC), purified by gel filtration on the Superdex200 10/300GL column in the buffer A for CycA(171-491) or buffer B for CycE(300-709) and concentrated by Vivaspin columns (Satorius). Protein concentration was measured by Bradford assay. The measurements were done in two different running buffers, buffer A for CycA(171-491) and buffer B for CycE(300-709). Both buffers were filtered and degassed before use. SPR data were collected at a flow rate of 20µl/min at 25º C with 120µl injection volume of increasing cyclins concentrations (31.25nM, 62.5nM, 75nM, 125nM, 150nM, 250nM, 300nM, 500nM and 1000nM) passed over the sensor chip with immobilized His_{10}-ZZ-frs (Figure 2).

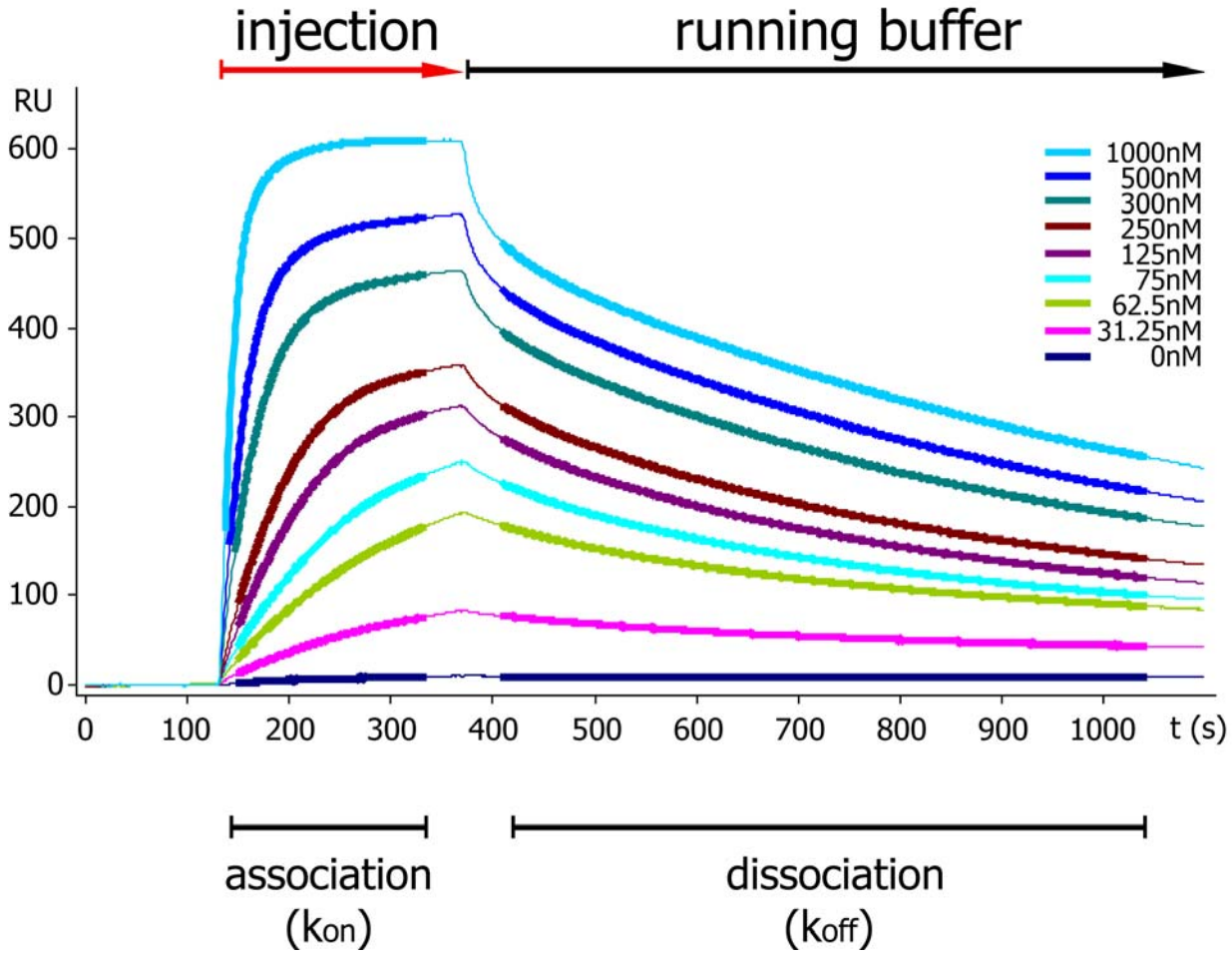

Figure 9. SPR association and dissociation kinetics with different concentrations of *Drosophila* CycA171-491. Injection part of the sensogram (red arrow) and chip washing procedure (black arrow) indicated above. The parts of the association and dissociation curves that were used for Koff, Kon and KD calculations are marked in bold and by black bars below the graph.

The signal of an uncoated reference cell was subtracted from the measurements. Data were collected at a rate of 1Hz. To calculate the binding constant of two interacting proteins information of the dissociation phase of the curves was analyzed in order to calculate the off-

rate using a double exponential fitting model. Using the determined off-rate and the information of the association phase of the curves, the on-rate was calculated by fitting to 1:1 langmuir binding model using a global fitting method from the BIAevaluation 4.0.1 software. Based on off-rate and on-rate the dissociation constant KD was determined.

18. Kinase assay

Immunocomplexes used in kinase assays were immunoprecipitated from *frs* deficient (w ; ΔKG7 e ca /ΔKG19 e ca) or from a cross of paired-Gal4 with UAS-Cdk2-Myc_6 0-12h embryos in IP buffer with the following antibodies: R Cdk1 (5µl serum/reaction), R CycA (2µl serum/reaction), M CycB (5µl ascites/reaction), R CycE (2µl serum/reaction) or anti-Myc (5µg M anti-c-Myc/reaction). In all cases the equivalent of 50 embryos (plain protein extract) was used per reaction unless otherwise mentioned. 10µl/reaction of ProteinA Sepharose CL-4B beads coupled with indicated immunocomplexes was incubated for 10min at 25ºC (or at 4ºC) with 2µCi [^{32}P] ATP/reaction in kinase buffer (Materials) in the presence of 3µM substrate protein and indicated amounts of Frs. The final volume of all kinase reactions was always 16µl. The substrates were expressed in *E.coli* and affinity purified - His_6-LaminDmO(1-179), GST-Rb(379-928) or purchased - HistoneH1 (Calbiochem). The kinase reaction was stopped by addition of SDS-PAGE sample buffer and loaded on the 12% SDS-PAGE gel. The gel was dried and autoradiography was performed with a FUJIFILM FLA-3000 phosphor-imager. For quantification of [^{32}P] incorporation the original picture was analysed in Image Reader V1.8E program.

In the kinase assay with total protein extract, Cdk1 immunocomplexes (50 embryo-equivalent per reaction coupled to 10µl of ProteinA Sepharose via R anti-Cdk1 antibodies 5µl/reaction) were incubated for 10min at 25ºC with 1µl of total protein extract (protein concentration about 20µg/µl) per reaction and 1µM GST, GST-*frs* and GST-*frs*86ASA in a total volume of 16µl.

19. In-gel tryptic digestion and LC-MS/MS analysis

Proteins present in the gel lane were visualized with colloidal coomassie staining. Visible bands were cut out with a scalpel. Gel slices were transferred to a 96-well plate and reduced, alkylated and digested with trypsin (Catrein et al., 2005) using a Digest pro MS liquid handling system (Intavis AG, Germany). Following digestion tryptic peptides were extracted from the gel pieces with 50% acetonitrile/0.1% TFA, concentrated nearly to dryness in a Speed-Vac vacuum centrifuge and diluted to a total volume of 30µl with 0.1% TFA. 25µl of the sample was analysed by a nanoHPLC system (Ultimate, Dionex, Netherlands equipped with a Famos

autosampler) coupled to a ESI QTOF hybrid mass spectrometer (Allied Biosystems). Sample was loaded on a C18 trapping column (Inertsil, LC Packings) with a flow rate of 20µl/min 0.1% TFA. Peptides were eluted and separated on an analytical column (75um x 150mm) packed with Inertsil 3µm C18 material (LC Packings) with a flow rate of 200nl/min in a gradient of buffer A (0.1% formic acid/ 5% acetonitrile) and buffer B (0.1% formic acid, 80% acetonitrile): 0-2min: 5% B; 2-50min: 5-40% B; 50-60min:40-60% B; 60-63min: 60-90% B. The column was connected with a nano-ESI emitter (New Objectives). 2000 V were applied via liquid junction. The QTOF MS operated in positive ion mode. One MS survey scan (0.7 sec) was followed by one information dependent product ion scan (3 sec). Only double and triple charged ions were selected for fragmentation. The peptide sequences of the phosphorylated peptides were confirmed by manual evaluation of the fragment spectra. The MS was done in cooperation with the ZMBH Core Facility for Biomolecular Chemistry division (Dr. Thomas Ruppert).

20. FACS analysis

For one FACS analysis 30 wing imaginal discs of 3rd instar larvae UAS-Frs[C] x MS1096 UAS-GFP transgene were cut in ice cold PBST buffer and trypsinized in 0.5ml Trypsin (0.5g/l) -EDTA (0.2g/l) solution (Gibco) 3.5h at 30ºC on the rotating wheel. As a negative control 30 wing imaginal discs of 3rd instar larvae MS1096 UAS-GFP were used. The discs were incubated in 5ml polystyrene round-bottom tubes (Falcon – Becton-Dickinson) and the cell suspension was subsequently transferred into new polystyrene round-bottom tube and filtered with cell strainer cap (Falcon – Becton-Dickinson). 0.3ml of the cell suspension was stained with Hoechst 33342 (0.5mg/ml) and 0.2ml was left as a control. Unstained and stained samples were sorted according to the GFP signal and analysed according to cell size and DNA staining (Becton Dickinson FACS AriaTM). The data were analysed with BD CellQuest Pro version 5.2 program (BD Bioscience).

21. Ventral furrow *frs* rescue phenotype

frs alleles used in the ventral furrow *frs* rescue experiment (except wild-type sequence) were site-directed mutagenised by PCR with JG182(BglII)/JG183(XbaI) primer pair and cloned into pBKS-frsΔCDS that contains *frs* genomic region (-1205 to 468, +1 transcription start site, amplified from P1 clone DS08110 by PCR with XhoI and ClaI sites, Großhans et al., 2003) with deleted wild-type sequence by XbaI/BglII. In the next step, *frs* allele with *frs* genomic region was recloned from pBKS-frsΔCDS-frs-allele by XhoI/XbaI into pCasper4 XhoI/XhoI

vector. Such prepared constructs were used for making transgenic flies. To get a respectively high number of embryos the flies were kept in plastic cages, about 50 transgenic for *frs* males and about 200 C(3) females. Collected embryos were staged 2-4h, dechorionated with 50% bleach, collected from the apple juice plates, fixed (methanol) and stained with hunchback β-Gal4 M Ab (1:5000) and pH3 R Ab (1:5000) primary antibodies and biotinylated secondary antibodies (1:500). Staining and developing procedures were done with DAB substrate kit for peroxidase (Vector Laboratories, Inc., USA) and VECTASTAIN Elite PK-6100 ABC kit according to the manufacturer protocols. No β-Gal4 staining indicated embryos deficient for *frs* whereas pH3 staining indicated cells during mitosis. Several steps of ethanol and acetone washing (50%, 75%, 100%) dehydrated stained embryos. Waterless embryos were mixed with acetone/araldite mixture (1:1) in a 1.5ml tube overnight at 4ºC, plated on the microscope glass plate and segregated. The embryos were counted for proper ventral furrow formation (according to Großhans et al., 2003) from following crosses: w; LyBke10/Tm3,hb x C(3), frs6; LyBke10/Tm3,hb x C(3), frs86ASA; LyBke10/Tm3,hb x C(3), frs11AxxA; LyBke10/Tm3,hb x C(3), frs22A48A; LyBke10/Tm3,hb x C(3).

22. *In vitro* GFP-Frs nuclear export assay in permeabilized HeLa cells

His_{10}-GFP-frs protein was expressed and purified by HisTrap HP affinity column with lysis/binding buffer (50mM Tris pH7.0, 200mM NaCl) and eluted with elution buffer (50mM Tris pH7.0, 200mM NaCl, 500mM imidazol) in the presence of 5mM β-mercaptoethanol (added already to the *E.coli* lysate before sonication) under standard conditions described in Protein expression and purification chapter of the methods section. 2mM EDTA was added to the eluted His_{10}-GFP-frs protein. In the next step of purification, Thiopropyl-activated Sepharose 6B was used. Thiopropyl-activated sepharose beads were first equilibrated with 10 volumes of EQ buffer (50mM Tris pH7.0, 200mM NaCl, 1mM EDTA) and incubated with His_{10}-GFP-frs protein 1h 4ºC, washed with EQ buffer and eluted with EL buffer (100mM Tris pH8.0, 20mM NaCl, 1mM EDTA and 80mM DTT added directly before use).

An interphase extract (low speed spin) from *Xenopus laevis* eggs was prepared as previously described by Leno and Laskey, 1991. Nuclear transport receptors were depleted from the extract with phenyl-Sepharose (low substitution, Pharmacia), using 500µl beads per ml of extract. Permeabilized HeLa B cells were prepared in suspension as described previously by Ribbeck et al., 1998. For export experiment 0.5µl HeLa nuclei were mixed with 20µl of Xenopus eggs extract, energy-regenerating complement (5mM creatine phosphate, 25µg/ml creatine kinase, 0.25mM GTP and 0.25mM ATP), 1µM Ran, 0.6µM NTF2 (import factor for

RanGDP), 0.5µM GFP-Frs, 2µg/ml DAPI and 0.5µM DmCrm1 protein in the *in vitro* nuclear export buffer. Export reactions were performed at 18°C. For confocal laser scanning microscopy, 2µl of each of the export sample was placed into a well of 10-well multi-test slide and covered with a cover slip. Chromatin was detected by DAPI staining (see above) and excitation at 405nm to indicate the positions of the nuclei. GFP was excited at 488nm. All materials used in this assay (except His_{10}-GFP-frs fusion protein and *in vitro* nuclear export buffer) were kindly provided by Dr.Theis Stüven (FG Görlich, ZMBH).

23. Transgenic flies

3µg DNA of pCasper4 carrying insert with appropriate transgene was precipitated with 1µg of pDelta2-3 turbo vector (contains transposase gene) and dissolved in ddH_2O DEPC to 0.2-0.6mg/ml DNA concentration. The embryos were collected (0-30 min) from the apple juice agar plates, aligned on the microscope glass plate and covered by oil (Voltalef H3S, ARKEMA, France). The DNA plasmid mixture was injected with a prepared glass needle into the pole plasma at the posterior tip of the *w* background embryo prior to pole cell formation. Injected embryos were incubated 48h at 25ºC and the larvae were transferred into fresh agar apple juice plate with a drop of liquid yeast. Close before pupation larvae were transferred into a small food vial. F1 flies were sorted according to color of the eyes (from bright yellow to intensive red, only one fly per vial because other flies may have this same insertion) and crossed with double balancer stock. In *frs* case it was w; Sp/CyO; LyBk10 e/Tm3, hb, Sb. Based on F2 generation flies the chromosome of *w+* insertion was determined and balanced stock was established.

24. Preservation and analysis of adult *Drosophila* wings

All analyzed adult *Drosophila* wings were dissected from the flies and mounted in Hoyer's/lactic acid solution on the microscope glass plates and analysed under bright-field illumination microscope.

Hoyer's/lactic acid solution - 30g Arabic gum was dissolved in 50ml dH_2O overnight on the rotating wheel. When Arabic gum was completely dissolved 200g of chloral hydrate was carefully added. Subsequently 20g glycerol was added and the solution was mixed and centrifuged for 1h at 13200rpm in order to get clarified. Hoyer's solution was mixed with lactic acid (1:1)(Roberts, D.B. 1998).

25. Cell cultures

Mammalian HeLa cells were kept in 6cm plates in complete DMEM medium containing 10% heat-inactivated fetal bovine serum (FBS) at 37ºC and 3.5% CO_2. *Drosophila* S2 cells were kept in 6cm plates in complete Schneider's *Drosophila* medium containing 10% FBS at 28ºC without CO_2. A penicillin-streptomycin solution was added to both media to a final concentration of 50 units penicillin G and 50µg streptomycin sulfate per milliliter of medium. HeLa cells were passaged after 5min trypsinization with 1:250 Trypsin-EDTA solution (0.5g/l trypsin, 0.2g/l EDTA, Gibco). Both cell lines were transfected with 1µg of *frs*-GFP plasmid DNA (pCS2-frs-GFP for HeLa cells and pMK26/ACTSV40BS-frs-GFP for S2 cells) and Effectene transfection reagent kit (Qiagen) according to manufacturer protocol (www.qiagen.com). The transfected cells were incubated for 24h and GFP signals in living cells were analyzed using an Olympus BX60 fluorescence microscope.

Results

1. Frühstart interacts with Nucleoporins, export factor Crm1 and CyclinE

1.1 Yeast-two-hybrid ovarian library screen for Frühstart protein interactors

It was already known that *frühstart* antagonizes *string (cdc25)* activity (Grosshans and Wieschaus 2000) but the molecular mechanism of this inhibition remained unknown. To investigate the molecular mechanism of *frs* activity the binding partners of *frs* were found by a yeast-two-hybrid ovarian cDNAs library screen. Frs interacting clones were isolated with lexA fused to full-length Frs with a lacZ and LEU2 reporter genes (Materials and Methods). Among 7.3 million of transformants analysed in the screen, 60 positive clones that interact with Frs bait protein were found. All Frs interacting clones that were isolated from the screen were amplified by PCR from the yeast DNA and sequenced (Table 3. The truncations are shown for selected examples).

Table 3. Interacting clones isolated in the *frs* yeast-two-hybrid ovarian library screen

Gene/CG number	Function	Frequency	Clones
nup50/CG2158	Nuclear pore component	23x	Full-length (4x), ΔN554, ΔN551(3x), ΔN535, ΔN533, ΔN524(2x), ΔN522, ΔN496(2x), ΔN443, ΔN416, ΔN409, ΔN385(2x), ΔN378, ΔN375, ΔN264
nup214/CG3820	Nuclear pore component	8x	ΔN905, ΔN876 (2x), ΔN645, ΔN572, ΔN508, ΔN413, ΔN322
nup358/CG11856	Nuclear pore component	5x	ΔN552, ΔN531 (2x), ΔN509, ΔN475
nup54/CG8831	Nuclear pore component	5x	ΔN560, ΔN546 (2x), ΔN545(2x)
nup153/CG4453	Nuclear pore component	1x	ΔN376
cyclinE/CG3938	G1/S Cdk2 activity regulator	2x	ΔN319, ΔN244
ctp/CG6998	Dynein ATPase/ microtubule motor	2x	-
hsc70-4/CG4264	Chaperone/ adenosinetriphosphatase	2x	-
dd4/CG2682	Transcription factor	1x	-
CG4639	Transcription factor	1x	-
bip2/CG2009	Transcription factor	1x	-
crc/CG8669	Transcription factor/calcium binding	1x	-
CG12163	Cathepsin F	1x	-
Msp-300/CG33715	larval muscle specific protein	1x	-
CG9986	Function unknown	1x	-
CG12114	Function unknown	1x	-
CG12797	Function unknown	1x	-
Unknown genes	Function unknown	3x	-

Based on the *frs* mitotic phenotype, and on the molecular function of the identified genes, two groups of clones that could be putative functional interactors were selected. The first group includes five different nucleoporins, CG2158/*nup50* (23 different clones), *nup214* (8 clones),

CG8831/*nup54* (5 clones), *nup358* (5 clones) and *nup153* (1 clone) and the second group, two independent clones of cyclinE. The rest of the genes that were found in the screen e.g. *hsc70-4* (chaperone) or CG33715 (larval muscle specific protein) do not seem to be correlated with the *frühstart* mitotic phenotype in the early embryo (Table 3).

To confirm the interaction specificity of Lex-Frs with JG-nucleoporins and JG-cyclinE in Y2H, a series of other Lex-fusion proteins was used. In the Y2H Frs interaction specificity test Lex-pelle, Lex-exuperantia, Lex-cactus and Lex-dynein light chain fusion proteins that do not play any role in cell cycle control machinery were tested (Figure 10). Y2H Frs interaction specificity test for CycE is presented in figure 23 of this section.

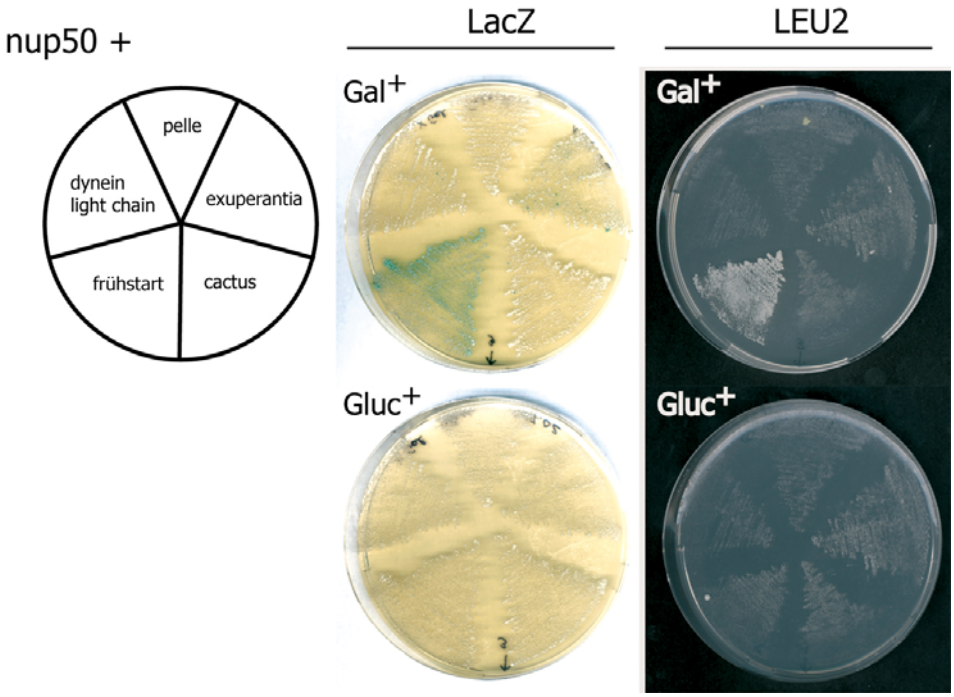

Figure 10. Specificity test of *frs* and *nup50* interaction in the Y2H β-Gal plate assay. Lex-Frs specifically interacts only with JG-Nup50. The interaction was tested with LacZ (blue color) and LEU2 (growth) reporter genes. As specificity control Lex-pelle, Lex-exuperantia, Lex-cactus and Lex-dynein light chain proteins were used. Galactose (Gal+) dependent promoter activates *nup50* gene expression. Gluc+ plates contain glucose instead of galactose.

The specificity test was done for all five nucleoporins found in the screen (only for one, the longest one clone from each gene) and for both clones of cyclinE. All tested clones showed specific interactions only with Lex-*frs* while no interactions with other Lex fusion proteins were observed (for Nup50 figure 10, for the rest of the nucleoporins data not shown, for cycE figure 23). This experiment showed that *frs*-interactors interactions that were found in the Y2H screen are specific.

1.2 *nup50* mRNA and Nup50 protein are present at mid-blastula transition

For further analysis of Frs-nucleoporins interactions I employed CG2158 gene called by me *nup50* because of its high structural homology to human *nup50* (often used old name of this gene was NPAP60 e.g. Lindsay et al., 2002) and mouse/rat *nup50* genes. Full-length *Drosophila nup50* gene was the strongest activator of the LacZ and LEU2 reporter genes in the *frs* Y2H screen. Additionally, *nup50* was the most frequent gene found in the Y2H screen and gave the highest number of accessible clones that were useful for further research. Moreover, the advantages of *nup50* for molecular engineering were its size (564aa, whereas e.g. Nup214 has 1751aa) and its high solubility when expressed in *E.coli* what facilitated the purification process necessary for further investigations.

The very first question was whether *nup50* gene is expressed during early development of *Drosophila* where the peak of *frs* anti-mitotic activity takes place. To address this question, *in situ* hybridization with *in vitro* synthesized anti-sense *nup50* RNA was performed (Materials and Methods, figure 11).

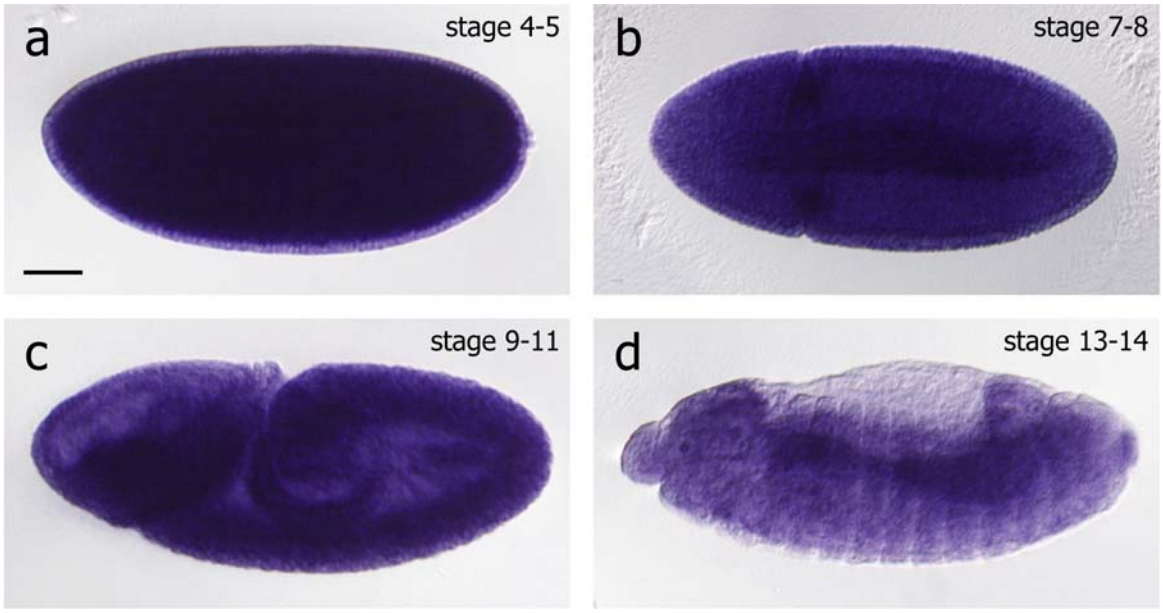

Figure 11. *In situ* hybridization showing the expression pattern of *nup50* gene during early embryonic development of *Drosophila*. **a**) *nup50* is maternally contributed. **b** and **c**) At the later stages *nup50* is ubiquitously expressed until stage 11. **d**) At stage 13-14 *nup50* expression is localized mostly to the body somites and gut. The scale bar represents 50μm.

In situ hybridization of wild-type OrR 0-12h embryos with anti-sense RNA revealed that *nup50* gene is maternally contributed (Figure 11a) and ubiquitously expressed during the embryonic development of *Drosophila* (Figure 11a-d). The next question was then whether Nup50 protein is available during early *Drosophila* development. To test it, rabbit polyclonal

antibodies against Nup50 were raised and affinity purified (Materials and Methods). Staged wild-type embryos were collected, fixed, stained with anti-Nup50 antibodies under standard conditions and analysed by confocal laser scanning microscopy (Figure 12-16).

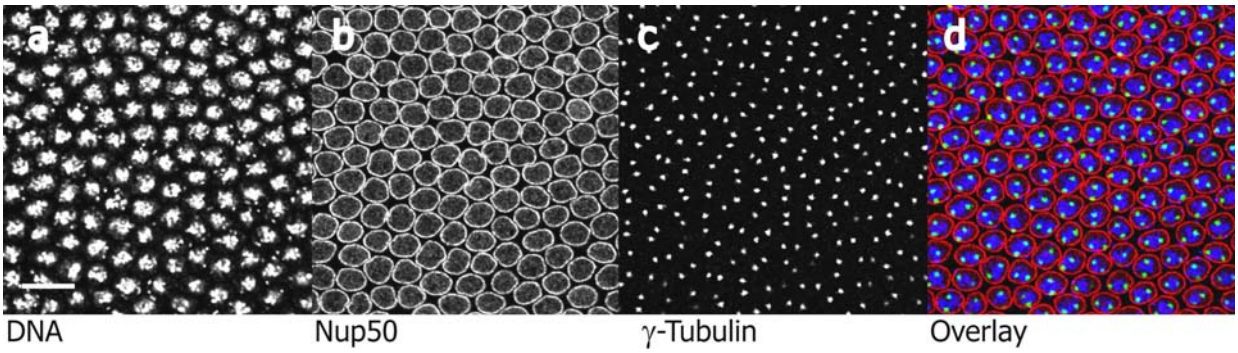

Figure 12. Polyclonal anti-Nup50 antibody staining of stage 5 (syncytial blastoderm) wild-type OrR embryo. **a**) DNA staining (DAPI), **b**) Polyclonal anti-Nup50 antibodies, **c**) Monoclonal γ-tubulin antibodies used as a control of the staining conditions, **d**) Overlay where DNA is marked blue, Nup50 red and γ-tubulin green. It was found that Nup50 protein is localized to the nuclear membrane of the cells (**b** and **d**). The scale bar represents 10μm.

The Nup50 antibody staining illustrated that Nup50 protein is present in the early embryo (Figure 12b,) as well as in the later stages (Figure 15 and figure 16) and is localized to the nuclear membrane during interphase (Figure 12b and d). As specificity control γ-tubulin antibodies were employed (Figure 12c). Both antibodies used in the staining showed independent place-specific localization what showed that Nup50 antibodies are specific and that staining conditions were established properly.

It was also found that during M-phase of *Drosophila* early embryo Nup50 protein colocalises with chromosomes and microtubules (Figure 13).

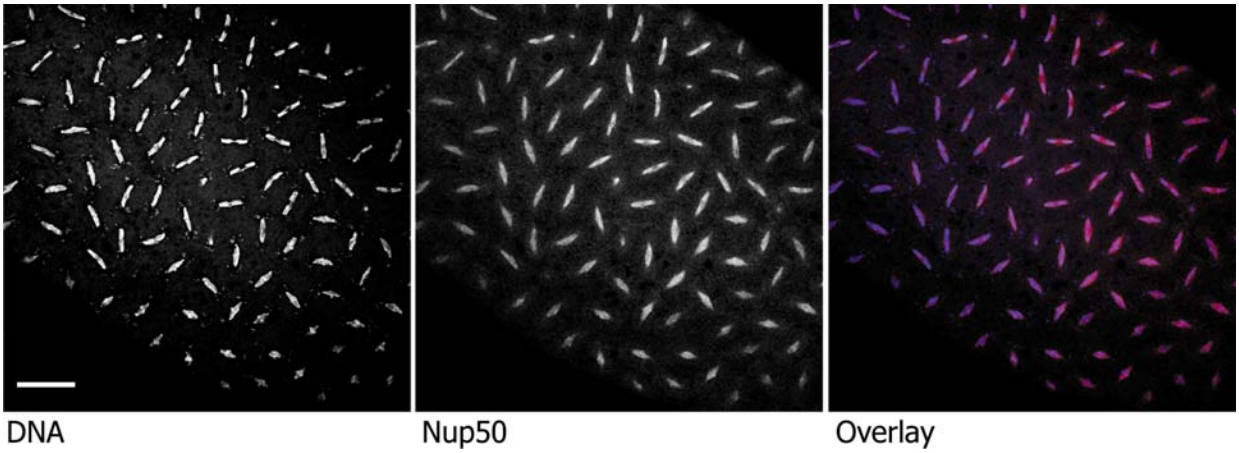

Figure 13. Polyclonal anti-Nup50 antibody staining of stage 3 (syncytial blastoderm) wild-type OrR embryo during mitotic division (anaphase). DNA staining was done with DAPI and marked in white or blue if overlay (left and right panels), whereas polyclonal anti-Nup50 antibodies are marked in white or red if overlay (middle and right panels). It was found that during mitotic division Nup50 protein localizes to the chromosomes and microtubules. The scale bar represents 20μm.

The question that remains open is whether the observed colocalization of Nup50 with chromosomes and microtubules has any functional meaning in the embryo or if it only is an unspecific interaction. The next observation was that the pole cells of the embryo are stained more strongly by Nup50 antibodies compared to the somatic cells (Figure 14).

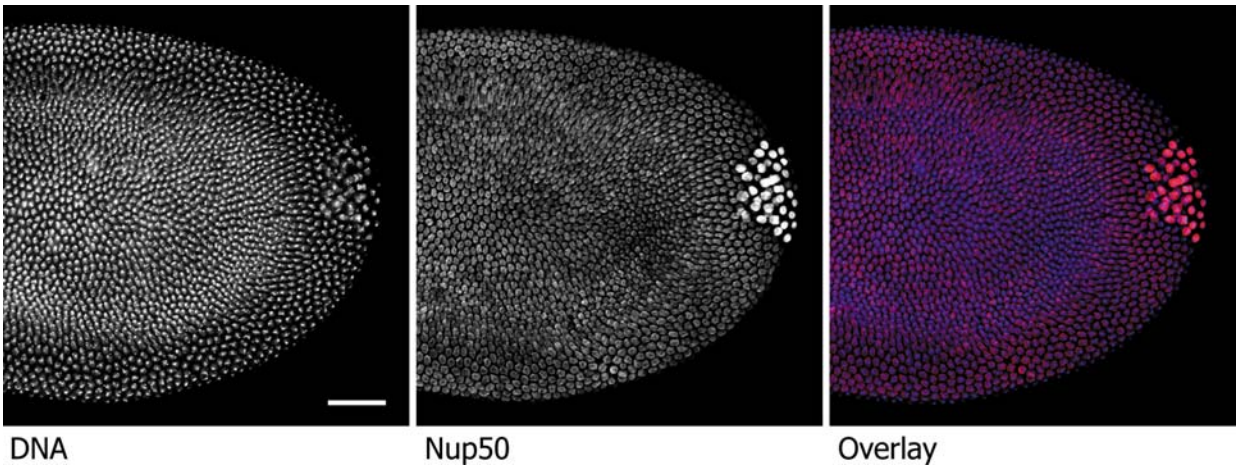

Figure 14. Polyclonal anti-Nup50 antibody staining of stage 4 (syncytial blastoderm) wild-type OrR embryo. DNA staining was done with DAPI, marked in white or blue if overlay and polyclonal anti-Nup50 antibody are marked in white or red if overlay. It was found that the pole cells are much strongly stained compared to the somatic cells. The scale bar represents 50μm.

It also remains unclear whether this phenomenon has any physiological significance and explanation. Stronger Nup50 antibody staining might be due to the fact that the pole cells e.g. might contain more Nup50 protein or that the pole cells are better penetrant for the antibody compared to the somatic cells.

Moreover, it was found that Nup50 protein is not only present in the early embryo but also later in subsequent developmental stages. Indeed, Nup50 protein is present in the cells during the entire embryonic development of *Drosophila* as well as in the epithelial cells of the larvae (Figures 15 and 16).

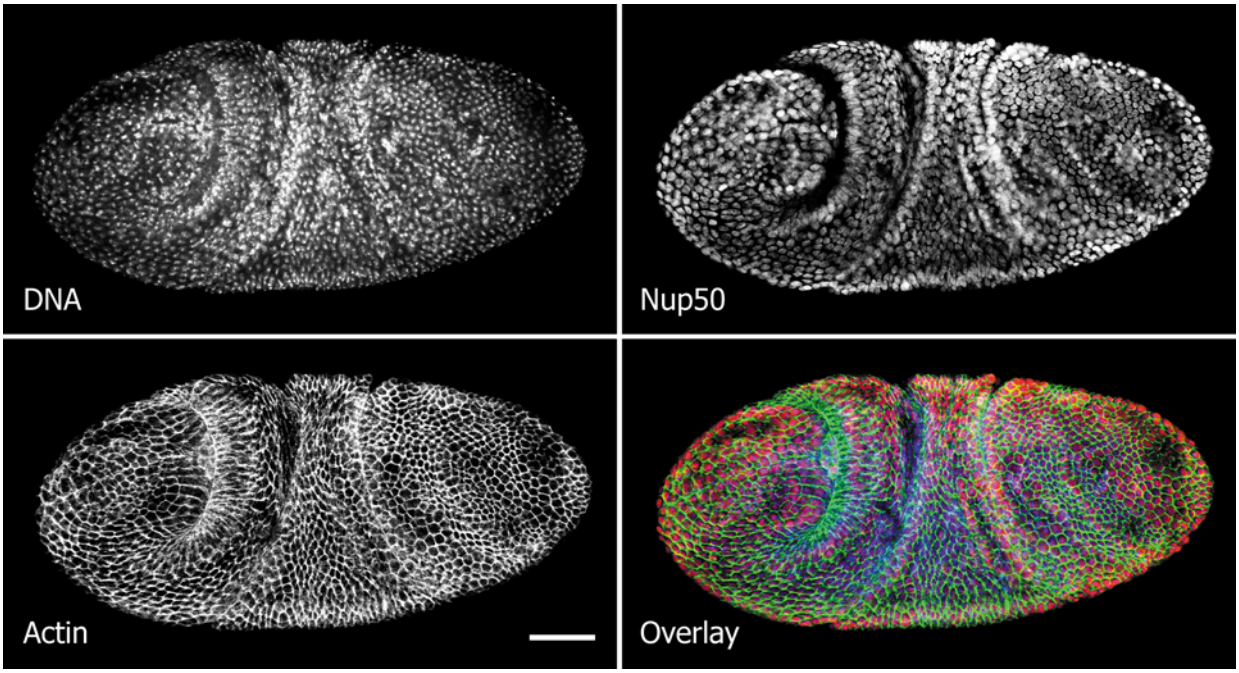

Figure 15. Polyclonal anti-Nup50 antibody staining of stage 8 wild-type OrR embryo. DNA staining was done with DAPI and marked in white or blue if overlay, polyclonal anti-Nup50 antibody staining is shown in white or red if overlay. To visualize cell compartments an actin staining was performed (phalloidin, Materials and Methods), here marked in white or in green if overlay. It was found that Nup50 protein is also present during later stages of *Drosophila* embryonic development. The scale bar represents 50µm.

In order to better visualize the wing imaginal disc epithelial cells nuclei the MS1096 Gal4 x UAS-Frs[D] flies were used for anti-Nup50 antibodies staining. Ectopic expression of Frs in the wing imaginal discs gives bigger, more diverse in size nuclei and disrupts the monolayer structure of the epithelium what makes the pictures much better for analysis. Transgenic for Frs wing imaginal discs were dissected, fixed, stained for Nup50 and tested for presence and localization of Nup50 (Materials and Methods, figure 16).

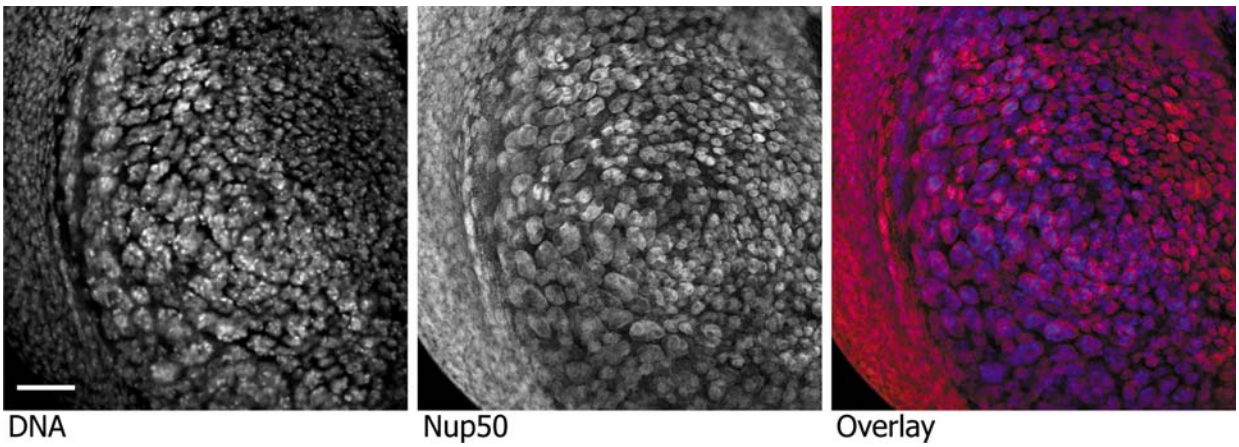

Figure 16. Polyclonal anti-Nup50 antibody staining of the wing imaginal disc of third instar MS1096 Gal4 x UAS-Frs [D] larvae. DNA staining was done with DAPI and marked in white or blue if overlay, polyclonal anti-Nup50 antibody staining is marked in white or red if overlay. It was found that Nup50 protein is also present during later stages of *Drosophila* development, here in the epithelial cells of the wing imaginal disc. The scale bar represents 50µm.

It was found that in the epithelial cells of wing imaginal discs, Nup50 is localized to the nuclear membrane as in the embryo. It was published before that rat Nup50 protein is a nucleoplasmically oriented component of the nucleoporin basket (Guan et al., 2000; Cronshaw et al., 2002). To test whether *Drosophila* Nup50 has a similar position electron microscopy staining and analysis would be required. In order to confirm in a different approach that Nup50 is present in the early *Drosophila* embryo, western blot analysis of embryonic total protein extract was performed. As in the case of embryonic staining, polyclonal anti-Nup50 antibody was used in a series of dilutions (Figure 17).

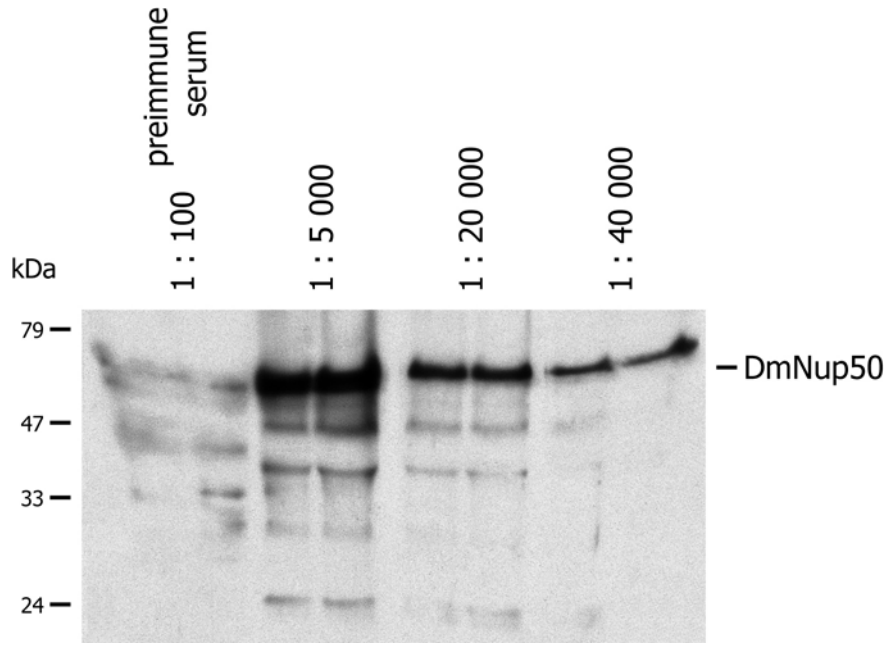

Figure 17. Western blot analysis of embryonic total protein extract with affinity purified rabbit polyclonal anti-Nup50 antibodies. In each line total protein extract from about 10 staged (0-4h) wild-type OrR embryos was loaded. The antibodies dilutions are indicated above the blot. As a negative control preimmune serum was used.

Western blot analysis of embryonic total protein extract confirmed the presence of Nup50 protein in the early *Drosophila* embryos and additionally showed the very high specificity of the rabbit polyclonal anti-Nup50 antibody in this technique. Anti-sense *nup50* RNA *in situ* hybridization and polyclonal Nup50 antibody staining in addition to western blot analysis revealed that *nup50* mRNA and Nup50 protein are present at mid-blastula transition where Frs acts as a mitotic inhibitor. This means that these two proteins that were found to interact in the Y2H system might also interact in the *Drosophila* embryo.

1.3 Frühstart interacts with the N-terminal part of Nup50 in Y2H system

The next question was whether all five nucleoporins that were found in the *frs* Y2H screen share a common binding motif or domain that is responsible for interaction with Frs. In order to

test this, the amino acid sequences of all of them were compared. The blast analysis did not show any similarities that could suggest the existence of a common Frs binding motif or domain and because of this, for further analysis of Frs-nucleoporins interactions, the *nup50* gene was used. Nup50 protein contains three main domains in its amino acid sequence. An Importin-α Binding Motif (IABM) is localized in the N-terminal part, a so called FG-repeats domain (FG) in the middle of the protein and a Ran Binding Domain (RanBD) in the C-terminal end. To determine which part of Nup50 is responsible for interaction with Frs all three domains were cloned into the JG4-5 vector (Materials and Methods, figure 18) and tested for interaction with full-length *frühstart* in the yeast-two-hybrid β-Gal plate assay. Full-length Nup50 and Nup50/67 constructs were used as referees (Figure 18). Nup50/67 was the shortest *nup50* clone found in the *frs* Y2H screen that showed interaction with Frs. As a negative control for Frs interaction full-length Dorsal protein was used.

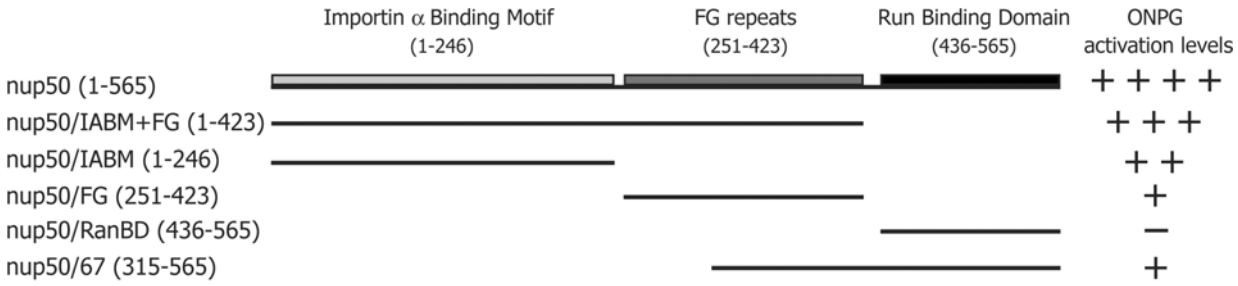

Figure 18. This scheme presents full-length Nup50 protein and a set of different deletion constructs that were used for mapping of the region that is responsible for interaction with Frs. Full-length Nup50 (1-564aa) and Nup50/67 (300-564aa) constructs were used as referees. Nup50/67 (300-564aa) was the shortest *nup50* clone found in the *frs* Y2H screen that showed interaction with Frs. ONPG activation levels part of the graph presents summary of an ONPG assay presented in table 4 and described below.

All constructs used in the test showed positive activation of LacZ and LEU2 reporter genes, except Nup50/RanBD. To quantify which fragment of Nup50 shows the strongest interaction with Frs, an ONPG test in Y2H liquid cultures was performed (Materials and Methods). The ONPG assay is based on the chemical reaction of 2-Nitrophenyl-β-galactopyranoside with β-galactosidase that is expressed during LacZ reporter gene activation by two interacting proteins in Y2H system. In this assay, the stronger the interaction between the two tested proteins, the higher is the β-galactosidase expression. The ONPG reaction with β-galactosidase gives a yellow staining that is measured at OD_{420} = ONPG units. All measurements were repeated three times for each tested interacting couple at the same time and averaged (Table 4).

Table 4. Mapping of the *nup50* region that is responsible for interaction with *frühstart* in the ONPG assay.

Interacting partners	Number of measurement	ONPG units	ONPG units (Averaged)
Frs + Nup50	1	122	**87**
	2	80.6	
	3	60.4	
Frs + Nup50/IABM+FG	1	37.4	**53**
	2	57.8	
	3	65.1	
Frs + Nup50/IABM	1	11.3	**10**
	2	9.4	
	3	9.7	
Frs + Nup50/FG	1	1.8	**2**
	2	1.8	
	3	1.8	
Frs + Nup50/RanBD	1	0.7	**1**
	2	0.5	
	3	0.8	
Frs + Nup50/67	1	1.9	**2**
	2	1.4	
	3	1.9	
Frs + Dorsal	1	0.6	**1**
	2	0.6	
	3	1	

The strongest interaction with Frühstart was exhibited by the construct that contained full-length Nup50 protein and the Nup50/IABM+FG fragment showed only slightly weaker interaction. Nup50/67 referee clone showed minimal activation of the LacZ reporter gene, which means that this fragment of the C-terminal *nup50* end is sufficient for interaction with *frs*, whereas no interaction was detected in the case of the Nup50/RanBD fragment (Table 4 and figure 18). Based on the β-Gal plate Y2H and ONPG Y2H in the liquid culture assays the interaction domain of Nup50 that is required for Frs interaction was determined. In these experiments it was shown that the N-terminal part of Nup50 is required and sufficient for interaction with Frs in Y2H system.

1.4 Frühstart interacts with [S^{35}] labelled Nup50 protein in an *in vitro* binding assay

The next question was whether the Frs-Nup50 interaction that was found in the *frs* Y2H screen is only Y2H specific or if it is possible to reproduce the result in a different approach. In order to confirm the Frs-Nup50 interaction an *in vitro* binding assay was performed. Two proteins, Nup50 and Pelle (used as a control) were expressed *in vitro* in a TNT Coupled Reticulocyte Lysate System in the presence of [^{35}S] methionine (Materials and Methods) and

tested for interaction with Frühstart. Glutathione sepharose beads coupled with GST-Frs fusion protein or GST alone were used as baits (Figure 19).

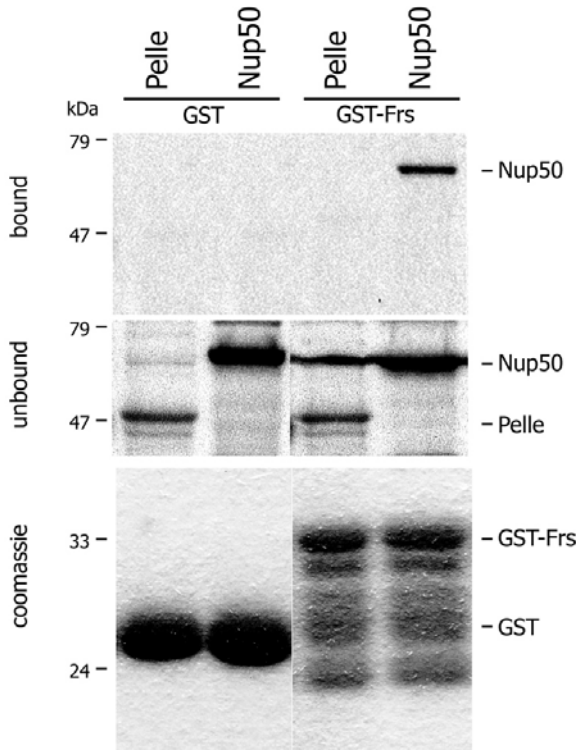

Figure 19. *In vitro* binding assay with Frühstart, Nup50 and Pelle. GST and GST-Frs proteins were used as baits. Frs interacts with [^{35}S] labelled Nup50 and does not interact with Pelle (bound panel). Unbound and coomassie panels are shown as protein loading controls.

In the *in vitro* binding assay it was found that Frs interacts with Nup50. This experiment was repeated three times and each time the result was positive. Surprisingly, when a new box of TNT kit was delivered, the binding signal from the Frs and Nup50 was gone. The problem with the TNT Coupled Reticulocyte Lysate kit is that it is a mixture of many undefined proteins. It is possible that the first batch of the TNT kit lysate contained the protein or proteins that contributed to the Frs-Nup50 complex formation. This could suggest that Frs indeed interacts with Nup50, but indirectly in the presence of other regulatory protein or proteins e.g. members of RanGTPase system (Görlich et al., 1999).

1.5 Nup214 affects Frühstart cytoplasmic localization *in vivo*

It was published before that Nup214 protein affects the function of *Drosophila* nuclear export machinery and the activity of the main nuclear export factor Crm1 (Roth et al. 2003). *nup214* was the only one available mutant out of all five nucleoporins found in the *frs* Y2H screen that could be used for Frs-nucleoporins interaction analysis *in vivo*. The question was then, whether

nucleoporin Nup214 affects Frs nucleocytoplasmic localization. To address this question, Frs was ectopically expressed in a *nup214* background. As the homozygous *nup214* mutant is lethal at late second instar larvae stage, expression of Frs was induced by 1h heat-shock procedure shortly before death of the larvae. The guts of GFP negative (homozygote for *nup214*) and positive (heterozygote) second instar larvae were dissected, fixed, stained with polyclonal anti-Frs antibody and analysed by confocal laser scanning microscopy (Materials and Methods, figure 20).

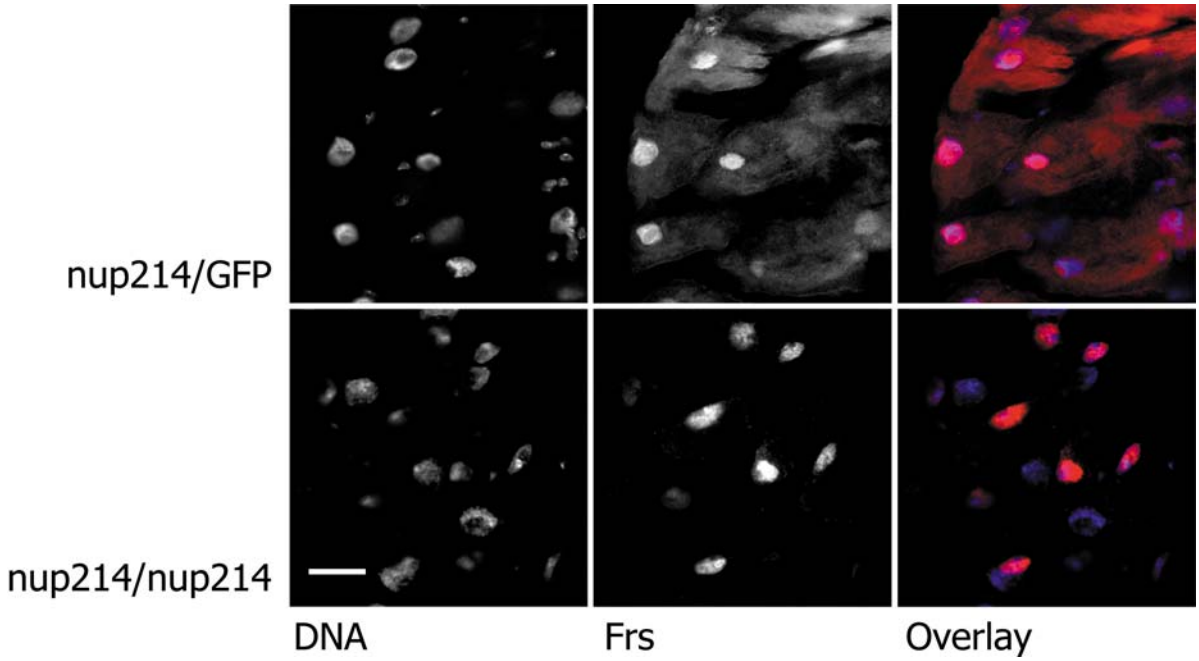

Figure 20. Nucleocytoplasmic localization of Frühstart in the *nup214* late second instar larvae gut cells. Nucleoporin Nup214 affects Frühstart cytoplasmic localization in the 2nd instar larvae gut cells. In the *nup214* heterozygous mutant Frs cytoplasmic localization is affected. Frs is localized mostly in the nucleus and in the cytoplasm whereas in the *nup214* homozygous larvae Frs is localized exclusively in the nucleus. DNA DAPI staining (white or blue if overlay), Frs antibody staining (white or red if overlay). Genotypes: w; Nup214{w+}/CyO, GFP{w+}; HS-Frs[5]{w+} for heterozygous larvae and w; Nup214{w+}/Nup214{w+}; HS-Frs[5]{w+} for homozygous. The scale bar represents 50μm.

In the wild-type stage 5 (syncytial blastoderm) embryos, Frs appears to be excluded from the nucleus, despite its positive charge and its size that is below the apparent exclusion limit of the nuclear pores (Großhans et al., 2003). In this experiment, ectopically expressed Frühstart localization in the gut cells of heterozygous *nup214*/GFP larvae was affected and strong nuclear localization was observed. In the *nup214* homozygous mutant, Frs was exclusively localized in the nucleus. Frs localization changes in *nup214*/GFP heterozygous and *nup214* homozygous mutant gut cells, suggesting that Nup214 protein is required for Frs cytoplasmic localization *in vivo*. It still remains unclear whether Frs localization has any functional significance. As Frs acts in the early embryo and Nup214 protein is maternally contributed it is not possible to do

the functional assay in this model. Nevertheless it would be interesting to test whether Frs cell localization is also affected in other mutants of the nucleoporins found in the *frs* Y2H screen.

1.6 Crm1 affects Frühstart cytoplasmic localization *in vivo*

As it was found that nucleoporin Nup214 affects Frs nucleocytoplasmic localization the next question was whether export factor Crm1 also plays a role in Frs cytoplasmic localization. In order to investigate this, Frs was ectopically expressed in an *embargoed* (*Drosophila crm1* homolog) mutant background. Similarly to *nup214*, homozygous *emb* mutant is lethal at late second instar larvae stage and because of that expression of Frs was induced by 1h heat-shock procedure shortly before death of the larvae. The guts of GFP negative (homozygote) and positive (heterozygote) second instar larvae were dissected, fixed, stained with polyclonal anti-Frs antibody and analysed by confocal laser scanning microscopy (Materials and Methods, figure 21).

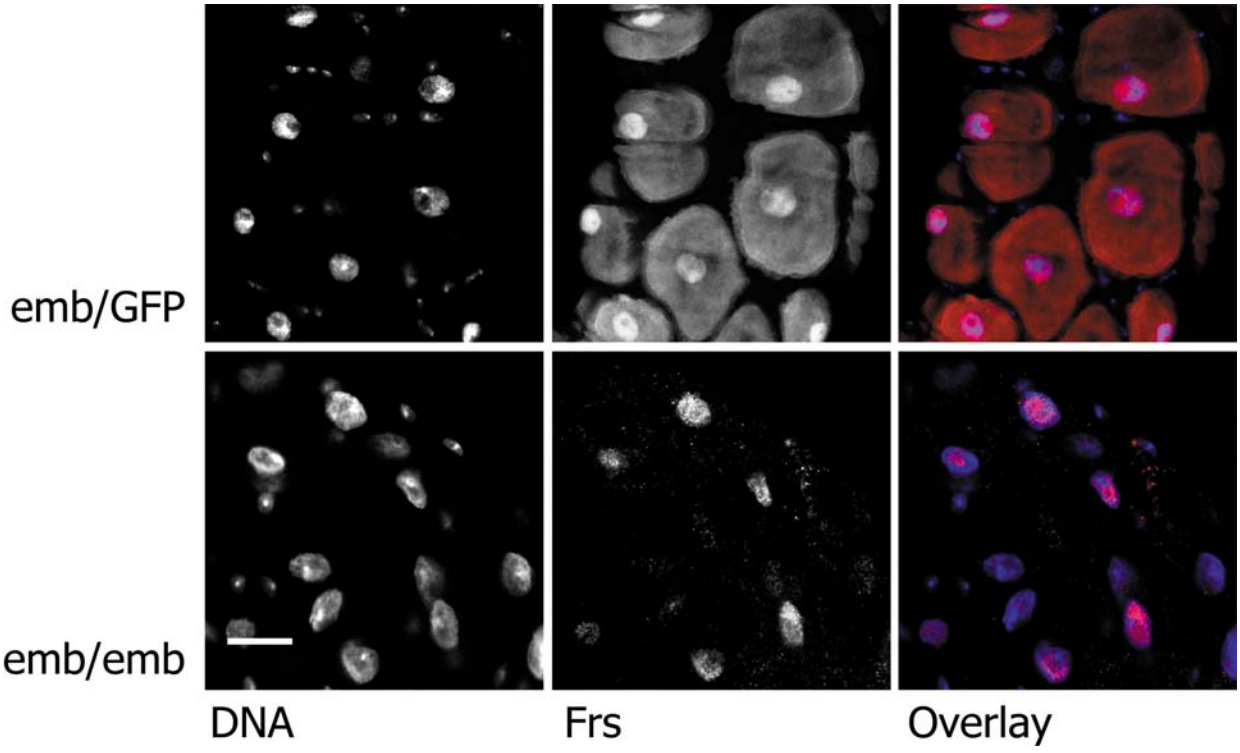

Figure 21. Nucleocytoplasmic localization of Frühstart in the export factor *emb* (*crm1*) late second instar larvae gut cells. In the *emb* heterozygous mutant Frs is localized mostly in the nucleus and in the cytoplasm whereas in the *emb* homozygous larvae Frs is localized exclusively in the nucleus (like in the case of *nup214* gene, figure 20). This experiment showed that export factor *emb* affects Frühstart cytoplasmic localization in the second instar larvae gut cells. Genotypes: w;emb[2]/CyO, GFP{w+};HS-frs[5]{w+} for heterozygous larvae and w;emb[2]/emb[2];HS-frs[5]{w+} for homozygous. The scale bar represents 50μm.

This experiment showed that nucleocytoplasmic localization of ectopically expressed Frs in the *emb*/GFP heterozygous second late instar larval gut cells is affected. In the *emb*/GFP gut

cells Frs was found to localize in the nucleus and in the cytoplasm, whereas in the *emb* homozygous mutant Frs was exclusively localized in the nucleus, what suggests that *Drosophila* Crm1 protein activity is required for Frs nucleocytoplasmic localization *in vivo*. It is not possible to perform a functional assay with Frs in *emb* mutant background during mid-blastula transition embryo because similarly to Nup214, Crm1 is maternally contributed.

To confirm nucleocytoplasmic Frs localization changes observed in the *emb* mutant an *in vitro* nuclear export assay in the permeabilized HeLa cells was done. The HeLa nuclei were incubated in a *Xenopus* egg extract, from which nuclear transport receptors had been depleted with the phenyl-Sepharose method and replenished with an energy-regenerating system (Ribbeck and Görlich., 2002; Stüven et al., 2003). The main task of the *Xenopus* egg extract was to stabilize HeLa nuclei. Frühstart was added as a GFP-fusion protein (Figure 22).

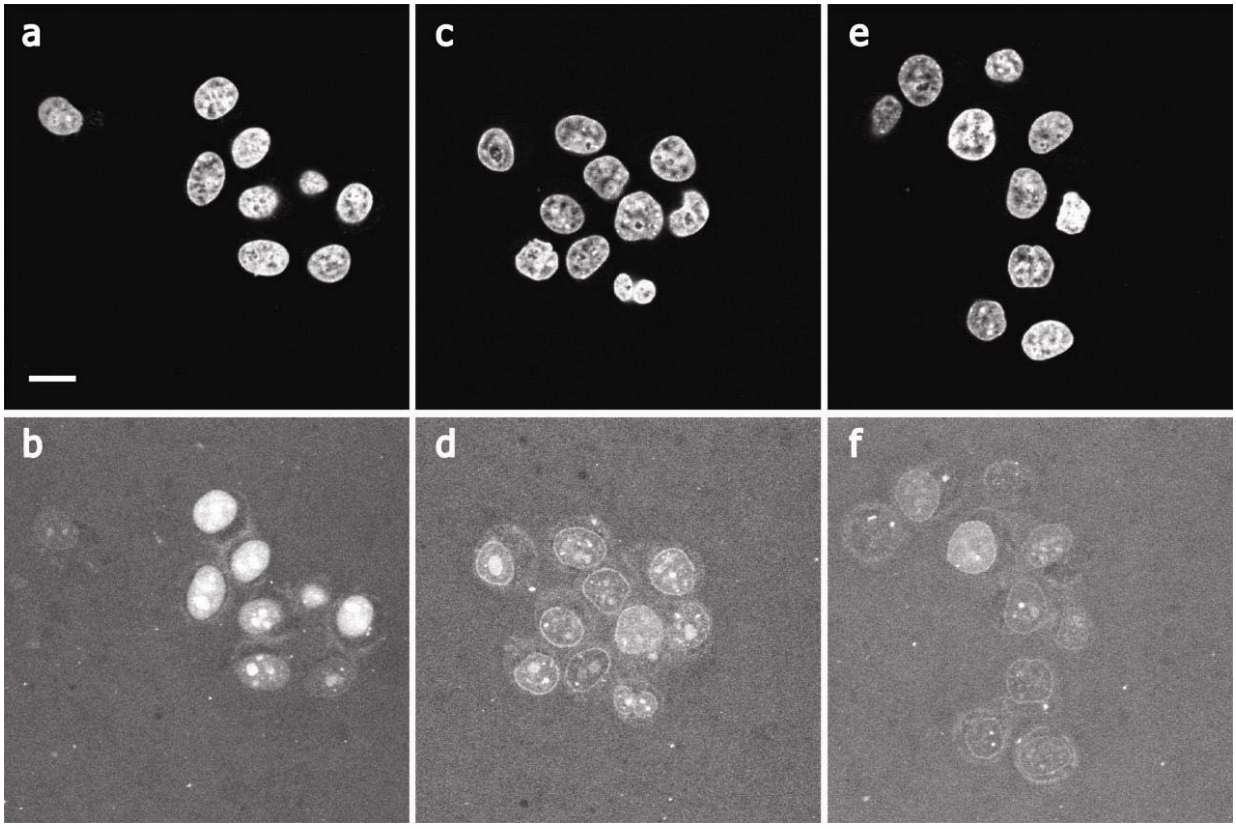

Figure 22. *In vitro* GFP-Frs nuclear export assay in permeabilized HeLa cells. Nuclei were incubated in a *Xenopus* egg extract, which had been previously depleted of endogenous nuclear transport receptors and replenished with an energy-regenerating system. Pictures **a**, **c** and **e** present DAPI staining used as a nuclear area marker. In the control samples (**b**) after 60 minutes incubation strong nuclear localization of GFP-Frs was observed. In the Crm1 samples after 15 minutes incubation (**d**) clear nuclear envelope localization of GFP-Frs was observed with similar effect after 60 minutes incubation (**f**). The scale bar represents 10μm.

In this experiment Frs was added to the sample and allowed to equilibrate between nuclei and cytoplasm. The sample was then split in two and *Drosophila* Crm1 was added to the first half,

and sample reaction buffer was added to the other half as a negative control. The distribution of the Frs export substrate was monitored 15 and 60 minutes later by confocal laser scanning microscopy (Materials and Methods). DAPI staining was used as a nuclear area marker (Figure 22a, c, e). In the control sample after 60 minutes of incubation, strong nuclear localization of Frs was observed (Figure 22b). In the sample containing Crm1 export factor, Frs was localized to the nuclear envelope already after 15 minutes (Figure 22d) and after the next 45 minutes of incubation the localization did not significantly change (Figure 22f). In the *in vitro* export assay, it was found that *Drosophila* main nuclear export factor Crm1 affects Frs nucleocytoplasmic localization in the HeLa nuclei *in vitro* (Figure 22), nevertheless it still remains unclear whether Frs cytoplasmic localization has any functional significance in the *Drosophila* embryo. The main role of Crm1 is to export proteins from the nucleus into the cytoplasm, surprisingly GST-Frs was not exported into the cytoplasm but localized to the nuclear envelope what may have at least two possible explanations. Firstly, the Crm1 complex with Frs tagged by GFP might have stuck in the nuclear envelope without any functional significance. The second explanation might be that the Crm1 complex with GST-Frs interacts stably with a set of nucleoporins (e.g. all five that were found in the *frs* Y2H screen) and by this it modifies or blocks the function of the nucleopores. This kind of modification or blocking could suppress the entry into the nucleus of proteins that trigger mitosis e.g. phosphatase String or kinase Twine. Nevertheless, no wild-type Frs colocalization to the nuclear envelope was observed in stage 5 embryos (Großhans et al. 2003).

2. Frühstart directly interacts with the hydrophobic patch of cyclins but does not stably interact with Cdk1 *in vitro*

2.1 Frühstart specifically interacts with CycE in the Y2H system

In the *frs* Y2H ovarian cDNAs library screen two sets of clones that interact with *frs* were found; the nucleoporins that were described above and two independent clones of G1/S *cyclinE* (Table 3). The question was then whether Frs - cycE interaction is specific, like the interaction of Frs with nucleoporins in the Y2H system. As a specificity control of Frs - cycE interaction three other LexA-fusion proteins were used: Lex-dynein light chain, Lex-cactus and Lex-tribblesΔN124 (Figure 23).

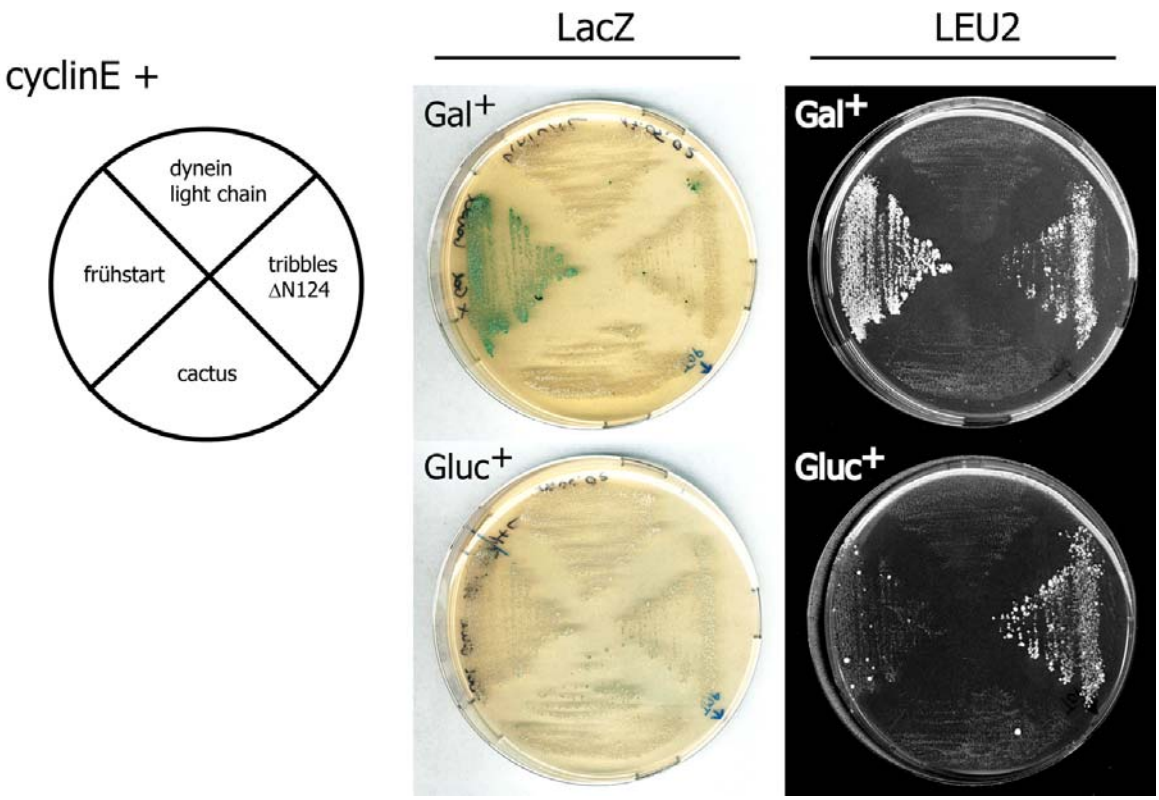

Figure 23. Specificity test of *frs* and *cyclinE* ΔN319 interaction in the Y2H β-Gal indicator plates assay. As specificity controls Lex-cactus, Lex-dynein light chain and Lex-tribblesΔN124 constructs were used. Lex-Frs specifically interacts only with JG-CycEΔN319. Galactose (Gal+) dependent promoter activates *cyclinE* gene expression. The interaction was tested with LacZ (blue color) and LEU2 (growth) reporter genes. Gluc+ plates contain glucose instead of galactose. Lex-tribbles ΔN124 clone showed auto activation with LEU2 reporter gene (LEU2 black panel).

In this experiment JG-*cyclinE*ΔN319 clone showed specific interaction only with Lex-*frs* whereas no interaction with other Lex fusion proteins was observed (Figure 23). Additionally, Lex-tribblesΔN124 construct showed auto activation of LEU2 reporter gene (Figure 23, LEU2 black panel). However, this auto activation has no significance for Frs-CyclinE interaction specificity. This experiment confirmed the specificity of the Frs-CycE interaction, found in the *frs* Y2H screen.

2.2 Frühstart interacts with [S^{35}] labelled CyclinA, B, B3 and E, but does not interact with Cdk1 in an *in vitro* binding assay

In order to confirm in a different approach the Frs-CycE interaction data provided by the *frs* Y2H screen, an *in vitro* binding assay was done (Materials and Methods). For this experiment, *Drosophila* CycE, CycA, CycB, CycB3 and Cdk1 proteins were *in vitro* expressed in TNT Coupled Reticulocyte Lysate System in the presence of [^{35}S] methionine (Materials and Methods). As baits, glutathione beads coupled with GST-Frs fusion protein and GST alone (negative control) were used (Figure 24).

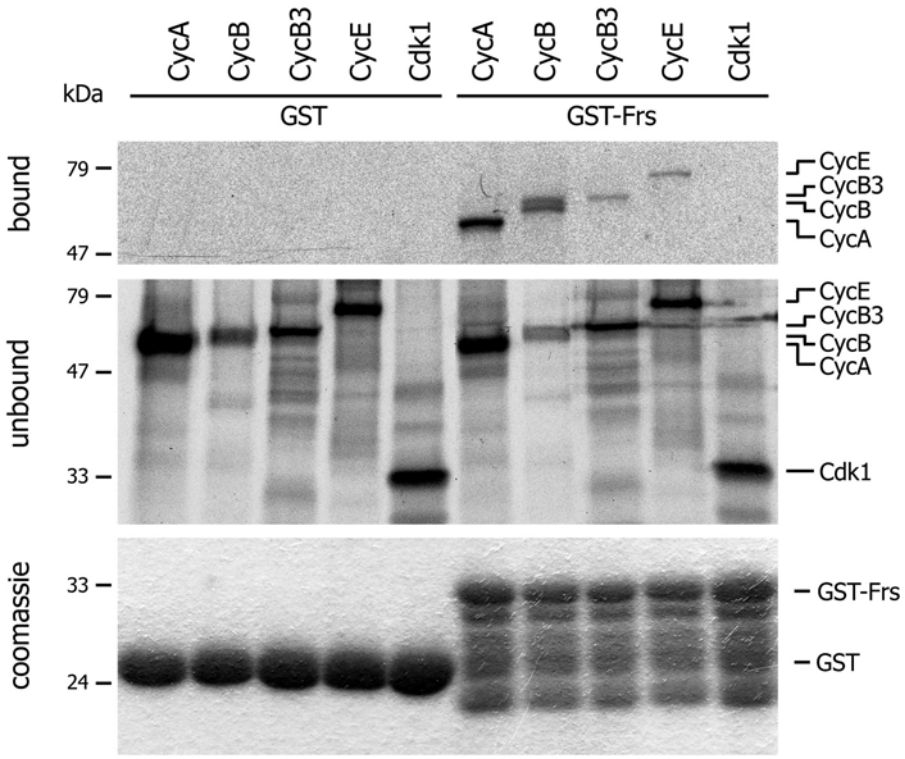

Figure 24. *In vitro* binding assay with Frühstart and [^{35}S] labelled *Drosophila* CyclinA, CyclinB, CyclinB3, CyclinE and Cdk1. As baits, GST and GST-Frs proteins were used. Frs interacts with all cyclins used in the experiment but does not interact with Cdk1 (bound panel). Unbound fractions and coomassie gel are showed as protein loading controls.

In the *in vitro* binding assay, it was found that Frühstart interacts not only with CyclinE but also with CyclinA, B and B3. In addition, no interaction with Cdk1 protein was observed. Nevertheless, this kind of binding assays where *in vitro* translated proteins are used, presents certain limitations. An *in vitro* translated protein mixture contains more than one [^{35}S] labelled proteins, there are many additional undefined proteins required for proper translation process. Base on this experiment we cannot assume whether the interaction that was found is direct or indirect.

2.3 Frühstart interacts with human CyclinA1 and CyclinB1 in the *in vitro* binding assay

To determine whether Frühstart – Cyclins interactions are specific only for *Drosophila* cyclins, two another proteins, human Cyclins A1 and B1 were *in vitro* expressed in the presence of [^{35}S] methionine and the *in vitro* binding assay was performed under standard conditions (Materials and Methods, figure 25).

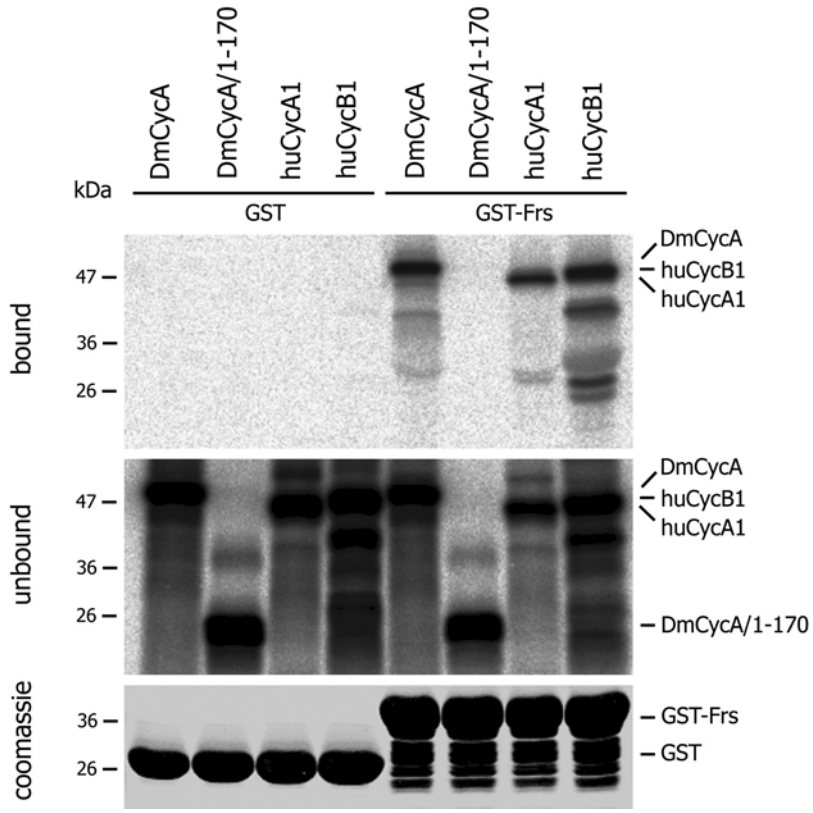

Figure 25. *In vitro* binding assay with Frühstart, human and *Drosophila* Cyclins. As baits GST and GST-Frs proteins were used. Frs interacts with [^{35}S] labelled DmCyclinA, huCyclinA1 and huCyclinB1 and does not interact with the N-terminal part of *Drosophila* CyclinA (DmCycA/1-170) protein that was used as a negative binding control (bound panel). Unbound fractions and coomassie gel are showed as protein loading controls.

In vitro binding assay showed that Frs interacts not only with *Drosophila* cyclins but also with two human cyclins huCycA1 and huCycB1. This experiment suggests that Frs or Frs-related proteins might act as mitotic inhibitors also in other organisms.

2.4 Frühstart interacts 2.5 times more strongly with CycA compared to CycE

In order to test whether Frs directly binds to Cyclins and to better characterize the formation of the Frs-Cyclins complex, the kinetic parameters of the binding were determined by real time surface plasmon resonance (SPR). Immobilized to the sensor chip Frs was analysed for interaction with *Drosophila* CyclinA and huCdk2 (Materials and Methods). In this experiment, human Cdk2 protein was used instead of *Drosophila* Cdk1 because DmCdk1 is hardly soluble in bacterial cells and because of this, difficult to isolate. Moreover, the binding effect of another cyclin kinase inhibitor, p27, on the huCycA and huCdk2 protein complex had been investigated by SPR before (Lacy et al. 2004).

It was found that CycA binds to Frs with a nanomolar binding constant KD=38nM. Additionally, no Frs-huCdk2 interaction was detected, what gives the KD>1μM (Figure 26).

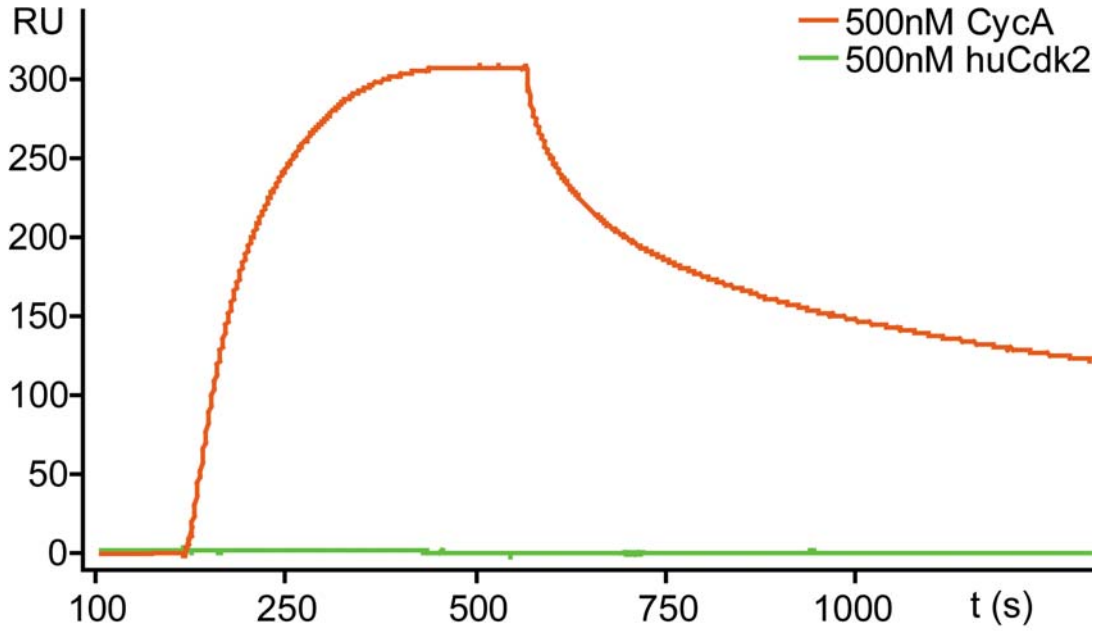

Figure 26. Association and dissociation kinetics of 500nM CycAΔN170 and 500nM His_{10}-ZZ-huCdk2 to immobilized His_{10}-ZZ-Frs measured by surface plasmon resonance. Frs directly binds to CycA but does not bind to huCdk2 *in vitro*. CycA association and dissociation curves showed in blue, huCdk2 curve showed in green. RU - response units, t - time in seconds. This experiment was done with kind help of dr. Rainer Nikolai (FG Bukau, ZMBH).

This experiment confirmed the data of the *in vitro* binding assay (Figure 24) and it additionally showed that Frs binds directly to CycA with high affinity and does not interact with huCdk2 *in vitro*. The next questions were whether Frs interacts with mitotic CycB and G1/S CycE as tightly as with CycA and whether Frs-CycA interaction affects CycA-huCdk2 complex stability. To address these questions real time surface plasmon resonance of Frs with CycB, CycE and CycA-huCdk2 complex was performed (Figure 27) and the binding constants were calculated (Materials and Methods).

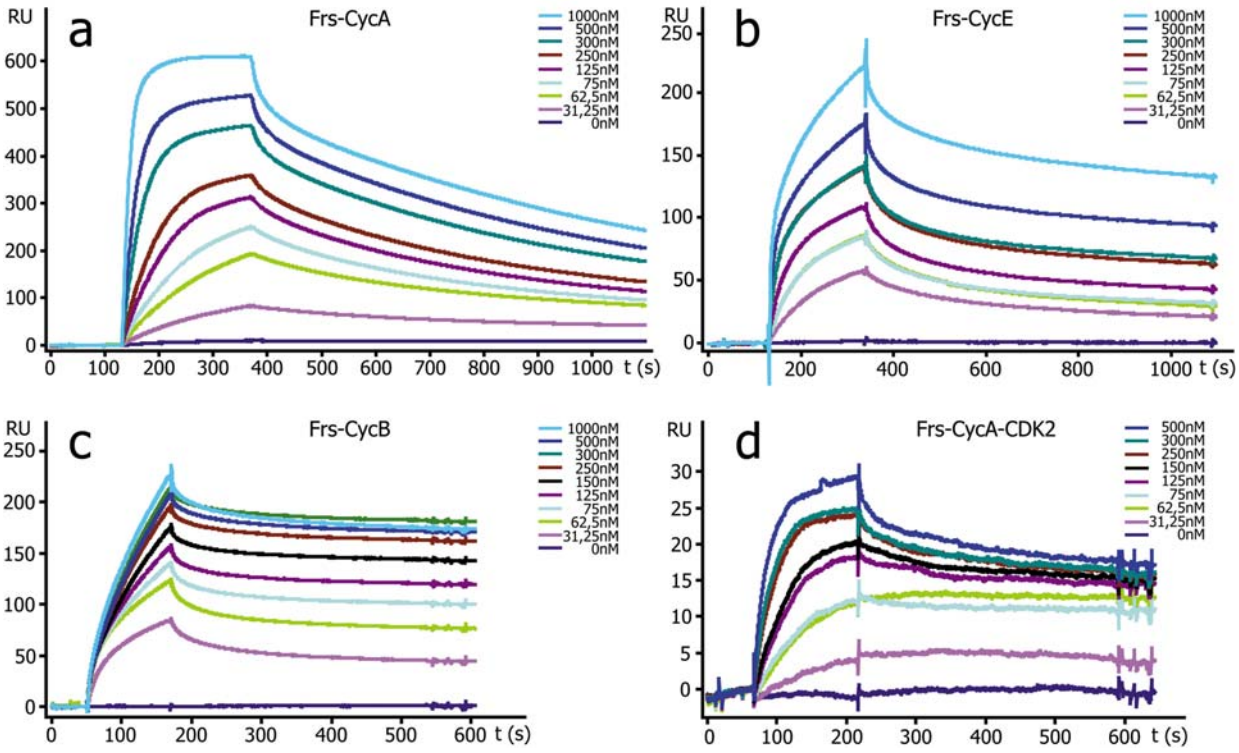

Figure 27. Dissociation (off-rate) and association (on-rate) kinetics of CycAΔN170 (**a**), CycEΔN299 (**b**), CycBΔN218 (**c**) and His_{10}-ZZ-huCdk2-CycAΔN170 complex (**d**) with immobilized to the sensor chip His_{10}-ZZ-Frs. RU - response units, t - time in seconds. Kinetic parameters of Frs-CycA, Frs-CycE and Frs-CycA-huCdk2 complex interactions are presented in table 5. These experiments were done with the kind help of dr. Rainer Nikolai and dr. Matthias Mayer (FG Bukau, ZMBH).

To calculate the binding constant of two interacting proteins, information from the dissociation phase of the curves was analyzed in order to calculate the off-rate using a double exponential fitting model. Taking into account the determined off-rate and the information of the association phase of the curves, the on-rate was calculated using a 1:1 langmuir fitting model. The dissociation constant KD was determined based on the off-rate and on-rate values (Table 5). In the case of CycA, CycE and Cdk2-CycA complex (Figure 27a, 27b and 27d) evaluation of the binding constants was possible because of the correct behavior of the interacting proteins on the sensor chip. In the case of CycB during the on-rate phase we observed an unspecific signal accumulation (Figure 27c) what cold be due to e.g. CycB-CycB complex formation or CycB-sensor chip unspecific interaction, and because of that Frs-CycB binding constant was not estimated. Nevertheless, based on the Frs-CycB on-rate and off-rate sensograms changes according to increasing amounts of CycB we can conclude that CycB interacts specifically and directly with Frs.

Table 5. Kinetic parameters of the Frs-Cyclins and Frs-CycA-huCdk2 complex interactions measured by SPR

Protein couple	**k_{off} (x10^{-3} s^{-1})**	**s.d.**	**k_{on}(x$10^{4}M^{-1}s^{-1}$)**	**s.d.**	**KD (nM)**	**s.d.**
Frs-CycA	2.8	0.01	7.3	0.03	38.4	0.2
Frs-CycE	6.78	0.05	7.04	0.09	96.3	1.4
Frs-CycB	-	-	-	-	-	-
Frs-CycA-huCdk2	4.39	0.04	4.0	0.03	111	1

s.d. - standard deviation.

The SPR data revealed that the interaction of Frs with mitotic CycA is 2.5 times stronger compared to the interaction with G1/S CycE. Such high Frs binding specificity might be an explanation of the *frs* mitotic phenotype in the early embryo on the molecular level. The remaining question in this hypothesis was only how highly is the concentration of Frs protein in the embryo during mid-cellularisation (see figure 29). The meaning of Frs-CycA-huCdk2 111nM binding constant is hard to interpret according to the proposed affinity model. The possible explanation might be that CycA alone and together with huCdk2 has different access to the Frs binding place, what might be a consequence of e.g. the conformational changes that takes place when Cyclins bind to Cdks. Moreover, based on the complex concentration dependent off-rate and on-rate sensograms changes we can assume that Frs binding to the CycA-huCdk2 complex does not lead to CycA-huCdk1 dissociation.

The purity of the proteins used in the surface plasmon resonance experiments is demonstrated in figure 28.

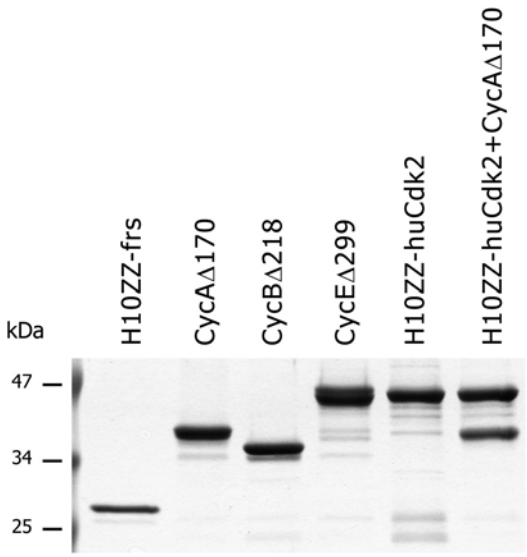

Figure 28. Polyacrylamide gel with *E.coli* purified protein preparations used in the surface plasmon resonance experiments. 2µg of each protein were analysed by 12% SDS-PAGE and stained with Coomassie to demonstrate the purity (The cloning and purification procedures are described in detail in the Materials and Methods sections of this work).

2.5 Frühstart reaches a physiological concentration of 100nM in the mid-cellularising embryo

It is known that *frühstart* is expressed during mid-blastula transition stage during *Drosophila* embryonic development (Großhans et al., 2003), but the *in vivo* concentration of the protein had not been estimated so far. To better characterize and understand the molecular mechanism and the biological function of Frühstart the concentration of the protein was measured. In order to estimate Frs concentration *in vivo* different amounts of recombinant His_{10}-ZZ-Frs and total extracts from precisely staged embryos (mid-cellularisation) were analysed by SDS-PAGE and western blot with polyclonal Frs antibody (Figure 29). Total protein extract from 20 embryos deficient for *frs* was loaded as a negative control (Materials and Methods).

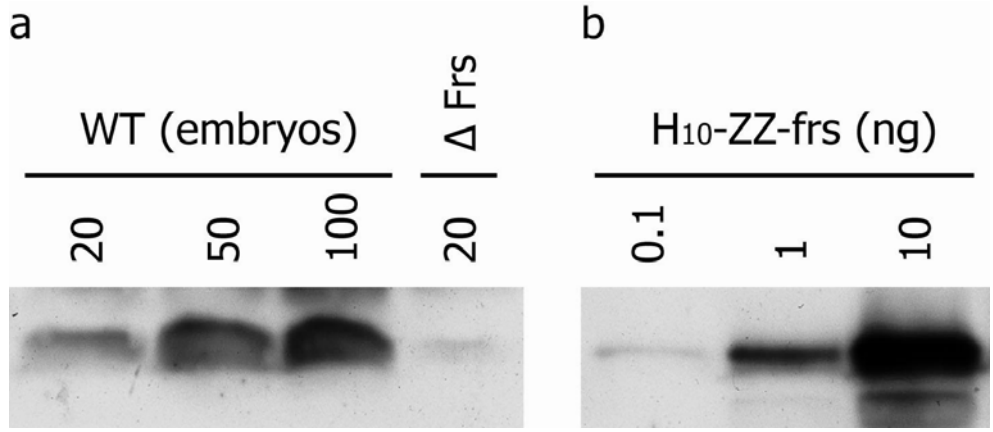

Figure 29. Western-blot analysis of mid-cellularisation embryos (stage 5) with polyclonal Frühstart antibody. **a**) To determine Frs physiological concentration indicated amounts of precisely staged WT embryos were analysed. As a negative control 20 Δfrs embryos were loaded. **b**) As a referee indicated amounts of recombinant His_{10}-ZZ-Frs protein were used. Frühstart physiological concentration in the embryo during mid-cellularisation reaches approximately 10^{-11} g. If volume of one embryo is 10^{-8} l then Frühstart reaches approximately 100nM concentration *in vivo*.

Frs *in vivo* concentration was estimated by comparing the optical density of the bands detected in western blot analysis. During mid-cellularisation, one embryo contains approximately 10^{-11}g of Frs. If 1 embryo weighs 10^{-5}g and we assume that the main ingredient of the embryo is water (>90%) so a volume of the embryo will be 10^{-8} l (1l of water equals 1kg), this gives at 10^{-7}M physiological concentration of Frühstart.

The nanomolar Frs concentration *in vivo* taken together with the nanomolar binding constants of Frs-CycA and Frs-CycE are consistent with the proposed affinity model for Frs mitotic CycA-Cdk1 complex inhibition (see also table 5).

2.6 Frühstart has two different activities

In the Y2H screen two different sets of clones were found, the nucleoporins and two independent clones of cyclinE what suggests that Frs has two different activities. For further analysis of the inhibitory mechanism of Frs, the residues that are responsible for its interaction with nucleoporins and cyclins were determined. Since Frs is a novel protein it was no possible to predict a putative binding interface by usual sequence comparison. In order to identify the residues that are responsible for the interaction of Frs with nucleoporins and cyclins a library of random *frs** mutants was prepared and was screened for Frs clones that bind to Nup50 but do not bind to CycE and for clones that bind to CycE and do not bind to Nup50, in the yeast two-hybrid system (Materials and Methods). The reason why the G1/S CycEΔN319 clone (Table 3) was used as bait instead of one of the mitotic Cyclins A, B or B3 was that expression of these proteins or even their small fragments in yeast is lethal. Out of about 15000 *frs** mutants that were screened, 23 showed the expected phenotype. Out of the 23 *frs** clones found in the screen, 18 clones interacted with Nup50 but did not interact with CycE, whereas 5 clones interacted with CycE but did not interact with Nup50 anymore. Every single mutated *frs** clone that did not interact with CycE or Nup50 in the Y2H assay was amplified by PCR and sequenced (Table 6).

Table 6. List of all clones isolated in the yeast-two-hybrid *frs** library screen

Clone number	*frs* residue	Original amino acid	Mutated amino acid	CycE interact.	Nup50 interact.	Type of mutation
1	9	CAA (Q)	CAC (H)	-	+	substitution
	15	AAC (N)	GAC (D)			substitution
	24	AAG (K)	AGG (R)			substitution
	32	CGC (R)	CGA (R)			substitution (R/R)
	60	GAA (E)	GAC (D)			substitution
	72	ATG (M)	ACG (T)			substitution
	86	AAA (L)	GAA (E)			substitution
2	28	GAG (E)	GGG (G)	-	+	substitution
	74	ACT (T)	TCT (S)			substitution
	80	AAT (N)	GAT (D)			substitution
3	58	CAA (Q)	CAG (Q)	-	+	substitution (Q/Q)
	60	GAA (E)	GAG (E)			substitution (E/E)
4	9	CAA (Q)	AAA (K)	-	+	substitution
	24	AAG (K)	GAG (E)			substitution
	27	AAT (N)	CGT (R)			substitution
	60	GAA (E)	GTA (V)			substitution
	69	CTG (L)	TTG (L)			substitution (L/L)
	86	AAA (K)	AAC (N)			substitution
5	34	TGC (C)	AGC (S)	-	+	substitution
	41	AAG (K)	GAG (E)			substitution
	49	CCC (P)	ACC (T)			substitution
	55	GGA (G)	AGA (R)			substitution

	65	CGC (R)	CTC (L)			substitution
	70	AAT (N)	TAT (Y)			substitution
	79	AAG (L)	TAG (stop)			substitution (stop codon)
6	8	AAC (N)	CAC (H)	-	+	substitution
	24	AAG (K)	AGG (R)			substitution
	58	CAA (Q)	TGA (stop)			double substitution (stop codon)
7	40	AAG (K)	TAG (stop)	-	+	substitution (stop codon)
8	24	AAG (K)	ATG (M)	-	+	substitution
	39	AGC (S)	GGC (K)			substitution
	40	AAG (K)	TAG (stop)			substitution (stop codon)
9	25	GAG (E)	GCG (A)	-	+	substitution
	28	GAG (E)	GTG (V)			substitution
	29	TTC (P)	CTC (L)			substitution
	33	GAG (E)	TAG (stop)			substitution (stop codon)
10	90	TAA (stop)	TAT (Y)	-	+	insertion (stop codon)
11	48	ACC (T)	CCC (P)	-	+	deletion (shifted ORF)
12	48	ACC (T)	CCC (P)	-	+	deletion (shifted ORF)
13	33	GAG (E)	GGG (G)	-	+	substitution
	47	GCC (A)	GCA (A)			deletion (shifted ORF)
14	14	CTG (L)	CTT (L)	-	+	substitution (L/L)
	16	AGC (S)	GGC (G)			substitution
	39	AGC (S)	TGC (C)			substitution
	46	CCA (P)	CAG (Q)			deletion (shifted ORF)
15	45	GTA (V)	GTT (V)	-	+	insertion (shifted ORF)
16	44	CTG (L)	CGG (R)	-	+	deletion (shifted ORF)
17	34	TGC (C)	TCT (S)	-	+	deletion (shifted ORF)
18	22	ACC (T)	CCC (P)	-	+	deletion (shifted ORF)
19	11	CTG (L)	CCG (P)	+	-	substitution
20	11	CTG (L)	CCG (P)	+	-	substitution
	36	TCC (P)	TCT (S)			substitution
	38	GAC (D)	GGC (G)			substitution
	73	TAC (Y)	AAC (N)			substitution
	81	TTC (F)	TCC (S)			substitution
21	8	AAC (N)	CAC (H)	+	-	substitution
	74	ACT (T)	CCT (P)			substitution
	79	AAG (K)	AGG (R)			substitution
22	20	GTG (V)	ATG (M)	+	-	substitution
	34	TGC (C)	CGC (R)			substitution
	48	ACC (T)	CCC (P)			substitution
	70	AAT (N)	CAT (H)			substitution
23	19	ATC (I)	TTC (F)	+	-	substitution

In this screen seven groups of *frs** mutants that affect Nup50 or CycE interactions were found:

- clones that had a point mutation (substitution) in one of the last six Frs amino acids sequence (clones 1 and 4).
- clone that has some C-terminal mutations but not among last six amino acids sequence (clone 2).

- clone that has changes in the nucleotide level but not in the amino acid level what can affect translation process (clone 3).
- clones with point mutations (single or double substitutions) that introduced a premature stop codon (clones 5-9).
- clone with a point mutation (substitution) in the stop codon, that caused no proper transcription termination (clone 10).
- clones with a point mutation (insertion or deletion) that changed the open reading frame (clones 11-18).
- clones that had a point mutation (substitution) in the leucine rich N-terminal part (clones 19-23). Schematic representation of all *frs** mutants found in the screen is shown in figure 30.

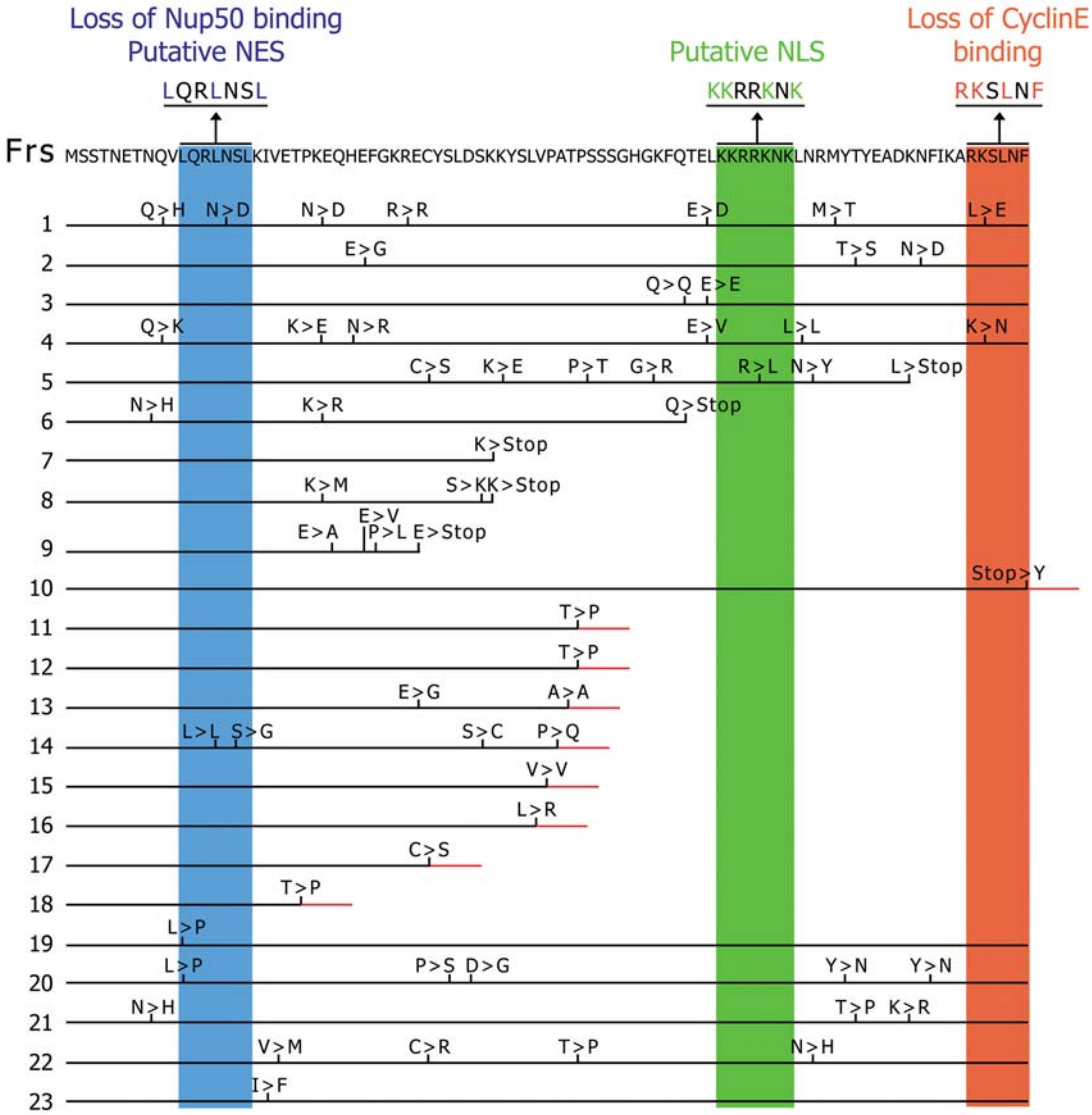

Figure 30. Schematic representation of Frs*-CycE (1-18) and Frs*-Nup50 (19-23) interacting mutants found in the *frs** Y2H screen. Over the *frs** clones the amino acid sequence of wild-type Frs is shown as an indicator for mutated residues. The blue panel shows the position of the putative nuclear export signal (NES) sequence, the green panel presents the putative, lysine rich nuclear localization signal (NLS) sequence whereas the red panel presents a cyclin binding motif (KxL) sequence. New C-terminal sequences, caused by frame-shift mutations are marked in red. This experiment was done with the help of Catherine Goursot.

This experiment showed that the N-terminal part of Frs is required for interaction with Nup50 whereas the C-terminal part of Frs is required for binding to CycE. Mutations among the leucine rich N-terminal fragment of Frs, that might be putative nuclear export signal (NES), abolished interaction with Nup50 in Y2H system. Amino acid analysis of the C-termini of Frs uncovered a KxL motif with a basic residue in front (RKxL) and subsequent phenylalanine (KxLxxP) (Appendix 1., Großhans J.). The KxL motif was already found and described in other Cdk inhibitors like mitotic *Drosophila* Roughex (Foley et al. 1999), M/G1-S-phase *S.cerevisiae* SIC1 (Sanchez-Diaz et al. 1998), G2/M-phase *S.cerevisiae* RUM1 (Moreno and Nurse 1994, Sanchez-Diaz et al. 1998) and Cdk phosphorylation substrates like Rb (Adams et al. 1999; Brown et al. 1999), E2F1 (Adams et al. 1996), p53 (Lowe et al. 2002), p21 (Adams et al. 1996; Chen et al. 1996), p27 (Lowe et al. 2002) and p107 (Zhu et al. 1995). Moreover, it was found that the putative nuclear localization signal (NLS) does not affect Frs-Nup50 or Frs-CycE interactions. To confirm that putative NES and KxL motifs are indeed responsible for Frs - Nup50 and Frs-CyclinE interactions in the Y2H system, two binding mutants were generated. In *frs*11AxxA mutant two leucines of the putative NES motif were substituted by alanines and in *frs*86ASA mutant the basic (K) and hydrophobic (L) amino acids of the KxL motif were mutated to alanines. The interaction test showed that *frs*11AxxA interacts with CycE but does not interact with Nup50, whereas *frs*86ASA mutant interacts with Nup50 but does not interact with CycE in the Y2H β-Gal plate assay (Appendix 2., Großhans J.). In summary, in the Y2H *frs** mutant library screen two interacting motifs were identified, a putative nuclear export sequence (NES) at the N-terminus that is responsible for interaction with Nup50 and a KxL motif at the C-terminal end that is responsible for interaction with CyclinE.

2.7 Mutation of Frs the KxL motif severely affects Frs-CyclinA complex formation *in vitro*

The next question was whether the Frs KxL motif is required and specific only for interaction with CycE or for interaction with another cyclins as well. To confirm the specificity of *frs* KxL motif found in the *frs** Y2H mutant library screen a competitive *in vitro* binding assay was performed. Equal amounts of *in vitro* expressed [^{35}S] CyclinA were preincubated with increasing amounts of Frs C16 peptide that contains the last 16 residues of Frs including the KxL motif, and tested for interaction with GST-Frs. GST-Frs86ASA and GST proteins were used as negative binding controls (Materials and Methods, figure 31).

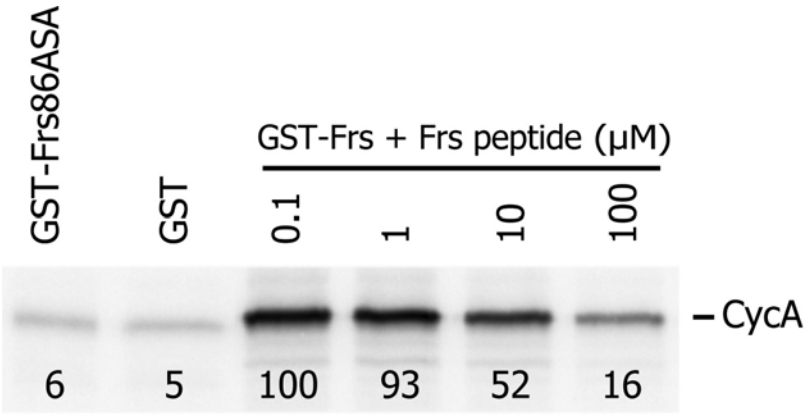

Figure 31. A competitive *in vitro* binding assay with Frühstart, [^{35}S] DmCyclinA and increasing concentrations of C16 peptide that contains last 16 C-terminal residues of Frs. GST-Frs86ASA, GST and GST-Frs proteins were used as baits. GST-Frs86ASA and GST were used as non-binding controls. The 16C peptide interferes with binding of CycA to GST-Frs. Concentration of the peptide and quantification of the autoradiograph are indicated by numbers.

It was found that in the competitive *in vitro* binding assay increasing amounts of C16 peptide affect Frs - CyclinA complex formation. This result, taken together with the data from the *frs** Y2H screen demonstrate that Frs KxL motif plays crucial role in the Frs-Cyclins complex formation in Y2H and *in vitro* binding assays.

2.8 Frühstart interacts with hydrophobic patch of CycA *in vitro*

After finding that the Frs KxL motif is responsible for interactions with cyclins, the next issue was which fragment of cyclins is required for the interaction with Frs. To test this, the amino acid sequences of all four *Drosophila* cyclins that were shown as Frs interactors in the *in vitro* binding assay (CycA, CycB, CycB3 and CycE) were compared. The blast analysis revealed that the most conserved region of all four cyclins is the cyclinbox domain, which has a size of about 100aa. Due to the mitotic phenotype of *frs*, mitotic CyclinA was used for further analysis of Frs-Cyclins interactions (Figure 32).

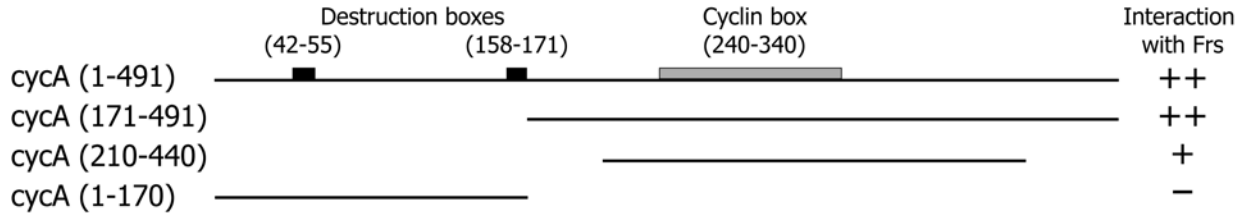

Figure 32. Schematic representation of *Drosophila* CyclinA protein and the truncations that were used to map a domain that is responsible for interaction with Frühstart in the *in vitro* binding assay (see also figure 33, bound panel). The CyclinA(1-491aa) construct contains full-length sequence of the protein, CyclinA(1-170aa), contains the N-terminus with destruction box region, CyclinA(171-491aa) contains the cyclinbox region and the entire C-terminal end and CyclinA(210-440aa) contains the cyclinbox region only.

To find the domain of CyclinA that is responsible for interaction with Frs three truncated forms of CycA were *in vitro* expressed in the presence of [^{35}S] methionine and tested in the *in vitro* binding assay. As a referee control full-length CyclinA was used (Figure 33).

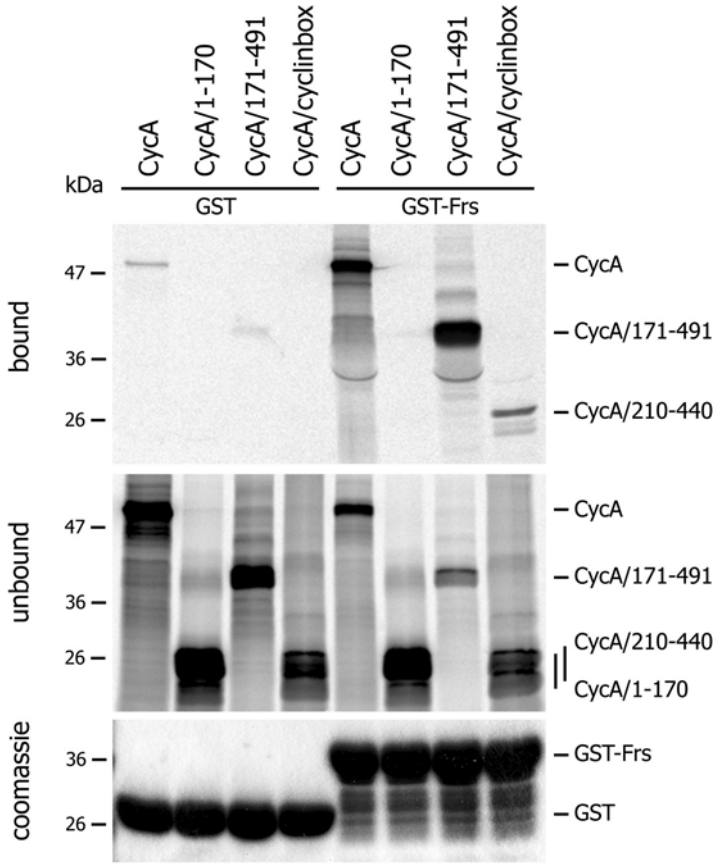

Figure 33. Mapping the interaction region of *Drosophila* CyclinA that is responsible for interaction with Frs in the *in vitro* binding assay. As baits GST and GST-Frs proteins were used. Frs interacts with [^{35}S] labelled full-length CyclinA(1-491aa), CyclinA(171-491aa) that contained the cyclinbox region and the entire C-terminal end and CyclinA(210-440aa) that contained cyclinbox domain only, but it does not interact with CyclinA(1-170aa) what means that the cyclinbox of CyclinA(210-440aa) domain is sufficient for interaction with Frühstart. Unbound fractions and coomassie gel are shown as protein loading controls.

The *in vitro* binding assay showed that Frs interacts with the cyclinbox domain of CyclinA and does not interact with the N-terminal end containing two destruction box domains. The cyclinbox as a Frs interacting domain and the presence of the KxL motif on the Frs amino acid sequence suggested that the hydrophobic patch of the cyclinbox could be the part of CyclinA that is required for interaction with Frs. To confirm the hypothesis that Frs binds to the hydrophobic patch of CyclinA, three amino acid residues that belonged to this motif were mutated to alanines (according to Schulman et al. 1998). The CycA-AAA hydrophobic patch mutant was *in vitro* expressed in the presence of [^{35}S] methionine and an *in vitro* binding assay was performed (Materials and Methods, figure 34).

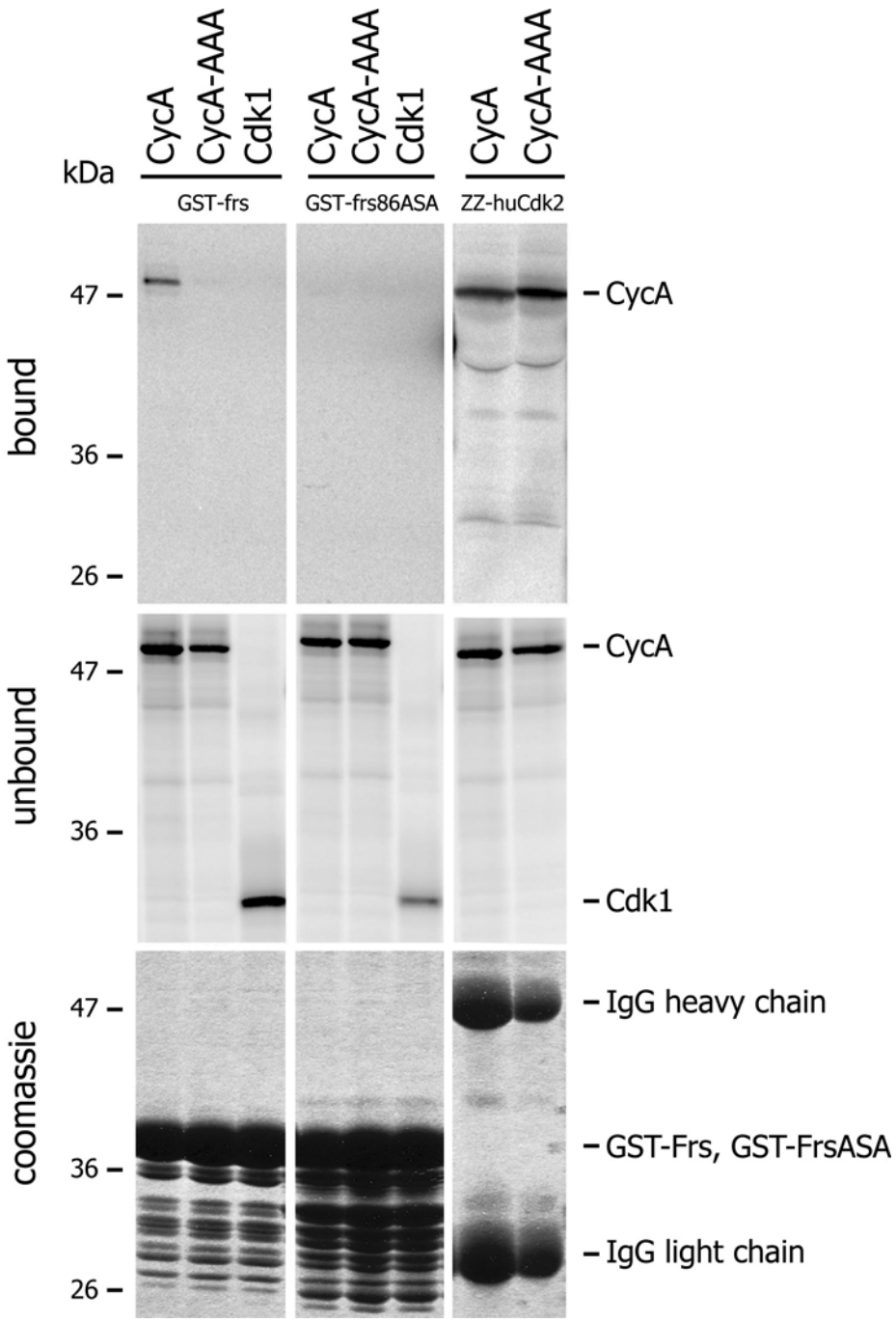

Figure 34. Mapping the interaction residues of the CyclinA cyclinbox domain that are responsible for interaction with Frs in the *in vitro* binding assay. Glutathione beats coupled with GST-*frs* and GST-*frs*86ASA or IgG beads coupled with His_{10}-ZZ-huCdk2 were used as baits. Frs interacts with [^{35}S] labelled *Drosophila* CycA but does not interact with *Drosophila* CycA-AAA (three residues of the hydrophobic patch were mutated to alanines) what means that the hydrophobic patch of the CycA cyclinbox domain is required for binding to Frs. Additionally, CycA-AAA mutation among the hydrophobic patch does not affect the complex formation with huCdk2. Bound and unbound fractions were analysed by SDS-PAGE and autoradiography. Unbound and coomassie fractions are shown as a protein loading controls.

Frs, huCdk2 and Frs86ASA (as cyclin non-binding control) proteins were used as baits. The *in vitro* binding assay showed that mutation among the CycA hydrophobic patch does not interfere with the formation of the CycA-huCdk2 complex but affects binding to Frs (Figure

34). In conclusion, the KxL motif found in the C-terminus of Frs is required for binding to the hydrophobic patch of CyclinA *in vitro*.

2.9 Frühstart forms a complex with CycA and Cdk1 *in vivo*

The next question was whether the Frs - Cyclin complex is also formed *in vivo*? In order to address this question an immunoprecipitation assay was performed. In this experiment embryos carrying a transgene with *frs* under control of a heat-shock promoter were used. Before immunoprecipitation experiment, the expression of the new construct was tested (Figure 35).

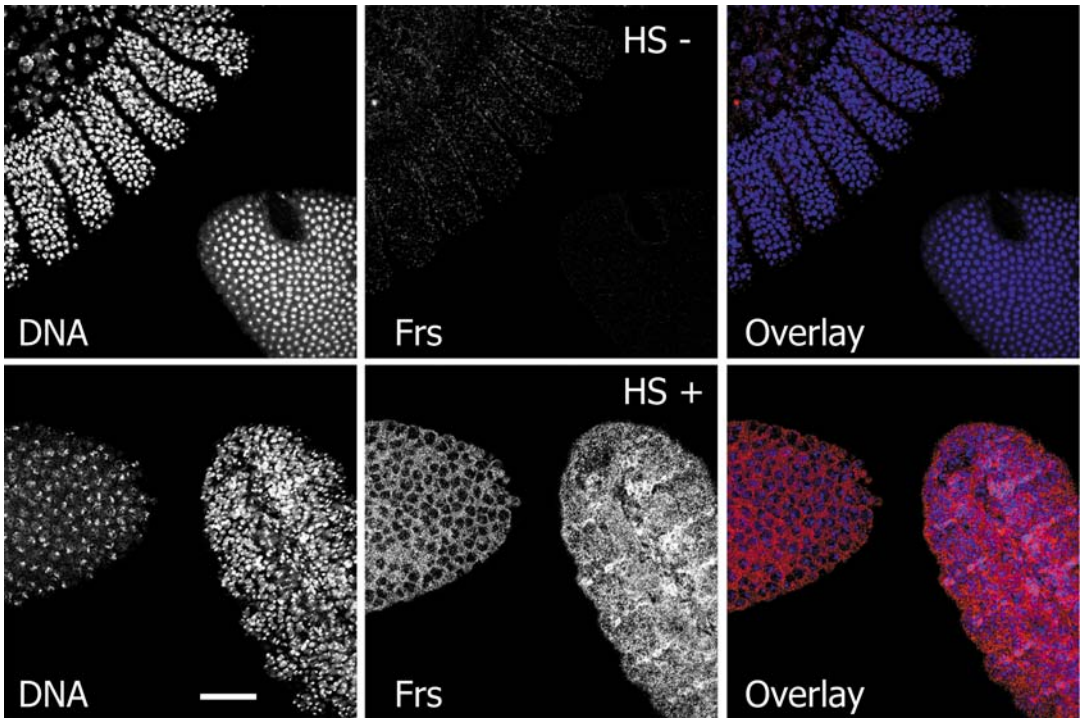

Figure 35. HS-Frs#5 transgene expression test of 0-12h embryos. Heat-shocked (HS+) and non heat-shocked (HS-, as a referee control) embryos were stained with anti-Frs antibodies under standard conditions (Materials and Methods). The pictures of Frs HS+ and Frs HS- were taken using the same settings at the confocal microscope. HS-Frs#5 transgenic embryos showed heat-shocked dependent expression of the *frs* gene. Scale bar represents 50 μm.

Anti-Frs staining confirmed that the HS-Frs#5 transgene is expressed in the embryo and can therefore be used for immunoprecipitation. HS-Frs#5 embryos were heat shocked to induce Frs expression, lysed and incubated with sepharose beads coupled with polyclonal CycA antibodies. Extract from *frs* deficient embryos was used as a negative control. Bound and unbound fractions were subjected to SDS-PAGE and analysed by western blotting with antibodies against CycA, Cdk1, Frs and α-tubulin (Materials and Methods, figure 36).

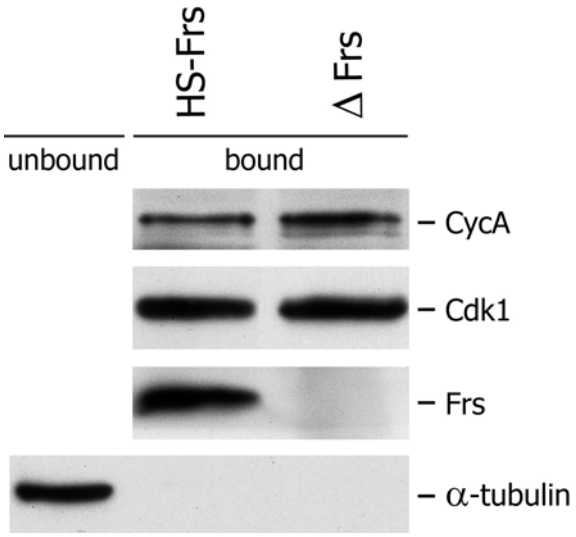

Figure 36. Western blot analysis of immunoprecipitated protein complexes from HS-*frs* and *frs* deficient embryos, using *Drosophila* CycA polyclonal antibodies. α-tubulin antibody was used as a specificity control and to show that washing of the ProteinA beads was done properly. The precipitates contained CycA together with Cdk1 and Frs, but not the control protein α-tubulin indicating that CycA-Frs interaction is specific also *in vivo*.

The immunoprecipitation assay showed that Frs-CycA complexes are formed also *in vivo* and can be immunoprecipitated from the embryos that ectopically expressed *frs*. The precipitates contained CycA together with Cdk1 and Frs, but not the control protein α-tubulin demonstrating that Frs-CyclinA association is specific *in vivo* (Figure 36).

2.10 Frs affects Cdk1 and Cdk2 kinase activity

The next question was whether Frs-Cyclins interactions have any functional meaning and whether they affect Cdk1 and Cdk2 kinase activity. In order to investigate this, a series of kinase assays were done. To test the influence of Frs on Cdk1 kinase activity, the Cdk1 complexes were immunoprecipitated from the embryonic lysate of *frs* deficient embryos by polyclonal antibodies raised against a peptide corresponding to the last 18 C-terminal residues of the Cdk1 kinase (Materials and Methods). In all kinas assays where Cdk1 was immunoprecipitated, the polyclonal anti-DmCdk1 antibodies were used as a plain not purified rabbit serum. As they were newly raised antibodies (according to Knoblich et al., 1994), it was first of all necessary to characterize their specificity.

To test whether Cdk1 serum is specific for Cdk1 protein and does not contain any additional antibodies that could recognize other kinases and by this affect the phosphorylation levels of Cdk1 substrates, immunoprecipitation and a kinase assay with Cdk1 and Nup50 rabbit serums (used as a negative control) were done (Figure 37). The immunocomplexes used in the kinase assay were immunoprecipitated from equal amounts of *frs* deficient embryos. *Drosophila* LaminDmO protein was used as a phosphorylation Cdk1 substrate (Materials and Methods).

Moreover, GST-Frs22A48A (a hypo-phosphorylated Frs allele) was used to test whether *E.coli* purified proteins used for further experiments were not contaminated during the purification process by some other kinases that could unspecifically increase Cdk1 phosphorylation activity signal and phosphorylation of the substrates.

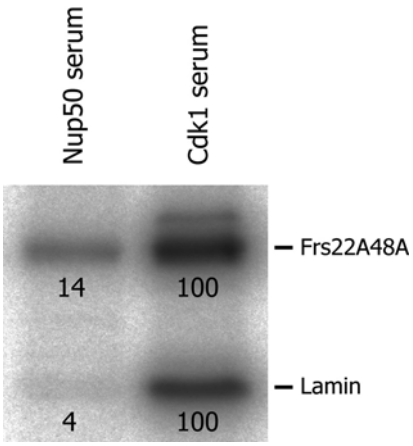

Figure 37. Specificity test of the anti-Cdk1 rabbit serum used in the kinase assays. Nup50 and Cdk1 immunocomplexes were isolated from embryonic lysates, incubated with His_6-Lamin(1-179aa) and GST-Frs22A48A hypo-phosphorylating Frs allele in kinase buffer in the presence of [^{32}P] γ-ATP. The reaction mixture was analysed by SDS-PAGE and autoradiography. The numbers indicate the quantification of the optical density of the bands. ProteinA sepharose beads coupled with Nup50 immunocomplexes showed minimal (4%) Lamin phosphorylation compared to the Cdk1 serum (100%) what means that Cdk1 antibodies from Cdk1 serum are specific. Additionally Frs22A48A incubation with Nup50 immunocomplexes showed 14% background phosphorylation compared to the Cdk1 serum (100%).

In the kinase assay, it was found that Nup50 immunocomplexes immunoprecipitated with anti-Nup50 serum showed minimal (4%) Lamin phosphorylation compared to the Cdk1 immunocomplexes immunoprecipitated with anti-Cdk1 serum (100%). This experiment proved that anti-Cdk1 antibodies are Cdk1 specific and that ProteinA sepharose beads coupled with anti-Cdk1 serum IgG do not associate unspecifically with another kinases available during immunoprecipitation. In addition, GST-Frs22A48A preparation did not significantly affect Lamin phosphorylation signal what means that the protein preparation was not contaminated by another unspecific kinases.

This same question concerning specificity was addressed in the case of the mouse monoclonal anti-c-Myc antibodies that were used to immunoprecipitate Cdk2 immunocomplexes from embryos transgenic for Cdk2-Myc_6. The Cdk2-Myc_6 immunoprecipitates and the unbound fractions were analysed by SDS-PAGE and western blot for presence of Cdk2 and Cdk1 proteins (Materials and Methods, figure 38).

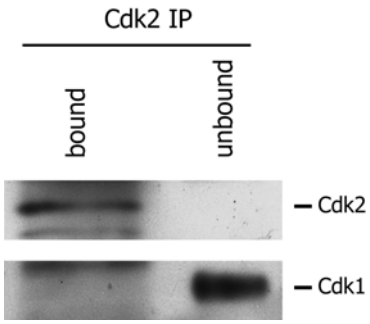

Figure 38. Western blot analysis of Cdk2-Myc_6 immunocomplexes immunoprecipitated with mouse anti-Myc antibody from paired-Gal4 x UAS-Cdk2-Myc_6 transgenic embryos. Unbound fractions were analyzed as a negative control. It was found that mouse monoclonal anti-c-Myc antibodies immunoprecipitate only Cdk2-Myc_6 protein kinase and do not co-immunoprecipitate Cdk1 from Cdk2-Myc_6 transgenic embryos.

Western blot analysis of the immunoprecipitated Cdk2-Myc_6 complexes showed that mouse monoclonal anti-c-Myc antibodies are specific for Cdk2-Myc_6 complexes and do not co-immunoprecipitate Cdk1 kinase protein.

The next important issue was to establish the optimal kinetic parameters of kinase assay conditions such as substrate concentration, kinase amount per reaction or reaction time of the experiment. The first question was then whether the amount of substrate is not a limiting factor in the assay. To test this, Cdk1 immunocomplexes isolated from embryonic lysate (100 embryo equivalents and 5µl Cdk1 serum per reaction) were incubated with 3µM GST-Rb substrate in kinase buffer with [^{32}P] γ-ATP for 1, 3, 10, 20 and 40 minutes at 25 ºC (Figure 39).

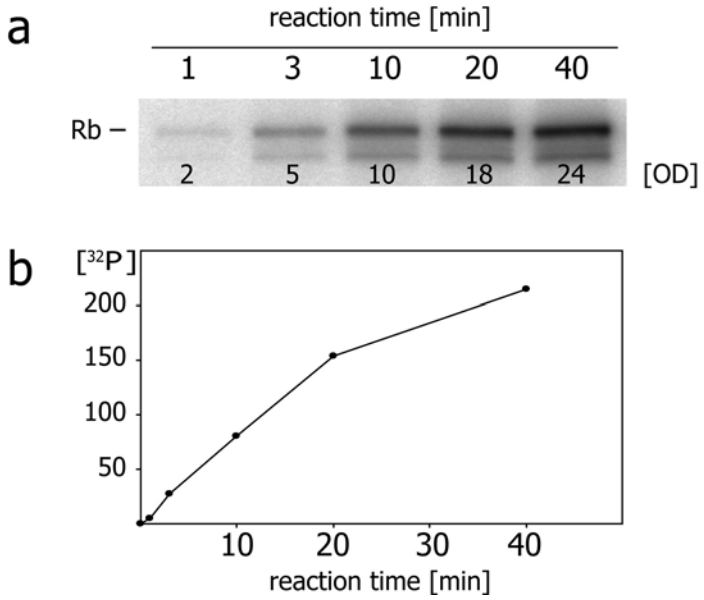

Figure 39. Kinase assay with Cdk1 immunocomplexes and GST-Rb(379-928) substrate. **a**) SDS-PAGE gel with [^{32}P] signal of phosphorylated GST-Rb from 1 minute up to 40 minutes. The measured optical density [OD] of the bands is indicated on the gel. **b**) Optical density values presented as a graph, which shows that the substrate is not a limiting factor in the assay if the reaction time is 10 minutes or even longer.

In the assay 3μM GST-Rb substrate was almost constantly being phosphorylated by immunoprecipitated Cdk1 protein kinase along the 40 minutes of reaction time. This means that under these conditions 3μM concentration of the substrate is not a limiting factor for Cdk1 immunoprecipitated from 100 embryos if the reaction time is 10 minutes or even longer.

It was also not clear whether Cdk1 immunocomplexes by themselves are not a limiting factor in the kinase assay. To test this, the Cdk1 immunocomplexes (5μl Cdk1 serum per reaction) were isolated from increasing amounts of *frs* deficient embryos (1, 10, 100 and 1000) and incubated with 3μM substrate in kinase buffer with [^{32}P] γ-ATP for 10 min at 25ºC (Figure 40).

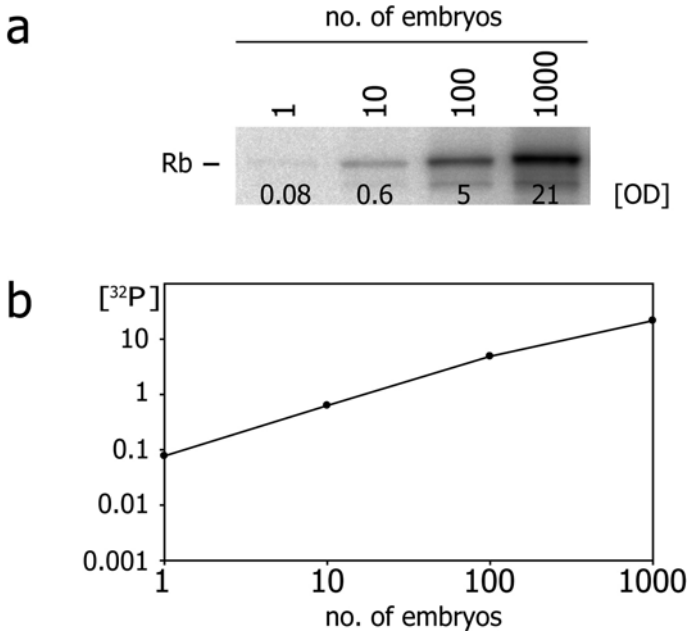

Figure 40. Kinase assay with Cdk1 isolated from increasing amounts of embryos. 3μM GST-Rb(379-928) was used as a substrate. **a**) SDS-Page gel with [^{32}P] signal of phosphorylated Rb substrate incubated 10 min at 25°C with Cdk1 immunocomplexes immunoprecipitated from 1, 10, 100 and 1000 *frs* deficient embryos. Increasing amounts of embryos are indicated above the gel. The optical density [OD] of the bands was measured and is indicated on the gel. **b**) Optical density values presented as a graph.

This experiment showed that the amount of Cdk1 kinase immunoprecipitated from 10-100 or even more embryos by 5μl of anti-Cdk1 serum used in the kinase reaction is not a limiting factor if the substrate concentration is 3μM.

Based on the test experiments that established the proper conditions of the kinase assay with immunoprecipitated native Cdk1 complexes the following reaction parameters were used for further Frs-Cyclins interactions: per reaction - Cdk1 immunocomplexes were isolated from 50 embryo equivalents by 5μl of anti-Cdk1 rabbit serum and incubated with 3μM substrate 10 minutes at 25°C unless otherwise mentioned (Materials and Methods).

When the kinase assay conditions with newly raised anti-Cdk1 antibodies were properly established the functional assay with Frs was performed. Because of the Frs mitotic phenotype *in vivo* the first question was whether Frs affects mitotic Cdk1 kinase activity.

To test the influence of Frs on Cdk1 function, Cdk1 immunocomplexes were isolated from embryonic lysate and incubated with increasing amounts of Frs in the presence of different Cdk1 *in vitro* substrates: HistoneH1, Rb or LaminDmO. The kinase assay reactions were done in the kinase buffer and [^{32}P] γ-ATP. As a referee GST and GST-Frs86ASA proteins were used. The samples were analysed by SDS-PAGE and autoradiography (Materials and Methods, figure 41).

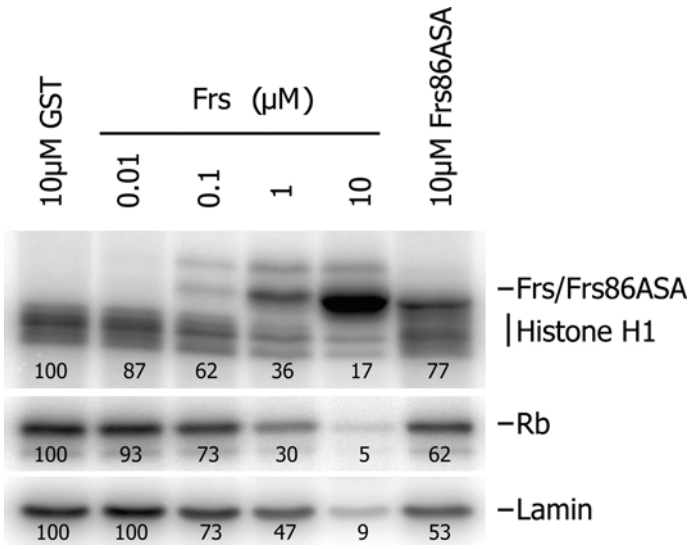

Figure 41. Kinase assay with Cdk1 immunocomplexes titrated by increasing amounts of Frs. Increasing amounts of Frs inhibited all three model substrates used in the assay. Cdk1 was immunoprecipitated from embryonic lysate by anti-Cdk1 serum, incubated with HistoneH1, Rb or LaminDmO substrate and increasing amounts of GST-Frs. As a negative control (100 = 100%) GST protein was used (first line). GST-Frs86ASA allele was used as a Cyclin non-binding control. All reactions were done in the kinase buffer with [^{32}P] γ-ATP, analysed by SDS-PAGE and autoradiography. The relative [^{32}P] incorporation by the substrates is indicated below the respective bands.

The Cdk1 kinase assay showed that Frs inhibited Cdk1 kinase activity and decreased the phosphorylation level of all three substrates used in the experiment. Moreover, GST-Frs fusion protein was a substrate for Cdk1 as well and was strongly phosphorylated. It was already known that Cdk1 triggers mitosis as a complex with CycA (essential) and as a complex with CycB (not essential). The next question was whether Frs is Cdk1-CycA or Cdk1-CycB complex specific inhibitor or if it can equally block both complexes. In order to address this question, Cdk1 complexes were immunoprecipitated from embryonic lysate by anti-Cdk1 serum, anti-CycA serum and anti-CycB antibodies separately and tested for Frs inhibition (Materials and Methods, figure 42).

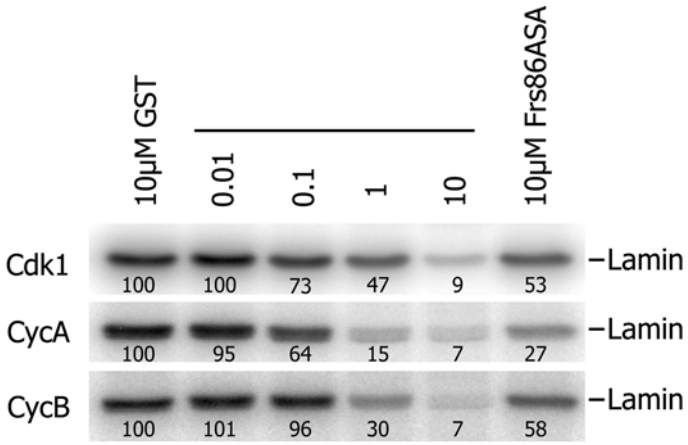

Figure 42. Kinase assay with Cdk1, CycA and CycB immunocomplexes titrated by increasing amounts of Frs. It was found that Frs inhibits kinase activity of Cdk1, CycA and CycB immunocomplexes to a comparable degree. The immunocomplexes were isolated from embryonic lysate by anti-Cdk1 serum, anti-CycA serum and anti-CycB antibodies and incubated with LaminDmO and increasing amounts of GST-Frs. GST protein was used as a negative control (100 = 100%). GST-Frs86ASA allele was used as a Cyclin non-binding control. All reactions were performed in the kinase buffer with [^{32}P] γ-ATP, analysed by SDS-PAGE and autoradiography. Relative [^{32}P] incorporation by the substrates is indicated below the respective bands.

No Frs specificity was observed in this experiment, as it equally inhibited Cdk1, Cdk1-CycA and Cdk1-CycB immunocomplexes kinase activity. The next question was then, whether Frs is only a mitotic Cdk1 specific inhibitor or if it is also able to inhibit G1/S Cdk2 kinase activity. To address this question, Cdk2-Myc$_6$ immunocomplexes were isolated from transgenic for Cdk2-Myc$_6$ transgenic embryos by anti-Myc antibodies and titrated by increasing amounts of Frs under standard conditions (Materials and Methods). Because in *Drosophila* G1/S Cdk2 kinase is active in the complex with CyclinE, the same experiment was done in parallel for CycE immunocomplexes that were isolated from *frs* deficient embryos (Figure 43).

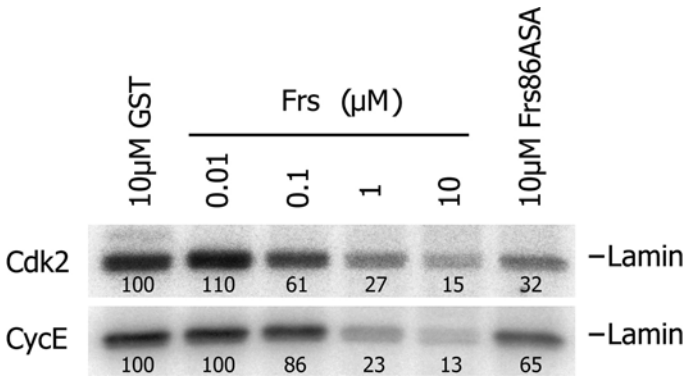

Figure 43. Kinase assay with Cdk2 and CycE immunocomplexes titrated by increasing amounts of Frs. Frs did not show any Cdk2 or CycE specificity and affected the kinase activity of both immunocomplexes to a comparable degree. The immunocomplexes were isolated from transgenic for Cdk2-Myc$_6$ embryos by anti-Myc antibodies, and from embryos deficient for *frs* by anti-CycE antibodies. The immunocomplexes were incubated with LaminDmO substrate and increasing amounts of GST-Frs. As a negative control (100 = 100%) GST was used. GST-Frs86ASA allele was used as a Cyclin non-binding control. All reactions were done in the kinase buffer with [^{32}P] γ-ATP, analysed by SDS-PAGE and autoradiography. Relative [^{32}P] incorporation by the substrate is indicated below the respective bands.

The kinase assay with Cdk2 and CycE showed strong kinase activity inhibition by Frs, like in the case of Cdk1 and CycA, and no specificity was found. The observed lack of Cdk specificity was very striking, especially in the context of the SPR data that showed 2.5x stronger Frs affinity to CycA compared to the CycE. For closer analysis of Cdk1 and Cdk2 kinase activity inhibition by Frs another kinase assay test was done. Cdk1 and Cdk2 immunocomplexes were incubated with a narrow range of Frs protein concentrations (0-1μM) that cover the nanomolar range of Frs-CycA and Frs-CycE binding constants values only. Each experiment was repeated three times with always this same immunocomplexes preparation and averaged (Materials and Methods, figure 44).

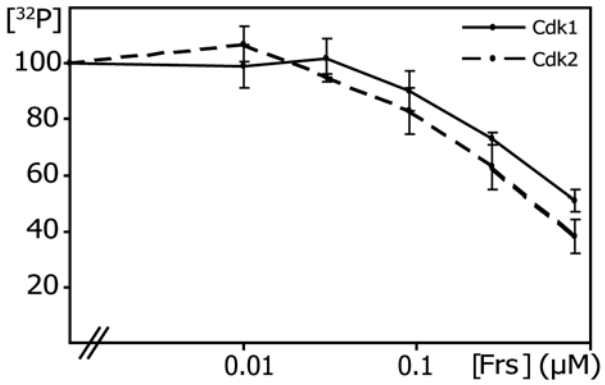

Figure 44. Kinase assay with Cdk1 and Cdk2 immunocomplexes titrated by increasing amounts of Frs. Both Cdk immunocomplexes were inhibited to a comparable degree. The immunocomplexes were incubated with LaminDmO used as a substrate and with increasing concentrations of GST-Frs in the kinase buffer. [^{32}P] incorporation was quantified following SDS-PAGE analysis and autoradiography. Each measurement was repeated three times and the average was calculated. Error bars represent standard deviations.

The *in vitro* kinase assays revealed that Frs equally inhibits phosphorylation of three model substrates by Cdk1 and no substrate specificity was observed. Moreover, Frs inhibited mitotic Cdk1 and G1/S Cdk2 kinase activity to a comparable degree, even though Frs has 2.5x higher affinity to CycA compared to the CycE. Another astonishing finding was that Frs inhibited Cdk1 and Cdk2 kinase activity at the micromolar range what is about ten times higher than the Frs-CycA, Frs-CycA-huCdk2 and Frs-CycE binding constants.

2.11 The hydrophobic patch is not required for HistoneH1, Rb and LaminDmO substrates interaction with Cdk1

In the kinase assay specificity test, it was found that Frs inhibits Cdk1 and Cdk2 kinase activity in the micromolar range that is about 10x higher than the binding constants of Frs-CycA, Frs-CycE and Frs-CycA-huCdk2 complex (Figure 44). A different activity was shown e.g. by p27 inhibitor that inhibits Cdk activity *in vitro* at the nanomolar range that is around its

nanomolar binding constant values (Toyoshima and Hunter 1994, Lacy et al. 2004). The difference between Frs binding constant values and Frs concentration that efficiently inhibits Cdk kinase activity *in vitro* suggests that binding of Frs to the hydrophobic patch of cyclins is not required for the inhibition of HistoneH1, Rb and LaminDmO model substrates phosphorylation. To investigate the role of the hydrophobic patch in Cdk1 substrate phosphorylation a competitive *in vitro* kinase assay was performed with the Frs C16 peptide that contains the last 16 C-terminal amino acids sequence of Frs with the KxL motif. Full-length wild-type Frs was used as a phosphorylation referee control (Materials and Methods, figure 45).

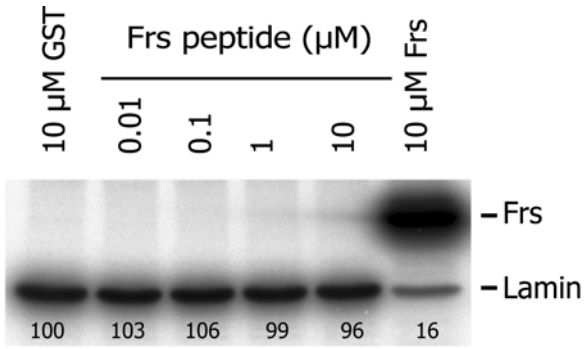

Figure 45. Competitive kinase assay with Cdk1 immunocomplexes titrated by increasing amounts of Frs C16 peptide. It was found that Frs C16 peptide does not inhibit Cdk1 kinase activity. Cdk1 was immunoprecipitated from embryonic lysate by anti-Cdk1 serum, incubated with LaminDmO substrate and increasing amounts of Frs C16 peptide. As a negative control (100 = 100%) GST protein was used (first line). GST-Frs was used as a referee control (last line). All reactions were performed in the kinase buffer with [^{32}P] γ-ATP and analysed by SDS-PAGE and autoradiography. Relative [^{32}P] incorporation by the substrates is indicated below the respective bands.

As it was demonstrated before, Frs C16 peptide affects Frs-CycA complex formation *in vitro* (Figure 31). The competitive kinase assay showed that Frs C16 peptide does not inhibit the Cdk1 kinase activity even at high 10µM concentration what shows that the hydrophobic patch is not required for LaminDmO substrate interaction with Cdk1 and most likely with two other model substrates HistoneH1 and Rb used in the previous kinase assay experiments.

2.12 Frs is a Cdk substrate *in vitro*

The kinase assay experiments revealed that Frs is also a Cdk substrate *in vitro* (Figures 37, 41 and 45). The question was then whether the observed phosphorylation of Frs has any functional meaning. In order to examine whether Frs phosphorylation affects Frs-CycA complex formation an *in vitro* binding assay with phosphorylated and unphosphorylated GST-Frs forms was performed. Frs86ASA allele was used as a non-binding control. The GSH beads coupled with Frs and Frs86ASA were mixed and incubated for 20min at 25ºC with ProteinA beads

coupled or not coupled with Cdk1 immunocomplexes in kinase buffer that contained [^{32}P] γ-ATP prior to the binding test with [^{35}S] labelled CyclinA (Materials and Methods). GSH bound and unbound fractions were analysed by SDS-PAGE and autoradiography (Figure 46).

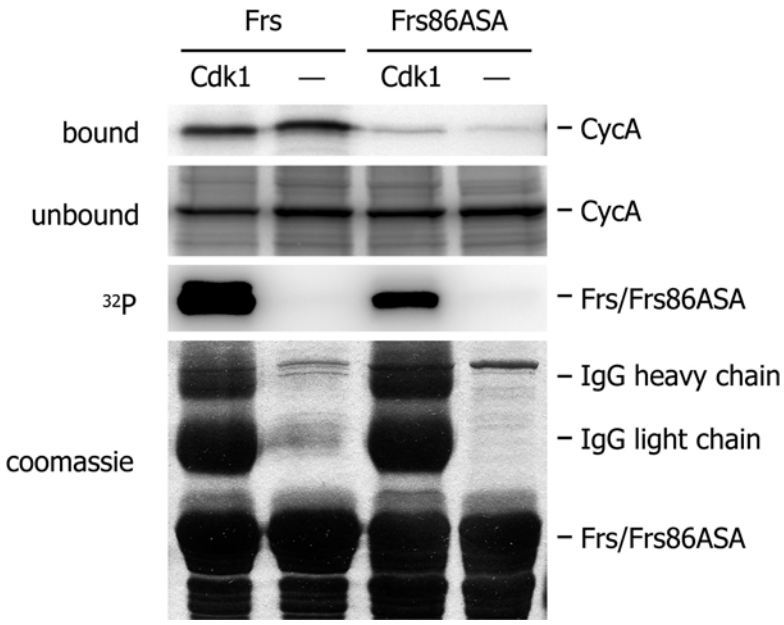

Figure 46. *In vitro* binding assay with phosphorylated and unphosphorylated forms of GST-Frs and [^{35}S] labelled *Drosophila* CyclinA. It was found that phosphorylated and non phosphorylated GST-Frs equally bind to [^{35}S] labelled *Drosophila* CyclinA (bound panel). GST-Frs and GST-Frs86ASA were used as baits. Unbound fractions and coomassie gel are shown as protein loading controls. Autoradiography (^{32}P) panel is shown as a Cdk1 kinase phosphorylation activity control.

The *in vitro* binding assays with phosphorylated and unphosphorylated Frs revealed that both forms equally bind to [^{35}S] labelled *Drosophila* CyclinA. This result together with Frs C16 competitive kinase assay (Figure 45) suggests that Frs might inhibit the Cdk1 and Cdk2 kinase activity via competition on the Cdk catalytic centre with the phosphorylation substrates used in the assay. In order to test this hypothesis, Frs phosphorylation sites were determined and a hypo-phosphorylated mutant was constructed. To determine the phosphorylation sites of Frs mass-spectroscopy analysis was applied. The Cdk1 phosphorylated and unphosphorylated forms of GST-Frs were subjected to SDS-PAGE and digested with trypsin. Cleaved peptides were separated with nanoHPLC system, high voltage protonised and analysed by mass-spectroscopy (Materials and Methods, figure 47).

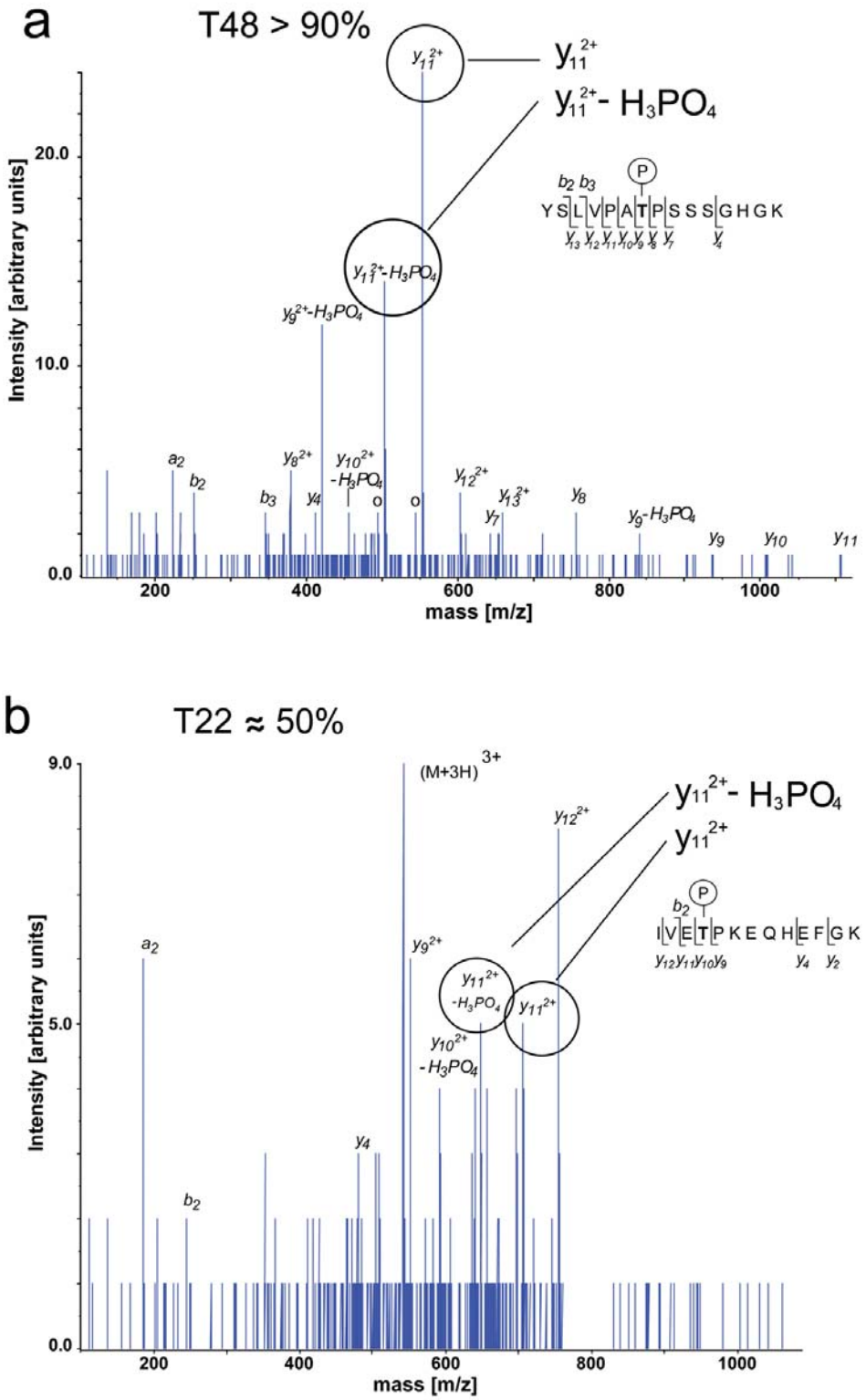

Figure 47. Mass-spectroscopy analysis of phosphorylated and unphosphorylated forms of Frs. GST-Frs phosphorylated by Cdk1 was trypsinized from SDS-PAGE gel, separated by nanoHPLC system and analysed by mass-spectroscopy. Unphosphorylated form of GST-Frs was used as a negative control. Mass-spectroscopy analysis revealed that Frs is phosphorylated at T48 (**a**) and T22 (**b**). Axis Y presents the intensity of the signal (arbitrary units), axis X presents the mass of the analyzed peptides (m/z is mass of peptide divided by charge of the ions). Each peak represents one peptide signal. Rings indicate spectra with and without phosphate groups. This experiment was done in cooperation with the ZMBH Core Facility for Biomolecular Chemistry division (Dr. Thomas Ruppert).

The mass difference between phosphorylated and unphosphorylated 11 amino acid Frs peptides was about 40 m/z (mass of peptide divided by charge of the ions). If the molecular weight of a phosphate group is 80Da and the peptide is double charged it means that the peptide contains one bound phosphate group (80Da : 2 ions = mass shift 40 m/z).

The mass-spectroscopy analysis revealed that Frs has two main phosphorylation residues, threonine 48 (Figure 47a) and threonine 22 (Figure 47b). It was also found that T48 is almost completely phosphorylated and T22 at about 50% under *in vitro* conditions. Both phosphorylated sites match the T/SP Cdk1 consensus sequence that is required for the substrates to be phosphorylated by Cdk1. To confirm the mass-spectroscopy data, Frs48A and Frs22A48 mutants, where T22 and T48 residues of Frs were submitted to alanines, were created by site-directed mutagenesis. Subsequently, the phosphorylation levels of both alleles were tested *in vitro* in the kinase assay. Wild-type Frs and Cyclin non-binding Frs86ASA alleles were used as a referee (Materials and Methods, figure 48).

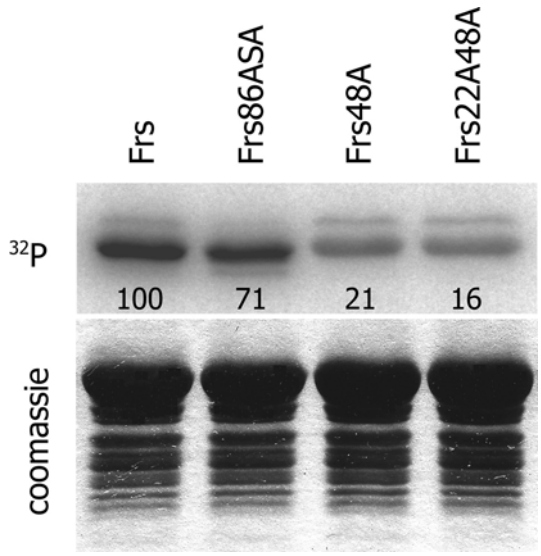

Figure 48. Kinase assay with equal amounts of GST-Frs, GST-Frs86ASA, GST-Frs48A and GST-Frs22A48A alleles phosphorylated by Cdk1. Frs22A48A allele with both its main phosphorylation sites mutated, is about five times less phosphorylated compare to the wild-type (^{32}P). GST-Frs was used as a fully phosphorylated referee (100 = 100%). The phosphorylation levels of the proteins were measured after SDS-PAGE and autoradiography. Coomassie gel is shown as a protein loading control.

The kinase phosphorylation test of Frs, Frs86ASA, Frs48A and Frs22A48A alleles showed that phosphorylation of Frs22A44A mutant is reduced to about 10-20% compared to the wild-type Frs (Figure 48). If we now consider that the unspecific kinase activity background of the IgG antibodies couplet with ProteinA sepharose used for Cdk1 immunoprecipitation equals about 14% (see Figure 37), we can assume that for Cdk1 kinase, Frs22A48A is a non-phosphorylating form of Frs.

The next question was then whether Frs phosphorylation affects Cdk kinase activity. To test the influence of non-phosphorylating Frs22A48A mutant on the Cdk1 activity the kinase assay was performed. Equal amounts of Cdk1 immunocomplexes were incubated with increasing concentrations of Frs22A48A and with LaminDmO in kinase assay buffer with [^{32}P] γ-ATP. Wild-type Frs and Frs86ASA alleles were used as a referees (Materials and Methods, figure 49).

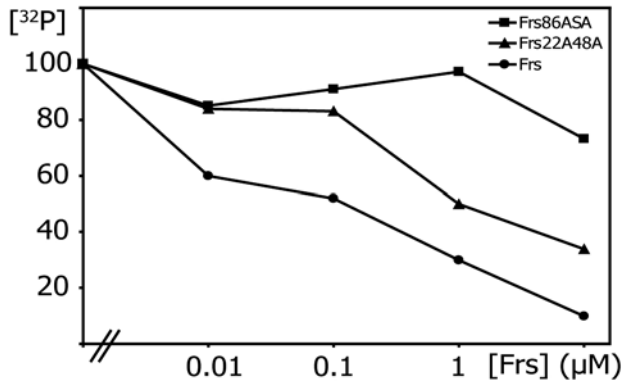

Figure 49. The diagram presents Cdk1 kinase activity in the presence of increasing amounts of GST-Frs, GST-Frs22A48A and GST-Frs86ASA. Frs22A48A is about 10x less active compare to the wild-type. The Cdk1 immunocomplexes were incubated with Lamin in kinase buffer and [^{32}P] γ-ATP. Relative degree of phosphorylation was quantified following SDS-PAGE and autoradiography.

The kinase assay with Cdk1 and Frs22A48A mutant revealed that the non-phosphorylating Frs allele is about 10 times less active compared to the wild-type Frs. Ten times higher amount of Frs22A48A protein was required for inhibition of Cdk1 kinase activity. In addition, Frs86ASA allele that does not bind to the cyclins was much less active even at high concentrations (Figure 49) what suggests that for efficient Cdk1 inhibition *in vitro*, Frs has to be bound to the Cyclin. This hypothesis seems to be true especially if we also consider the fact that Frs86ASA is usually much less phosphorylated in the kinase assay compared to the normally bound to cyclin wild-type form of Frs (Figure 41).

It was estimated before that during mid-cellularisation stage Frühstart reaches approximately 100nM concentration *in vivo* (Figure 29), whereas the *in vitro* kinase assay data showed that Frs is able to inhibit Cdk1 kinase activity at about ten times higher concentration (Figure 49). In consequence, unphysiologically high concentration of Frs may inhibit Cdk phosphorylation by substrate competition *in vitro*. This shows that the cyclin hydrophobic patch is not critical for the recognition of the used in the kinase assay model substrates *in vitro*.

The next question was whether it is possible to find substrates the phosphorylation of which is independent of even high Frs concentration *in vitro*. In order to find such substrates, the kinase

assay with Cdk1 and total embryonic protein extract was done (Materials and Methods, figure 50).

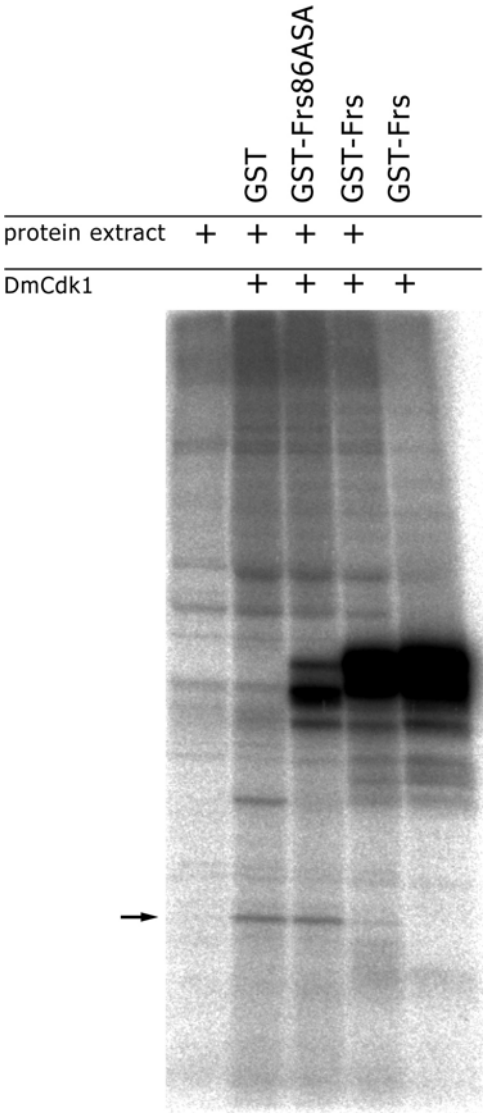

Figure 50. Kinase assay of embryonic total protein extract with Cdk1. Cdk1 immunoprecipitates were incubated with embryonic total protein extract and GST-Frs in the kinase buffer containing [^{32}P] γ-ATP. As controls equal amounts of GST and GST-Frs86ASA were used. The first line shows [^{32}P] γ-ATP incubated with total protein extract only to demonstrate the kinase activity of internal kinases. The last lane shows Cdk1 immunocomplexes incubated with GST-Frs to present Cdk1 kinase activity. It was found that at least one Cdk1 substrate is inhibited by GST-Frs (black arrow) and is not inhibited by control proteins GST and GST-Frs86ASA.

One undefined Cdk1 substrate that is affected by Frs and is not affected by control proteins GST and Frs86ASA was found in the kinase assay with embryonic total protein extract (Figure 50). Unfortunately, no protein that is substrate of Cdk1 and is not inhibited by Frs was detected. Moreover, this experiment showed that in the *Drosophila* embryo there are some Cdk1 substrates (at least one) that are inhibited by Frs. The limitation in this experiment was the high [^{32}P] background that made phosphorylated proteins hard to detect.

The purity of the proteins used in the kinase assays is demonstrated in figure 51.

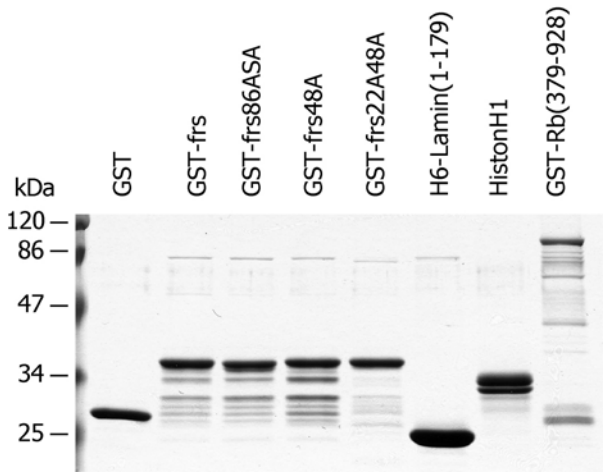

Figure 51. Polyacrylamide gel with *E.coli* purified protein preparations used in the kinase assays. 2µg of each protein were analysed by 12% SDS-PAGE and stained with Coomassie to demonstrate the purity (Cloning and purification procedures are described in detail in the materials and methods section of this work).

2.13 Binding of Frs to the Cyclins is essential for its function *in vivo*

To test whether 86KxL, 11LxxL motifs and the two phosphorylating threonines (T22 and T48) of *frs* play an essential role for *frs* mitotic function *in vivo*, *frs*86ASA, *frs*11AxxA and *frs*22A48A mutations were introduced into genomic rescue constructs and tested for their ability to complement the *frs* ventral furrow phenotype. The embryos from the C(3) x *frs* rescue constructs crosses were fixed, stained with β -galactosidase and phospho-histone3 and counted for premature mitosis in the mesoderm anlage and proper ventral furrow formation according to Großhans et al., 2003 (Materials and Methods, table 7).

Table 7. Statistics of ventral furrow rescue phenotype embryo stainings.

Genotype of male	normal VF	open VF	penetrance (%)
Df *frs*/TM3,hb	100	78	88
frs^{+};Df *frs*/TM3, hb	120	20	28
*frs*86ASA;Df *frs*/TM3, hb	59	53	94
*frs*11AxxA;Df *frs*/TM3, hb	121	19	27
*frs*22A48A;Df *frs*/TM3, hb	55	25	62

The numbers indicate amounts of embryos obtained from C(3) flies crossed with *frs* rescue transgenes (Genotype of male) that were scored for proper ventral furrow formation according to Grosshans et al. 2003. The penetrance means percentage of the homozygous for *frs* transgene embryos that rescue ventral furrow phenotype. The embryos were stained with β -galactosidase and phospho-histone3. Only embryos without β-galactosidase staining were scored as deficient for endogenous wild-type *frs*. In this class the expected proportion of Df *frs* hemizygous embryos is 50%.

The ventral furrow rescue phenotype data showed that the wild-type sequence and the *frs*11AxxA allele (where the putative NES is mutated) complemented, whereas the *frs*86ASA allele did not complement (Table 7), suggesting that the physiological function of *frs* requires binding to the hydrophobic patch of cyclins. Nevertheless, *frs*11AxxA allele still showed cytoplasmic localization (Figure 53c and d) what suggests that mutation of two leucines among the putative nuclear export signal is not sufficient to disrupt *frs* nuclear export activity. To test whether *frs* nucleocytoplasmic localization plays or does not play a role in the *frs* anti-mitotic activity it might be necessary to mutate the third leucine that belongs to the putative NES sequence. If *frs*11AxxAxxA allele would not be exclusively cytoplasmic anymore the *frs* ventral furrow rescue experiment with this transgene should finally clarify the connection between *frs* localization and *frs* anti-mitotic function *in vivo*. Another possible way to test the correlation between *frs* function and localization might be the *frs* ventral furrow rescue experiment with transgenic flies expressing GFP-*frs* fusion protein. The GFP-*frs* fusion protein is accumulating exclusively in the nucleus when expressed in *Drosophila* Schneider cells or human HeLa cells (Figure 52a and 52b).

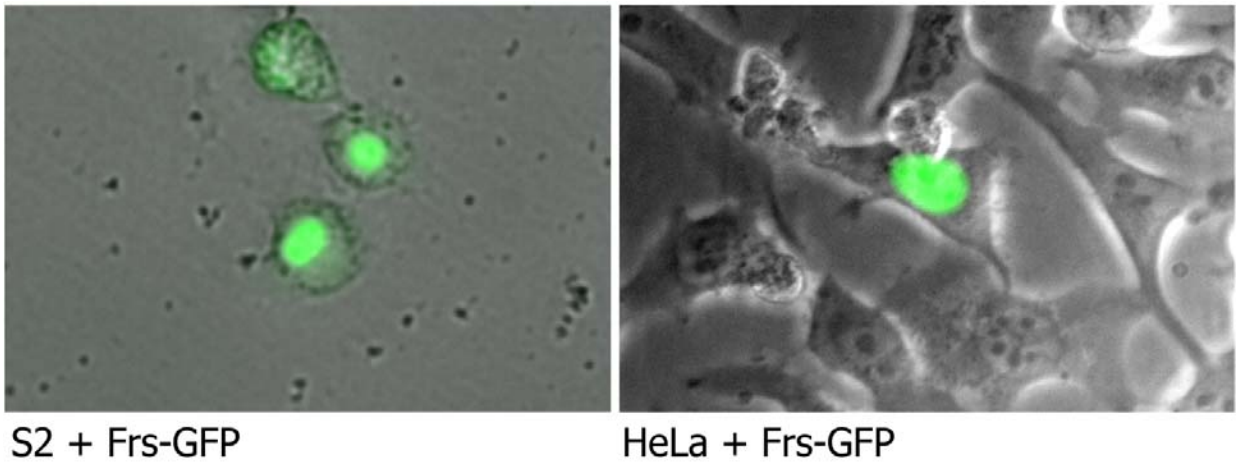

Figure 52. Cell culture expression of GFP-*frs* constructs. **a**) *Drosophila* Schneider cells expressing GFP-frs fusion protein. **b**) Human HeLa cells expressing GFP-frs fusion protein.

It has not been tested yet whether GFP-*frs* construct is still functional in the fly, but this might be possible to check by injecting early *Drosophila* embryos with *in vitro* translated GFP-*frs* RNA (according to method described already by Grosshans et al., 2003).

*frs*22A48A transgene complemented the *frs* ventral furrow phenotype only to about 60% (Table 7). The explanation for this could be that phosphorylation of Frs by Cdk1 somehow contributes to the Frs mitotic phenotype or that the *frs*22A48A allele used for the assay had lower expression level of the transgene (Figure 53f).

For proper interpretation of the ventral furrow phenotype rescue data it was necessary to check whether the *frs* transgenes that were used in the assay are expressed in the embryo and whether the expression levels of all of them are comparable. In order to test the expression levels of the *frs* transgenes, stage 5 embryos were stained with anti-Frs antibodies. Additionally, an anti-β -galactosidase antibody staining was done to distinguish the embryos that are deficient for endogenous Frs protein (Materials and Methods, figure 53).

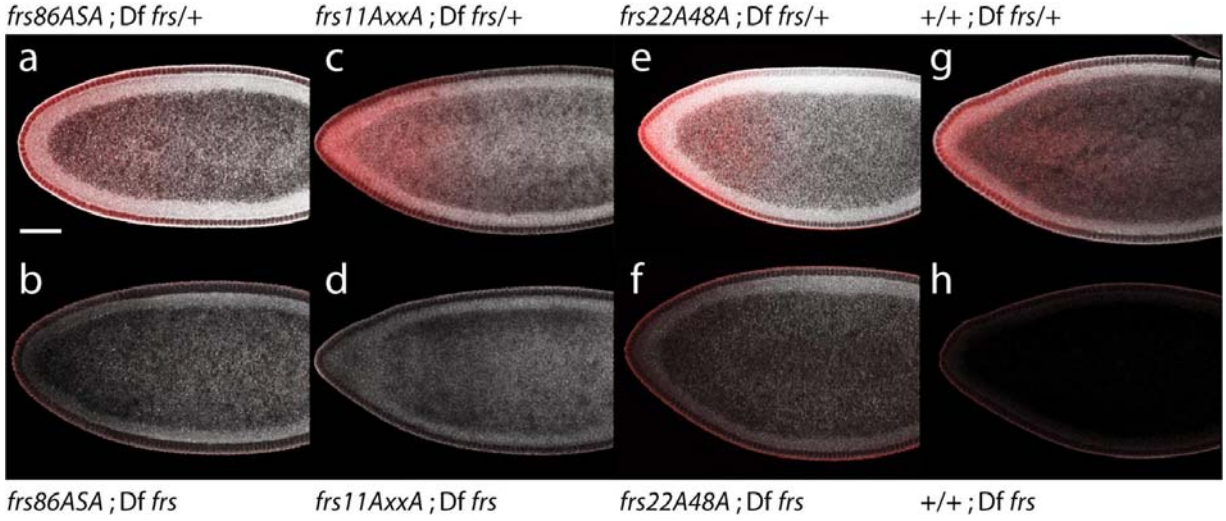

Figure 53. Expression test of *frs* transgenes used in the VF rescue phenotype assay. Embryos from stocks carrying *frs* deficiency and *frs*$^{+}$ transgenes were fixed and stained with Frs (white) and β-galactosidase (red) antibodies (Materials and Methods). Endogenous Frs deficient embryos were distinguished by the absence of β-galactosidase staining. Scale bar represents 50μm. Genotypes of stained transgenes: **a**) *frs*86ASA ; Df(3L)BK10 / TM3, hb-lacZ, **b**) *frs*86ASA ; Df(3L)BK10 / Df(3L)BK10, **c**) *frs*11AxxA ; Df(3L)BK10 / TM3, hb-lacZ, **d**) *frs*11AxxA ; Df(3L)BK10 / Df(3L)BK10, **e**) *frs*22A48A ; Df(3L)BK10 / TM3, hb-lacZ, **f**) *frs*22A48A ; Df(3L)BK10 / Df(3L)BK10, **g**) +/+ ; Df(3L)BK10 / TM3, hb-lacZ, **h**) +/+ ; Df(3L)BK10 / Df(3L)BK10.

The Frs antibody staining with *frs*86ASA (Figure 53a and 53b) and *frs*11AxxA (Figure 53c and 53d) transgenes demonstrated proper Frs expression levels. *frs*22A48A transgene (Figure 53e and 53f) showed slightly lower level of Frs expression compared to the *frs*86ASA and *frs*11AxxA. As a negative control, embryos deficient for Frs were stained (Figure 53g and 53h) and no Frs staining was observed (Figure 53h).

The test of Frs expression level of the transgenes positively confirmed the ventral furrow rescue phenotype data (Table 7). The lower expression level of Frs22A48A transgene compared to the rest of tested transgenes might explain the not complete rescue of the ventral furrow phenotype.

3. Frühstart is G2/M specific inhibitor *in vivo*

3.1 Ectopically expressed Frs during the last (16th) zygotic division blocks mitosis but does not affect S-phase

In order to put the *in vitro* data into a physiological context, the cell cycle specificity of Frs *in vivo* was defined. In *frs* mutant embryos the precocious 14th mitosis during ventral furrow formation showed that Frs inhibits entry into mitosis (Großhans et al. 2000). The question then was in which step of the cell cycle Frs acts. Does Frs directly inhibit only the G2/M transition or are G1/S and S phases also affected? To determine whether *frs* also affects the S-phase of the cell cycle, it was ectopically expressed in a striped pattern during mid-embryogenesis (stage 10). The ectopic expression of Frs inhibited the last zygotic cell cycle (cycle 16) as shown by 50% reduced cell density. Moreover, the embryos did not show inhibition of S-phase because BrdU was incorporated in S phase 16 (Appendix 2b and 2c., Großhans J.).

3.2 Wing imaginal disc epithelial cells that ectopically express *frs* are bigger and have a several fold higher DNA content compared to the wild-type

For further analysis of the *frs* phenotype, *frs* was ectopically expressed in the epithelial cells of wing imaginal discs. This expression revealed strong morphological defects in pupal wing discs and adult wings. Microscopy analysis showed that disc cells were several times larger and had bigger nuclei with enormously strong DNA staining compared to the wild-type. Moreover, the wing hairs were grouped and had disturbed polarity (Appendix 3b and 3c., Großhans J.).

To confirm the Frs ectopic expression phenotype in the epithelial cells of wing imaginal discs the FACS analysis was done (Figure 54). Wing imaginal discs from third instar larvae (Figure 54a and 54b) were dissected and trypsinized (Materials and Methods). Following staining with Hoechst, cells were sorted according to the GFP signal (Figure 54c and 54d) and analysed according to cell size (Figure 54e) and DNA staining (Figure 54f).

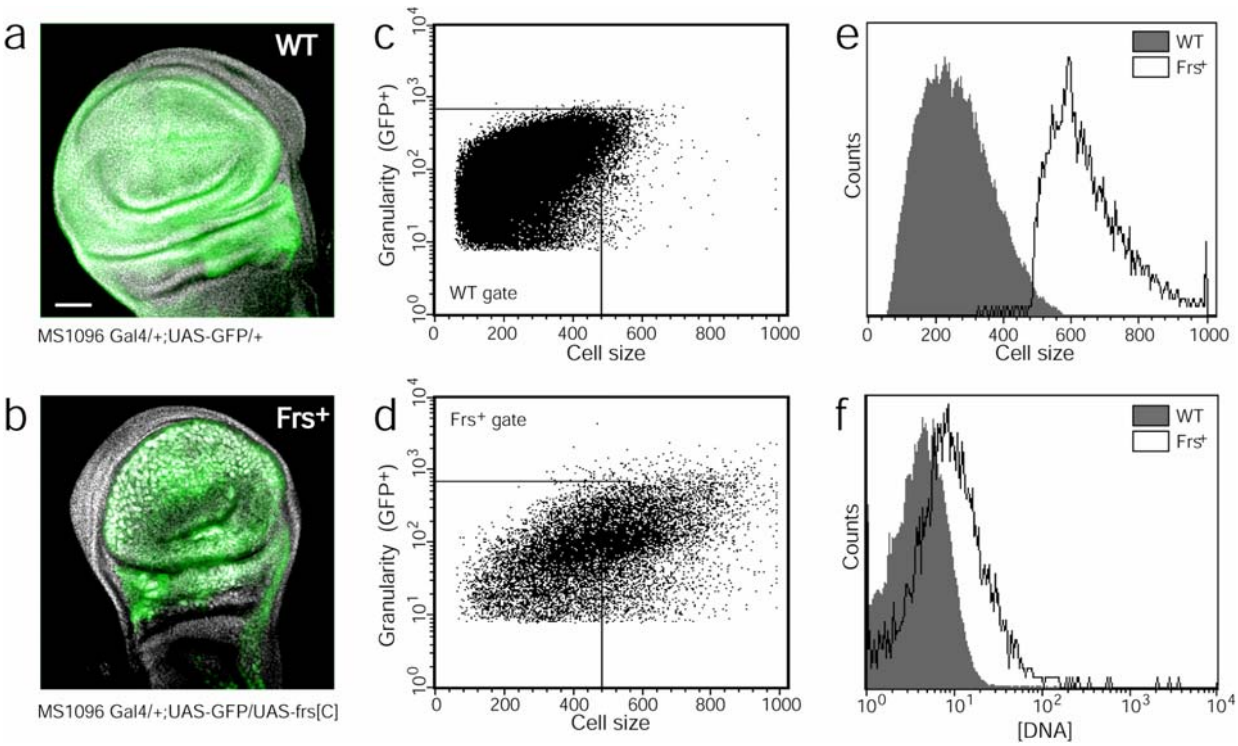

Figure 54. Ectopic expression of *frs* in the epithelial cells of wing imaginal discs. **a, b**) *frs* expression domains are indicated by GFP expression signal (green), DNA (white). **c, d**) Dissociated cells of larval wing discs that did or did not express Frs were stained with Hoechst, sorted by GFP expression and analysed according to cell size (**e**) and DNA staining (**f**). Selected cell population from the discs without Frs (**c**, WT gate) and population of large cells from the *frs* expressing discs (**d**, Frs+ gate) were analysed. Scale bar represents 50µm. Genotypes: **a**) w,1096-Gal4 ; UAS-GFP. **b**) w,MS1096-Gal4/+; UAS-GFP/UAS-frs[C].

The FACS analysis complemented the previous microscopy observations. The epithelial wing imaginal disc cells with ectopically expressed Frs were several times bigger and indeed contained several times more DNA compared to the wild-type cells (Figure 54e and 54f). The higher DNA content suggests that in the wing epithelial cells *frs* induces endocycles what is typical Cdk1 or CycA in *Drosophila* and mitotic Cdk phenotype in yeast (Sauer et al. 1995; Hayashi et al. 1996; Weigmann et al. 1997; Vidwans et al. 2002).

3.3 Larval salivary gland cells ectopically expressed *frs* show normal growth of the tissue compare to the wild-type

To test whether *frs* has an effect on the naturally occurring endocycles, ectopic expression of *frs* in *Drosophila* larval salivary glands was performed (Figure 55).

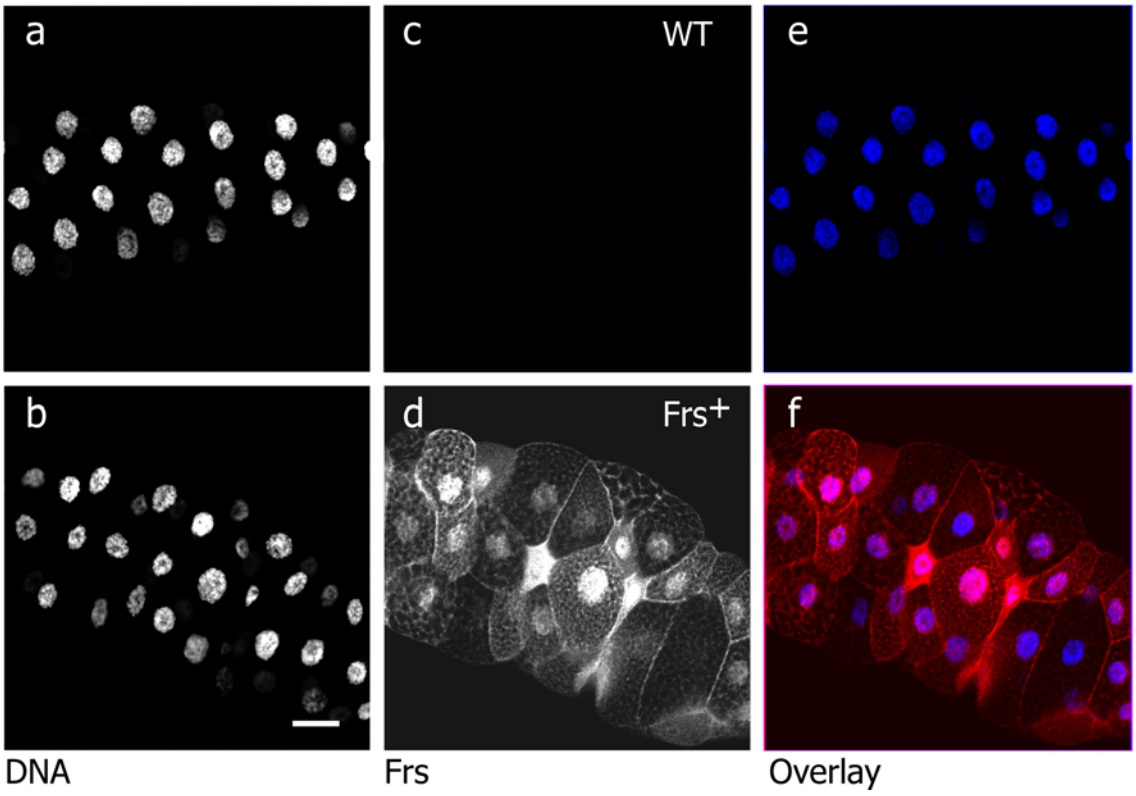

Figure 55. Ectopic expression of *frs* in third instar larval salivary glands. Ectopic expression of *frs* does not affect salivary glands formation and naturally occurring endoreplication. The glands were stained for DNA with DAPI (**a**,**b**., white or blue if overlay) and for Frs (**c**,**d**., white or red if overlay). Scale bar 50 µm. Genotypes: WT - w;patched-Gal4. Frs+ - patched-Gal4/UAS-frs[C].

This experiment showed that ectopic expression of *frs* allowed the growth of the salivary gland tissue (Figure 55b, 55d and 55f), what indicates that ectopic *frs* does not affect naturally occurring endocycles. To test the expression pattern of UAS-*frs* in the salivary glands of patched-Gal4 line, the UAS-GFP transgene was used first and analysed according to GFP localization and expression level. Transgenic patched-Gal4/UAS-GFP salivary glands showed strong and ubiquitous expression of GFP marker protein (data not shown).

4. Frühstart genetically interacts with CycA, CycB, CycB3 and CycE

4.1 Frühstart genetically interacts with CycB3 in the *Drosophila* eyes

A genetic interaction test was performed in order to further analyse the biological function of Frühstart in the fly. *Drosophila cyclinA, cyclinB, cyclinB3* and *cyclinE* genes were over-expressed in the *Drosophila* eyes with and without ectopically expressed *frs*. In this experiment GMR-Gal4 flies were crossed with UAS-*frs*[I], UAS-*cycA*, UAS-*cycB*, UAS-*cycB3* and UAS-*cycE* transgenes (Materials and Methods). Surprisingly, only mitotic *cycB3* showed genetic interaction with Frs (Appendix 4., Bartoszewski S.). Over-expression of *cyclins A, B, B3, E* and *frühstart* in the eyes separately caused a rough eyes phenotype (e.g. appendix 4a. for *frühstart*,

4b. for cycB3. Bartoszewski S.). When *cyclins A, B,* or *E* were over-expressed together with *frs* no rescue phenotype was observed (data not shown), whereas cyclinB3 over-expressed together with *frs* restored the rough eye phenotype to wild-type. This demonstrates that *frs* genetically interacts with *cycB3* in the *Drosophila* eye. To confirm eyes genetic interaction data, *cycA*, *cycB*, *cycB3*, *cycE* and *frs* were also over-expressed in the epithelial cells of *Drosophila* wings (Figure 56).

4.2 Frühstart genetically interacts with *cycA, cycB* and *cycE* in the *Drosophila* wing imaginal discs

To reconfirm genetic interaction data achieved in the *Drosophila* eyes the genetic interaction of *frs*, *stg*, *cycA*, *cycB*, *cycB3*, and *cycE* genes were tested in the wings (Figure 56).

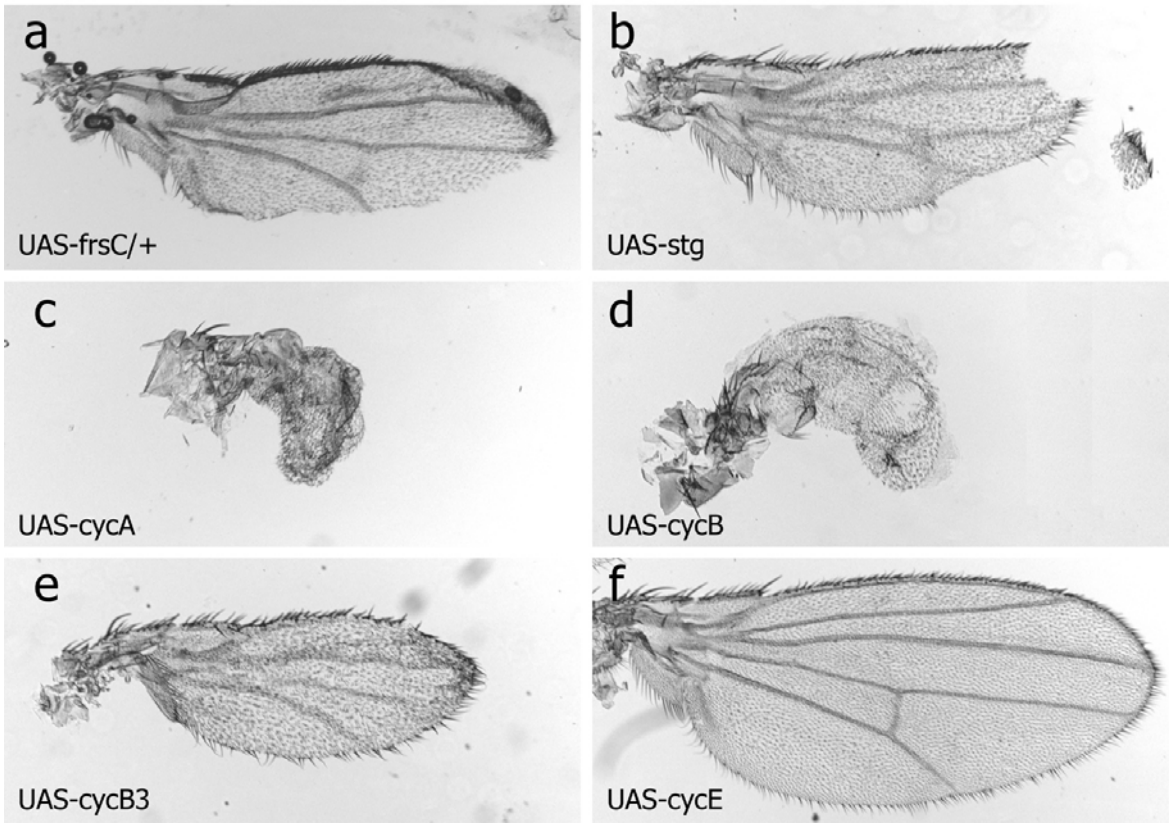

Figure 56. The pictures present *Drosophila* wings with ectopically expressed *frühstart* alone (**a**) or in the presence of *stg* (**b**), *cycA* (**c**), *cycB* (**d**), *cycB3* (**e**) or *cycE* (**f**) co-expressed genes. It was found that in the *Drosophila* wings *frs* genetically interacts with *cycA*, *cycB* and *cycE*. Genotypes: **a**) w,MS1096-Gal4/+;UAS-*frs*C/+. **b**) w,MS1096-Gal4/+;UAS-*frs*C/+;UAS-*stg*/+. **c**) w,MS1096-Gal4/+;UAS-*frs*C/UAS-*cycA*. **d**) w,MS1096-Gal4;UAS-*frs*C/UAS-*cycB*. **e**) w,MS1096-Gal4;UAS-*frs*C/UAS-*cycB3*. **f**). w,MS1096-Gal4/+;UAS-*frs*C/+;UAS-*cycE*/+.

When *frs* is ectopically expressed in the wings by MS1096-Gal4 driver, it gives a slightly hypomorphic, contracted wing phenotype (Figure 56a). When it is ectopically expressed in parallel with *string*, the *frs* phenotype is not affected (Figure 56b). *frs* ectopically expressed

together with *cycB3* seems to only very slightly enhance the *frs* phenotype (Figure 56e), the wings become more hypomorphic compared to the wings where *frs* is expressed alone. Two mitotic cyclins, *cycA* and *cycB*, when over-expressed with *frs* strongly enhanced the *frs* phenotype, the size of the wings is severely reduced (Figure 56c and 56d). The G1/S *cycE* gene when over-expressed with *frs* restored *frs* wing phenotype to the wild-type (Figure 56f). It showed that in the assay *frs* genetically interacts with *cycA* (enhanced *frs* phenotype), *cycB* (enhanced *frs* phenotype) and *cycE* (suppressed *frs* phenotype). All analyzed wings were dissected from adult flies, mounted in Hoyers/lactic acid (Materials and Methods; Roberts, D.B. 1998) and observed under bright-field illumination microscope.

Discussion

The aim of this study was biochemical, molecular and genetic characterization of the *Drosophila* CG17962 zygotic gene called z600 (Schulz and Miksch 1989; Schulz et al., 1989; Galewsky et al., 1990) or *frühstart* (Großhans and Wieschaus, 2000). Originally, *frühstart* (*frs*) was identified in screens for mutations that disrupt mesoderm invagination during gastrulation process (Müller et al., 1999; Seher and Leptin 2000). Further analysis revealed that *frs* is a mitotic inhibitor that specifically counteracts protein phosphatase *string* and in this way delays mitosis in the ventral furrow cells. This inhibition prevents the interference of mitotic events and morphogenetic movements during ventral furrow formation (Großhans and Wieshaus 2000). Subsequent studies demonstrated that *frs* is also sufficient and partially required for pausing the rapid nuclear cycles after the last (13th) cleavage division during celularisation (Großhans et al., 2003). The premature entry into mitosis 14 of the ventral cells that affects proper ventral furrow formation in the homozygote mutant of *frs* indicated the physiological function of this gene in G2/M transition in the embryo. Moreover, ectopically expressed *frs* in the epidermal cells of the embryo caused inhibition of the 16th (and last) zygotic mitosis whereas the 16th S-phase occurred normally (Appendix 3, Großhans J.), what once again confirmed the mitotic specificity of *frs*.

This study revealed, at least partially, the molecular mechanism of *frs* anti-mitotic activity and demonstrated how Frs might inhibit Cyclins-Cdk1 activity and mitosis *in vivo*.

In *Drosophila*, full activation of Cdk1 kinase requires its association with a mitotic cyclin (A, B or B3), phosphorylation of Thr 161 in the T-loop domain and dephosphorylation by protein phosphatase String/Twine (Cdc25 homologues) of Thr14 and Tyr15 phosphorylation sites phosphorylated before by Wee1/Myt1 kinases. The molecular features of Frs, like its primary amino acid structure (Frs is not a kinase or phosphatase) and its association with nucleoporins and cyclins suggest that Frs affects Cdk1 kinase activity via protein inhibitory mechanism rather than by Cdk1 phosphorylation. This study showed that Frs negatively regulates entry into mitosis by high affinity binding to the hydrophobic patch of mitotic CyclinA *in vitro* and *in vivo*. The remaining question then is how Frs-CyclinA interaction affects the mitotic function of Cdk1. The first possible explanation could be that Frs acts as a nucleocytoplasmic transport factor that modulates nucleocytoplasmic localisation of mitotic proteins like e.g. Cyclins, Cdk1 or String.

Is Frs a new nucleocytoplasmic transport factor?

Drosophila Cdk1 kinase complex with the only essential mitotic cyclinA (Jacobs et al., 1998) is cytoplasmic during interphase and accumulates in the nucleus during prophase (Lehner et al., 1989; Dienemann and Sprenger 2004). It is then possible that Frs might act as a molecular "anchor" where its C-terminus directly binds to the hydrophobic patch of CycA via the KxL motif and its N-terminus indirectly interacts with nucleoporins and by this interferes with the entry and accumulation of Cdk1 into the nucleus before mitosis 14. Frs might also have an opposite activity and promote the export of Cdk1-cyclin complexes, which can be another way of preventing the nuclear accumulation of Cdk1 that is required for entry into mitosis (Figure 57).

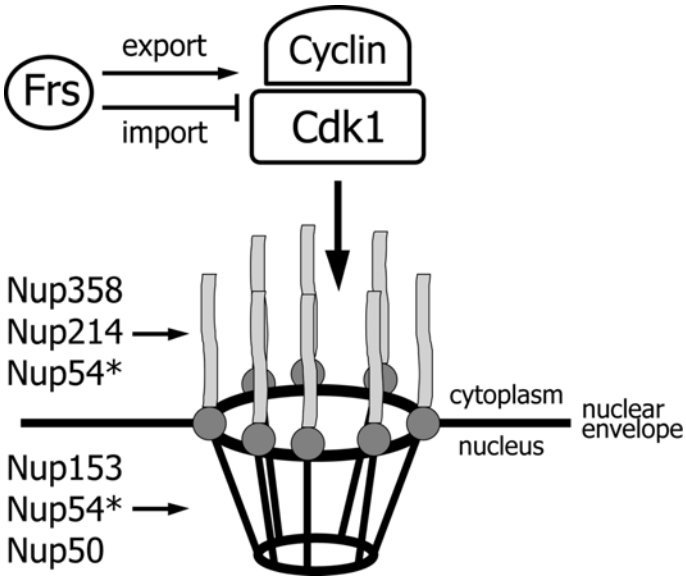

Figure 57. Frs might inhibit nuclear accumulation (import) or promote nuclear exclusion (export) of Cdk1-cyclins complexes before entry into mitosis 14. In the nuclear pore basket model, the nucleocytoplasmic localization of nucleoporins found in *frs* Y2H screen is indicated. *) Nup54 is localized to the cytoplasmic and nuclear parts of the nuclear pore.

This theory is indirectly supported by the fact that Frs interacts with a set of nucleoporins and with the main export factor Crm1 *in vitro* and *in vivo*. The clear association of GFP-Frs with the nuclear envelope in the nuclear export assay performed in permeabilized HeLa cells could also be an argument in favor of the proposed mechanism. Nevertheless, no localization of wild-type Frs to the nuclear envelope in stage 5 embryos where Frs anti-mitotic activity takes place was previously observed (Großhans et al. 2003). There are also several arguments that seem to contradict this hypothetic model.

It is rather unlikely that Frs is a new transport receptor, as it is not a hydrophobic protein like almost all nuclear transport receptors (Görlich and Kutay 1999). Frs is a basic polypeptide that

contains 19 basic residues (Schulz and Miksch 1989; Großhans et al., 2003). In addition, Frs is a cytoplasmic protein, despite its positive charge and its size that is below the 40kDa exclusion limit of the nuclear pores (Großhans et al., 2003; Görlich and Kutay 1999), contains two predicted NLS and NES motifs and is actively exported from the nucleus on the Crm1 dependent way. Moreover, it was published before that almost all nucleoporins (Nup50, Nup214, Nup358, Nup153) that were identified as Frs interactors in the Y2H screen, are involved in the Crm1 nuclear export pathway (Askjaer et al., 1999; Smitherman et al., 2000; Guan et al., 2000; Bernad et al., 2004). The fact that Frs interacts with so many nucleoporins that do not associate with one particular fragment of the nucleopore complex but are spread all over the pore (Fan et al., 1997; Allen et al., 2000; Guan et al., 2000; Cronshaw et al. 2002; Figure 57) might also argue against this theory. Another argument that the interaction of Frs with nucleoporins has no connection to its anti-mitotic activity might be *frs* ventral furrow phenotype rescue experiment data with non-Nup50 interacting frs11AxxA allele that showed complete rescue of the Frs ventral furrow phenotype (Results, table 5). Nevertheless, the *frs*11AxxA allele still showed cytoplasmic localization (Results, figure 53c and d) what suggests that mutation of two leucines among the predicted nuclear export signal is not sufficient to disrupt *frs* nuclear export activity and by this makes difficult to reach a final conclusion. Remarkable might also be an observation made by Smitherman, et al., 2000. They found that another cell cycle inhibitor $p27^{CIP}$ interacts with Nup50 protein in the Y2H screen (similarly to Frs) and that in the Nup50-null mouse embryo fibroblasts $p27^{CIP}$ cell cycle activity is not affected.

Taken together, the above data suggest that Frs is not a new nucleocytoplasmic transport factor and that the observed Frs-nucleoporins interactions are due to its nucleocytoplasmic shuttling.

Does Frs belong to the INK4 cyclin dependent kinase inhibitors family?

Currently, there are two known cyclin dependent kinase inhibitors families, INK4 and KIP/CIP. The INK4 family includes p15, p16, p18 and p19 proteins that specifically bind to Cdk4 and Cdk6 and act as inhibitors of CycD. Crystal structure analysis of p19 - Cdk6 complex (Russo et al., 1998; Brotherton et al., 1998) revealed that mammalian p19 inhibitor binds exclusively to Cdk6 and does not interact with the cyclin subunit. Frs *in vitro* binding assays together with surface plasmon resonance data clearly show that Frs binds with high affinity to the Cyclins and does not stably interact with the kinase subunit, suggesting that Frs does not share a common molecular mechanism with p19 and does not belong to the INK4 inhibitor family.

Is Frs a member of the KIP/CIP cyclin dependent kinase inhibitors family?

Among the members of the KIP/CIP family are the p27, p57 and p21 inhibitors. The best characterized member of this family is the G1/S inhibitor p27 and its *Drosophila* homolog *dacapo*. The 3D structure of p27 revealed that its N-terminus is extended along the surface of huCdk2-CyclinA complex, forming hydrophobic contacts with regions on both cyclin and kinase (Russo et al., 1996; Barberis et al., 2005). p27, similarly to Frs, binds to the Cyclin hydrophobic patch via its KxL motif. This binding blocks the hydrophobic patch that is required for proper phosphorylation of some Cdk protein substrates and Cdk protein inhibitors like Rb (Adams et al., 1999) E2F1 (Adams et al., 1996), p53 (Lowe et al., 2002), p21 (Adams et al., 1996; Chen et al., 1996), p27 (Lowe et al., 2002; Brown et al., 1999), p107 (Zhu et al., 1995; Schulman et al., 1998; Brown et al., 1999) and many more (Loog and Morgan, 2005). In parallel p27 binds to the catalytic center of Cdk2, disrupts its active site and blocks ATP binding to Cdk2 (Russo et al., 1996). Even if both p27 and Frs stably bind with high affinity to the hydrophobic patch of the cyclin subunit (p27-huCycA KD=25nM, Lacy et al. in 2004; Frs-CycA=38nM, this work) it seems that they do not share a common molecular mechanism, because Frs does not bind stably to the Cdk subunit. Moreover, it was found that in the *in vitro* kinase assay Frs inhibits Cdk1 and Cdk2 kinase activity in the micromolar range that is about ten times higher than the binding constants of Frs-CycA, Frs-CycE and Frs-CycA-huCdk2 complex (Results, figure 35). A different activity was exhibited by the p27 inhibitor, which inhibits Cdk2 activity *in vitro* at the nanomolar range that is around its nanomolar binding constant values (Toyoshima and Hunter 1994, Lacy et al. 2004).

Does Frs belong to a new family of inhibitors?

There is also a third, informal and poorly characterized group of cell cycle inhibitors that do not belong to any of the previously described families. This group includes M/G1-S Sic1 (*Saccharomyces cerevisiae*), M/G1 Rum1 (*Shizosaccharomyces pombe*), mitotic Rux (*Drosophila melanogaster*) and G2/M Frs (*Drosophila melanogaster*). It was published before that Sic1, Rum1 and Rux are able to functionally replace each other *in vivo* (Sanchez-Diaz et al., 1998; Foley and Sprenger, 2001) even if there is no obvious sequence homology between these proteins and their sequence similarity is negligible. Nevertheless, all members of the third class of cell cycle inhibitors contain the KxL motif among their primary amino acid sequence (Rux contains even three KxL motifs). Moreover, it was found that Sic1 and Rux, similarly to Frs, directly interact with mitotic cyclins via their RxL motif and specifically inhibit mitotic cyclin-Cdk1 complexes *in vitro* (Hodge and Mendenhall, 1999; Avedisov et al., 2000; Foley

and Sprenger 2000; this work). Additionally, Frs, Sic1 and Rux, when over-expressed, they induce cycles of endoreplication in proliferating epithelial cells of *Drosophila* wing imaginal discs (Foley at al., 1999; Thomas et al., 1997; this work) what shows their common mitotic specificity also *in vivo*. We can also include among their similarities the fact that all of these proteins are non-essential, as they cooperate with other mechanisms such as cyclin proteolysis (for Frs not yet investigated) and that all of them are phosphorylated and subsequently degraded through the ubiquitin-dependent proteolytic pathway (Benito et al., 1997; Verma et al., 1997; Foley et al., 1999; in the case of Frs the significance of its phosphorylation still remains not completely understood). All the similarities described above, might indicate that all these proteins share a common molecular mechanism to inhibit the cell cycle. Nevertheless, there are also some important differences that might suggest that Frs has its own, individual way of regulation the cell cycle.

The zygotic gene *rux* is expressed throughout most of *Drosophila* development at low levels, that cannot be detected by *in situ* hybridization (Foley and Sprenger, 2001), whereas the zygotic gene *frs* is expressed only at the beginning of cell cycle 14, reaches at narrow peak during cellularisation and persists until the end of gastrulation (Großhans et al., 2003). In contrast to *rux*, the level of *frs* mRNA expression is high enough to be easily detect by *in situ* hybridization. Furthermore, Frs is a site-specific inhibitor of mitosis and even if it is ubiquitously expressed all over the embryo, it affects only a narrow stripe of the ventral cells that invaginate to form a mesoderm anlage (Großhans et al., 2003), whereas expression and activity patterns of *rux* tightly match each other (Foley and Sprenger, 2001). Another important difference is the fact that Frs and Rux block two different aspects of mitosis. Frs blocks the entry into mitosis (G2/M transition, Großhans and Wieschaus, 2000) whereas Rux regulates the exit from mitosis (metaphase/anaphase transition, Foley and Sprenger, 2001).

Another important difference between Frs and Rux was revealed by functional assays. *In vitro* kinase assays demonstrated that Frs inhibits mitotic Cdk1 and S phase Cdk2 kinase activity to a comparable degree, whereas when ectopically expressed in the later stages of embryonic development, Frs does not inhibit Cdk2-dependent progression through S phase. In contrast to Frs, Rux does not inhibit Cdk2 kinase activity *in vitro* and when over-expressed in the embryo, it does not inhibit Cdk2-dependent S phase progression (Foley et al., 1999; Thomas et al., 1997). Unfortunately, we still do not have enough molecular data to make clear statements about the inhibitory mechanisms of Sic1, Rum1, Rux and Frs.

This study showed that the anti-mitotic activity of Frs is directly correlated with the function of the hydrophobic patch of mitotic CyclinA. The cyclin non-binding *frs*86ASA allele did not

rescue the *frs* ventral furrow phenotype, what was direct evidence supporting this statement. Further kinase assay analysis with Cdk1 and Cdk2 immunocomplexes revealed that increasing amounts of Frs inhibit the phosphorylation of LaminDmO, Histone H1 and Rb substrates. Phosphorylation of the substrates by Cdk1 and Cdk2 was inhibited to comparable degree, even if the SPR data revealed that Frs preferentially binds to CycA compared to CycE. Another striking observation was that complete inhibition of Cdk1 and Cdk2 kinase activity was achieved only with ten times higher Frs concentration compared to its nanomolar binding constants. This phenomenon suggests that Frs-hydrophobic pocket interaction by itself cannot be the reason of the decrease in Cdk kinase activity. This hypothesis was confirmed by the kinase assay performed with the C16 peptide that contained the last 16 residues of Frs and the KxL motif that compromised Frs-CycA complex formation in the *in vitro* binding assay. In this assay it was shown that even high concentration of C16 peptide (10µM) was not able to affect Cdk kinase activity. This evidence clearly demonstrates that the hydrophobic pocket is not essential for phosphorylation of the substrates used in the *in vitro* kinase assays. The fact that Frs is also a Cdk substrate, might suggest that the observed decrease of the kinase activity at so high Frs concentration is not due to binding to the hydrophobic patch but due to Frs competition on the Cdk catalytic cleft with the phosphorylation model substrates used in the assay. The kinase assay with non-phosphorylating frs22A48A allele revealed that this allele is about ten times less active compared to the wild-type *in vitro* what supports this assumption. In comparison, cyclin non-binding Frs86ASA allele was even less active than Frs22A48A.

These results show that at non physiologically high concentration Frs may inhibit Cdk kinase activity by competing on the catalytic cleft of Cdk with other substrates *in vitro*. It also suggests, that in order to achieve efficient inhibition of Cdk1 kinase activity by Frs, binding of Frs to the hydrophobic pocket of the cyclins is at least partially required *in vitro*. The question that naturally followed was then whether so high phosphorylation of Frs has any functional significance. It was found in the *in vitro* binding assay, that the prephosphorylated form of Frs interacts with CyclinA as strongly as the unphosphorylated form, what shows that Frs phosphorylation does not affect Frs-CycA complex formation. Moreover, the rescue construct carrying the Frs22A48A allele rescued up to 62% mitotic ventral furrow phenotype of Frs, what implies that phosphorylation of Frs has a functional meaning, even if it is not a major aspect of the anti-mitotic activity of Frs in the mid-blastula embryo.

Taking all together, a possible role of Frs in the inhibition of mitotic Cyclin-Cdk1 complexes might rely on occupying the hydrophobic pocket on the Cyclin subunit what would block the cyclin binding site for an undefined yet group of *Drosophila* Cdk1 mitotic substrates that in

order to be efficiently phosphorylated by Cdk1 require to bind to CycA subunit as well. This hypothesis is supported by the fact that there are already identified such Cdk substrates (e.g. Rb, p107 or p27) that to be efficiently phosphorylated by Cdk have to first bind to the hydrophobic pocket on the cyclin subunit (Brown et al., 1999; Lowe et al., 2002; Lacy et al., 2004; Loog et al., 2005).

The reason why in this study we were not able to show Frs substrate specificity is the fact that in general not many Cdk substrates have been identified and characterized so far. I could test only one *Drosophila* specific substrate, LaminDmO, which was far not enough. In parallel, the tested calf HistoneH1 and human Rb substrates did not solve this problem either.

The substrate specificity correlated with hydrophobic pocket function was recently described in detail in the yeast. Loog and Morgan, 2005 demonstrated that mitotic Cdk1-Clb2 complex equally phosphorylates all 150 substrates tested in the kinase assay, whereas in the case of G1/S Cdk1-Clb5 there was a group of about 24% of the substrates containing the KxL motif that were more strongly phosphorylated in comparison to the rest of the substrates. We then wondered, whether similar situation exists in *Drosophila*. It is possible that most of the mitotic Cdk1 kinase substrates are phosphorylated by direct interaction with the kinase (Figure 58a) and blocking the hydrophobic pocket by Frs does not affect their phosphorylation level (Figure 58b). Nevertheless, the phosphorylation of a small group of yet undefined *Drosophila* Cdk1 substrates that in order to be efficiently phosphorylated (activated) first have to bind to the cyclin hydrophobic pocket (Figure 58c), might be inhibited by Frs (Figure 58d).

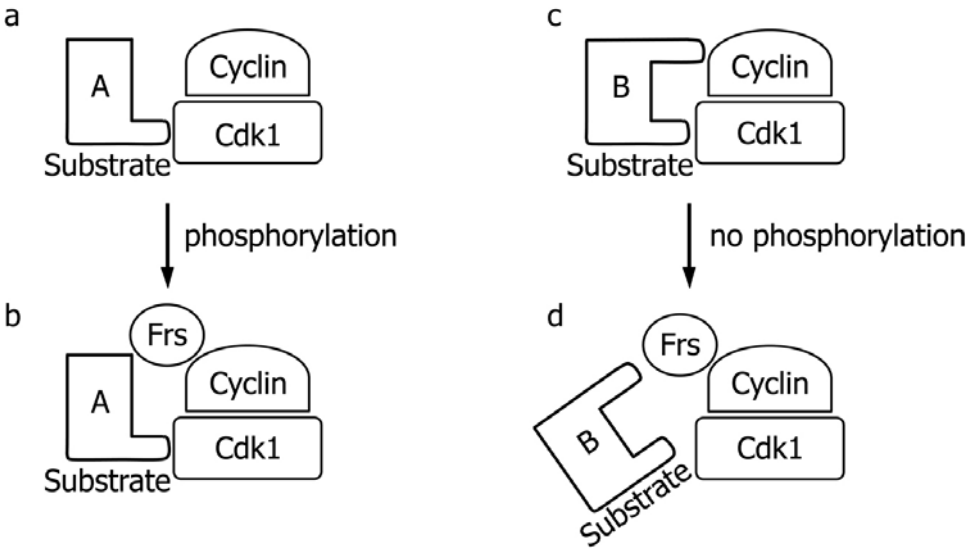

Figure 58. Molecular model of the inhibitory mechanism of Frs. Substrates without KxL motif like HistoneH1 are phosphorylated normally without (**a**) and with Frs (**b**). The mitotically specific substrates with KxL motif are properly phosphorylated without Frs (**c**) and are not properly phosphorylated in the presence of Frs. Substrate A is equally phosphorylated with or without Frs (**a** and **b**) whereas Substrate B phosphorylation is inhibited (weakened) by blocking of the hydrophobic patch by Frs (**c** and **d**).

The substrate specificity that is observed in yeast may contribute a potential explanation for the Frs-Cyclin hydrophobic patch interaction requirement in the embryo, with the difference that in the yeast it plays a role in the G1/S transition whereas in *Drosophila* it is important for the entry into mitosis. Further proteomic studies can reveal more *Drosophila* Cdk1 and Cdk2 specific substrates, thus leading in the elucidation of not only anti-mitotic function of Frs but also another *Drosophila* mitotic inhibitor, Rux.

Literature

Adachi, Y., and Yanagida, M. Higher order chromosome structure is affected by cold-sensitive mutations in a *Schizosaccharomyces pombe* gene *crm1*C which encodes a 115-kD protein preferentially localized in the nucleus and its periphery. *J. Cell Biol.* 108, 1195–207 (1989).

Adams, P.D., Sellers, W.R., Sharma, S.K., Wu, A.D., Nalin, C.M., and Kaelin, W.G. Jr. Identification of a cyclin - cdk2 recognition motif present in substrates and p21-like cyclin-dependent kinase inhibitors. *Mol Cell. Biol.* **16**, 6623-6633 (1996).

Adams, P.D., Li, X., Sellers, W.R., Baker, K.B., Leng, X., Harper, J.W., Taya, Y., and Kaelin W.G. Jr. Retinoblastoma protein contains a C-terminal motif that targets it for phosphorylation by cyclin-cdk complexes. *Mol. Cell. Biol.* **19**, 1068-1080 (1999).

Alberts, B., Johnson, A., Lewis, J., Raff, M., Roberts, K., and Walter, P. Molecular biology of the cell. In: The cell cycle and programmed cell death. Published by Garland Science NY, pp. 995-996 (2002).

Allemand, E., Dokudovskaya, S., Bordonne, R., and Tazi, J. A conserved Drosophila transport-serine/arginine-rich (SR) protein splicing factors and their antagonist repressor splicing factor 1. *Mol. Biol. Cell* **13**, 2436-2447 (2002).

Allen, T. D., Cronshaw, J. M. Bagley, S., Kiseleva, E., and Goldberg, M. W. The nuclear pore complex: mediator of translocation between nucleus and cytoplasm. *J. Cell Sci*. **113**, 1651-1659.

Ashburner, M. Drosophila, a Laboratory Handbook. Published by Cold Spring Harbor, NY (1989).

Askjaer, P., Bachi, A., Wilm, M., Bischoff, F. R., Weeks, D. L., Ogniewski, V., Ohno, M., Niehrs, C., Kjems, J., Mattaj, I. W., Fornerod, M. RanGTP-regulated interactions of CRM1 with nucleoporins and a shuttling DEAD-box helicase. *Mol. Cell. Biol*. **19**, 6276-6285 (1999).

Avedisov, S. N., Krasnoselskaya, I., Mortin, M., Thomas, B. J. Roughex mediates G1 arrest through a physical association with cyclin A. *Moll. Cell Biol*. **20**, 8220-8229 (2000).

Barberis, M., de Gioia, L., Ruzzene, M., Sarno, S., Coccetti, P., Fantucci, P., Vanoni, M., and Alberghina, L. The yeast cyclin-dependent kinase inhibitor Sic1 and mammalian $p27^{Kip1}$ are functional homologues with a structurally conserved inhibitory domain. Biochem. J. 387, 639-647 (2005).

Benito, J., Martín-Castellanos, C. and Moreno, S. Regulation of the G1 phase of the cell cycle by periodic stabilization and degradation of the p25rum1 Cdk inhibitor. *EMBO J.* **17**, 482-497 (1997).

Bernad, R,. van der Velde, H., Fornerod, M., and Pickersgill, H. Nup358/RanBP2 attaches to the nuclear pore complex via association with Nup88 and Nup214/CAN and plays a supporting role in CRM1-mediated nuclear protein export. *Mol. Cell. Biol.* **24**, 2373-2384 (2004).

Bhattacharya, A., and Steward, R. The Drosophila homolog of NTF-2, the nuclear transport factor-2, is essential for immune response. *EMBO Rep*. **3**, 378-383 (2002).

Bogerd, H. P., Fridell, R. A., Benson, R. E., Hua, J., Cullen, B. R. Protein sequence requirements for function of the human T-cell leukemia virus type 1 Rex nuclear export signal delineated by a novel in vivo randomization-selection assay. *Mol. Cell. Biol.* **16**, 4207-4214 (1996).

Brotherton, D. H., Dhanaraj, V., Wick, S., Brizuela, L., Domaille, P. J., Volyanik, E., Xu, X., Parisini, E., Smith, B. O., Archer, S. J., Serrano, M., Brenner, S. L., Blundell, T. L. & Laue, E. D. Crystal structure of the complex of the cyclin D-dependent kinase Cdk6 bound to the cell-cycle inhibitor p19INK4d. *Nature* **395**, 244-250 (1998).

Brown, N.R., Noble, M.E. Endicott, J.A., and Johnson, L.N. The structural basis for specificity of substrate and recruitment peptides for cyclin-dependent kinases. *Nature Cell Biol.* **1**, 438-443 (1999).

Catrein, I., Hermann, R., Bosserhoff, A., and Ruppert, T. Experimental proof for a signal peptidase I like activity in Mycoplasma pneumoniae, but absence of a gene encoding a conserved bacterial type I SPase. *FEBS J.* **272**, 2892-900 (2005).

Chen, Y.N., Sharma, S.K., Ramsey, T.M., Jiang, L., Martin, M.S., Baker, K., Adams, P.D., Bair, K.W., and Kaelin, W.G. Jr. Selective killing of transformed cells by cyclin/cyclin-dependent kinase 2 antagonists. *Proc. Natl. Acad. Sci. USA* **96**, 4325-4329 (1999).

Chi, N. C., Adam, E. J. H., Visser, G. D., and Adam, S. A. 1996. RanBP1 stabilises the interaction of Ran with p97 in nuclear protein import. *J. Cell Biol.* **135**, 559-569 (1996).

Collier, S., Chan, H. Y. E., Toda, T., McKimmie, C., Johnson, G., Adler, P. N., O'Kane, C., and Ashburner, M. The Drosophila embargoed gene is required for larval progression and encodes the functional homolog of Schizosaccharomyces Crm1. *Genetics* **155**, 1799-1807 (2000).

Cronshaw, J. M., Krutchinsky, A. N., Zhang, W., Chait, B. T., and Matunis M. J. Proteomic analysis of the mammalian nuclear pore complex. *J. Cell Biol.* **158**, 915-927 (2002).

De Bondt, H. L., Rosenblatt, J., Jancarik, J., Jones, H. D., Morgan, D. O., and Kim, S. H. Crystal structure of cyclin-dependent kinase 2. *Nature* **363**, 595-602 (1993).

Dienemann, A. and Sprenger, F. Requirements of Cyclin A for mitosis are independent of its subcellular localization. *Curr. Biol*. **14**, 1117-1123 (2004).

Edgar, B.A., and O'Farrell, P.H. Genetic control of cell division patterns in the Drosophila embryo. *Cell* **57**, 177–187 (1989).

Edgar, B. A., and O'Farrell, P. H., The three postblastoderm cell cycles of Drosophila embryogenesis are regulated in G2 by string. *Cell* **62**, 469-80 (1990).

Edgar, B. A., Lehman, D. A., and O'Farrell, P. H. Transcriptional regulation of string (cdc25): a link between developmental programming and the cell cycle. *Development*. **11**, 3131-43 (1994).

Edgar, B. A., and Orr-Weaver, T. L. Endoreplication cell cycles: more for less. *Cell* **105**, 297-306 (2001).

Emmerich, J., Meyer, C. A., de la Cruz, A. F., Edgar, B. A., and Lehner, C. F. Cyclin D does not provide essential Cdk4-independent functions in Drosophila. *Genetics* **168**, 867-75 (2004).

Fan, F., Liu, C.-P., Korobova, O., Heytig, C., Offenberg, H. H., Trump, G., and Arnheim, N. cDNA cloning and characterization of Npap60: a novel rat nuclear pore-associated protein with an unusual subcellular localization during male germ cell differentiation. *Genomics* **40**, 444–453 (1997).

Fasken, M. B., Saunders, R., Rosenberg, M., and Brighty, D. W. A leptomycin B-sensitive homologue of human CRM1 promotes nuclear export of nuclear export sequence-containing proteins in *Drosophila* cells. J. Biol. Chem. 275, 1878-1886 (2000).

Finley, R. L. Jr. and Brent, R. Gene Probes – A practical Approach. Hames B. D., Glover D. M., editors. Oxford, U.K.: Oxford Univ. Press (1995).

Foe, V. F. Mitotic domains reveal early commitment of cells in Drosophila embryos. *Development* **107**, 1-22 (1989).

Foe, V.F., Odel, G.M., and Edgar, B.A. Mitosis and morphogenesis in the Drosophila embryo: point and counterpoint. In: The Development of Drosophila melanogaster, M. Bate and A. Martinez-Arias,eds. (Cold Spring Harbor, NY:CSHL Press), pp. 149-300 (1993).

Fogarty, P., Campbell, S. D., Abu-Shumays, R., de Saint Phalle, B., Yu, K. R., Uy, G. L., Goldberg, M. L. and Sullivan, W. The Drosophila grapes gene is related checkpoint gene chk1/rad27 and is required for late syncytial division fidelity. *Curr. Biol*. **7**, 418-426 (1997).

Foley, E., O'Farrell, P., and Sprenger, F. Rux is a cyclin-dependent kinase in hibitor (CKI) specific for mitotic cyclin-Cdk complexes. *Curr. Biol*. **9**, 1392-1402 (1999).

Foley, E., and Sprenger, F. The cyclin-dependent kinase inhibitor Roughex is involved in mitotic exit in Drosophila. *Curr. Biol*. **11**, 151-160 (2001).

Fornerod, M., Ohno, M., Yoshida, M., and Mattaj, I. W. Crm1 is an export receptor for leucine rich nuclear export signals. *Cell* **90**, 1051-1060 (1997).

Galewsky, S., Xie, X. L., and Schulz, R. A. The Drosophila melanogaster z600 gene encodes a chromatin-associated protein synthesized in the syncytial blastoderm. *Gene* **96**, 227-232 (1990).

Görlich, D., Prehn, S., Laskey, R. A., and Hartmann, E. Isolation of a protein that is essential for the first step of nuclear protein import. *Cell* **79**, 767–778 (1994).

Görlich, D., Vogel, F., Mills, A. D., Hartmann, E., and Laskey, R. A. Distinct functions for the two importin subunits in nuclear protein import. *Nature* **377**, 246–248 (1995).

Görlich, D., Henklein, P., Laskey, R. A., and Hartmann, E. 1996a. A 41 amino acid motif in importin alpha confers binding to importin beta and hence transit into the nucleus. *EMBO J.* **15**, 1810-1817 (1996).

Görlich, D., Pante, N., Kutay, U., Aebi, U., and Bischoff, F. R. Identification of different roles for RanGDP and RanGTP in nuclear protein import. *EMBO J.* **15**, 5584–5594 (1996).

Görlich, D., and Kutay, U. Transport between the cell nucleus and the cytoplasm. *Annu. Rev. Cell Dev. Biol*. **15**, 607-660 (1999).

Großhans, J., Schnorrer, F., and Nüsslein-Volhard, C. Oligomerisation of Tube and Pelle leads to nuclear localisation of Dorsal. *Mech. Dev*. **81**, 127-138 (1999).

Großhans, J., and Wieschaus, E. A genetic link between morphogenesis and cell division during formation of the ventral furrow in Drosophila. *Cell* **101**, 523-531 (2000).

Großhans, J., Müller, A., and Wieschaus, E. Control of cleavage cycles in Drosophila embryos by frühstart. *Dev. Cell* **5**, 285-294 (2003)

Guan, T., Kehlenbach, R. H., Schirmer, E. C., Kehlenbach, A., Fan, F., Clurman, B. E., Arnheim, N., and Gerace, L. Nup50, a nucleoplasmically oriented nucleoporin with a role in nuclear protein export. *Moll. Cell. Biol.* **20**, 5619-5630 (2000).

Harper, J.W., Elledge, S.J., Keyomarsi, K., Dynlacht, B., Tsai, L.-H., Zhang, P., Dobrowolski, S., Bai, C., Connel-Crowley, L., Swindell, E., Fox, M.P., and Wei, N. Inhibition of cyclin-dependent kinases by p21. *Mol. Biol. Cell* **4**, 387-400 (1995).

Hayashi, S. A Cdc2 dependent checkpoint maintains diploidy in Drosophila. *Development* **122**, 1051-1058 (1996).

Hodge, A., and Mendenhall, M. The cyclin-dependent kinase inhibitory domain of the yeast Sic1 protein is contained within the C-terminal 70 amino acids. *Mol. Gen Genet*. **262**, 55-64 (1999).

Iwasaki, T., Matsuki, R., Shoji, K., Sanmiya, K., Miyao, M., and Yamamoto, N. A novel importin alpha from rice, a component involved in the process of nuclear protein transport. *FEBS Lett.* **428**, 259–262 (1998).

Jacobs, H. W., Knoblich, J. A., and Lehner, C. F. Drosophila Cyclin B3 is required for female fertility and is dispensable for mitosis like Cyclin B. *Genes Dev*. **12**, 3741-51 (1998).

Kaelin, W. G. Jr., Pallas, D. C., DeCaprio, J. A., Kaye, F. J., and Livingston, D. M. Identification of cellular proteins that can interact specifically with the T/E1A-binding region of the retinoblastoma gene product. *Cell*. **64**, 521-32 (1991).

Kaspar, M., Dienemann, A., Schulze, Ch., and Sprenger, F. Mitotic degradation of cyclin A is mediated by multiple and novel destruction signals. *Curr. Biol*. **11**, 685-690 (2001).

King, R. W., Jackson, P. K., and Kirschner, M. W. Mitosis in transition. *Cell* **79**, 563-571(1994).

Knighton, D. R., Zheng, J. H., Ten, Kyck L. F., Ashford, V. A., Xuong, N. H., Taylor, S. S. & Sowadski, J. M. Crystal structure of the catalytic subunit of cyclic adenosine monophosphate-dependent protein kinase. *Science* **253**, 407-414 (1991).

Knoblich, J.A., Sauer, K., Jones, L., Richardson, H., Saint, R., Lehner, C.F. Cyclin E controls S phase progression and its down-regulation during Drosophila embryogenesis is required for the arrest of cell proliferation. *Cell* **77**, 107-120 (1994).

Kolonin, M. G., and Finley, R. L. Jr. A role for cyclin J in the rapid nuclear division cycles of early Drosophila embryogenesis. *Dev Biol.* **227**, 661-72 (2000).

Kutay, U., Bischoff, F. R., Kostka, S., Kraft, R., and Görlich, D. Export of importin alpha from the nucleus is mediated by a specific nuclear transport factor. *Cell* **90**, 1061–1071 (1997).

Lacy, E.R., Filippov, I., Lewis, W.S., Otieno, S., Xiao, L., Weiss, S., Hengst, L., and Kriwacki, R.W. p27 binds cyclin-CDK complexes through a sequential mechanism involving binding-induced protein folding. *Nat. Struct. Mol. Biol.* **11**, 358-364 (2004).

Lane, M.E., Sauer, K., Wallace, K., Jan, Y.N., Lehner, C.F., and Vaessin, H. Dacapo, a cyclin-dependent kinase inhibitor, stops cell proliferation during Drosophila development. *Cell* **87**, 1225-1235 (1996).

Lawrence P. A. The making of a fly. Published by Blackwell Publishing. (1992).

Lee, L.A., and Orr-Weaver, T.L. Regulation of cell cycles in Drosophila development: intrinsic and extrinsic cues. *Annu. Rev. Genet*. **37**, 545-578 (2003).

Lehner, C. F., and O'Farrell, P. H. Expression and function of Drosophila cyclin A during embryonic cell cycle progression. *Cell* **56**, 957-68 (1989).

Leptin, M. Drosophila gastrulation: from pattern formation to morphogenesis. *Annu. Rev. Cell Dev. Biol*. **11**, 189–212 (1995).

Lindsay, M. E., Plafker, K., Smith, A. E., Clurman, B. E., and Macara, I. A. Npap60/Nup50 is a tri-stable switch that stimulates importin-α:β-mediated nuclear protein import. *Cell* **110**, 349-360 (2002).

Lindsey, D. L., and Zimm, G. G. The Genome of *Drosophila melanogaster*. Academic Press, Inc. (1992).

Loog, M., and Morgan, D.O. Cyclin specificity in the phosphorylation of cyclin-dependent kinase substrates. *Nature* **434**, 104-108 (2005).

Lowe, E.D., Tews, I., Cheng, K.Y., Brown, N.R., Gul, S., Noble, M.E., Gamblin, S.J., and Johnson, L.N. Specificity determinants of recruitment peptides bound to phospo-CDK2/cyclin A. *Biochemistry* **41**, 15625-15634 (2002).

Matsusaka, T., Imamoto, N., Yoneda, Y., and Yanagida, M. Mutations in fission yeast Cut15, an importin alpha homolog, lead to mitotic progression without chromosome condensation *Curr. Biol.* **8,** 1031-1034 (1998).

Meyer, C.A., Jacobs, H.W., Datar, S.A., Du, W., Edgar, B.A., and Lehner, C.F. Drosophila Cdk4 is required for normal growth and is dispensable for cell cycle progression. *EMBO J*. **19**, 4533-4542 (2000).

Millar, J. B., and Russell, P. The cdc25 M-phase inducer: an unconventional protein phosphatase. *Cell* **68**, 407-101992 (1992).

Moreno, S., and Nurse, P. Regulation of progression through the G1 phase of the cell cycle by the rum1+ gene. *Nature* **367**, 219-220 (1994).

Morgan, D. O. Cyclin-dependent kinases: engines, clocks, and microprocessors. *Annu. Rev. Cell Dev. Biol.* **13**, 261-291 (1997).

Müller, H.-A.J., Samanta, R., and Wieschaus, E. Wingless signaling in the Drosophila embryo: zygotic requirements and the role of the frizzled genes. *Development* **126**, 577–586 (1999).

Müller, D., Thieke, K., Bürgin, A., Dickmanns, A., and Eilers, M. Cyclin E-mediated elimination of p27 requires its interaction with the nuclear pore-associated protein mNPAP60. EMBO J. 19, 2168-2180 (2000).

Nicolas, F. J., Zhang, C., Hughes, M., Goldberg, M. W., Watton, S. J., and Clarke, P. R. Xenopus Ran-binding protein 1: molecular interactions and effects on nuclear assembly in Xenopus egg extracts. *J. Cell Sci.* **110**, 3019-3030 (1997).

Nurse, P. Ordering S phase and M phase in the cell cycle. *Cell* **79**, 547-550 (1994).

Nüsslein-Volhard, Ch. The identification of genes controlling development in flies and fishes. Nobel lecture, 08.12. 1995 Stockholm.

Pavletich, N.P. Mechanisms of cyclin-dependent kinase regulation: structures of Cdks, their cyclin activators, and Cip and INK4 inhibitors. *J. Mol. Biol.* **287**, 821-828 (1999).

Pines, J., and Hunter, T. The differential localization of human cyclins A and B is due to a cytoplasmic retention signal in cyclin B. *EMBO J.* **13**, 3772–3781 (1994).

Polyak, K., Lee, M. H., Erdjument-Bromage, H., Koff, A., Roberts, J. M., Tempst, P., and Massague, J. Cloning of p27Kip1, a cyclin-dependent kinase inhibitor and a potential mediator of extracellular antimitogenic signals. *Cell* **78**, 59-66 (1994).

Rexach, M., and Blobel, G. Protein import into nuclei: association and dissociation reactions involving transport substrate, transport factors, and nucleoporins. *Cell* **83**, 683-692 (1995).

Ribbeck, K., and Görlich, D. The permeability barrier of nuclear pore complexes appears to operate via hydrophobic exclusion. *EMBO J*. **21**, 2664-2671 (2002).

Roberts, D.B. Drosophila, A Practical Approach. Oxford: Oxford University Press (1998).

Roth, P., Xylourgidis, N., Sabri, N., Uv, A., Fornerod, M., and Samakovlis, Ch. The Drosophila nucleoporin DNup88 localizes DNup214 and Crm1 on the nuclear envelope and attenuates NES-mediated nuclear export. *Jour. Cell Biol.* **163**, 701-706 (2003).

Russell, P., and Nurse, P. cdc25+ functions as an inducer in the mitotic control of fission yeast. *Cell* **45**, 145-53 (1986).

Russell, P., and Nurse, P. Negative regulation of mitosis by wee1+, a gene encoding a protein kinase homolog. *Cell* **49**, 559-67 (1987).

Russo, A. A., Jeffrey, P. D., Patten, A. K., Massague, J. and Pavletich, N. P. Crystal structure of the p27Kip1 cyclin-dependent-kinase inhibitor bound to the cyclin A-Cdk2 complex. *Nature* **382**, 325-331 (1996).

Russo, A. A., Tong, L., Lee, J. O., Jeffrey, P. D., and Pavletich, N. P. Structural basis for inhibition of the cyclin-dependent kinase Cdk6 by the tumor suppressor p16INK4a. *Nature* **395**, 237-243 (1998).

Sambrook, J., Fritsch, E., and Maniatis, T. Molecular cloning: a laboratory manual. Cold Spring Harbor Laboratory Press (1989).

Sanchez-Diaz, A., Gonzalez, I., Arellano, M., and Moreno, S. The Cdk inhibitors p25rum1 and p40SIC1 are functional homologues that play similar roles in the regulation of the cell cycle in fission and budding yeast. *J. Cell Sci*. **111**, 843-851 (1998).

Sauer, K., Knoblich, J.A., Richardson, H., and Lehner, C.F. Distinct modes of cyclin E/cdc2c kinase regulation and S-phase control in mitotic and endoreduplication cycles of Drosophila embryogenesis. *Genes Dev*. **9**, 1327-1339 (1995).

Schnorrer, F., Bohmann, K., and Nusslein-Volhard, Ch. The molecular motor dynein is involved in targeting Swallow and bicoid RNA to the anterior pole of Drosophila oocytes. *Nat. Cell. Biol.* **2**, 185-90 (2000).

Schulman, B. A., Lindstrom, D. L., and Harlow, E. Substrate recruitment to cyclin-dependent kinase 2 by a multipurpose docking site on cyclin A. *Proc. Natl. Acad. Sci. USA* **95**, 10453-10458 (1998).

Seher, T., and Leptin, M. Tribbles, a cell-cycle brake that coordinates proliferation and morphogenesis during Drosophila gastrulation. *Curr. Biol.* **10**, 623-629 (2000).

Schulz, R. A. and Miksch, J. L. Dorsal expression of the Drosophila z600 gene during early embryogenesis. *Dev. Biol*. **136**, 211-221(1989).

Schulz, R. A., Shlomchik, W., Cherbas, L., and Cherbas, P. Diverse expression of overlapping genes: the Drosophila Eip28/29 gene and its upstream neighbors. *Dev. Biol*. **131**, 515-523 (1989).

Sherr, C. J. G1 phase progression: cycling on cue. *Cell* **79**, 551-555 (1994).

Sherr, C. J., Kato, J., Quelle, D. E., Matsuoka, M., and Roussel, M. F. D-type cyclins and their cyclin-dependent kinases: G1 phase integrators of the mitogenic response. *Cold Spring Harbor Symp. Quant. Biol.* **59**, 11-9 (1994).

Sibon, O. C. M., Stevenson, V. A., and Theurkauf, W.E. DNAreplication checkpoint control at the Drosophila midblastula transition. *Nature* **388**, 93–96 (1997).

Sibon, O. C. M., Laurenc¸on, A., Hawley, R. S., and Theurkauf, W. E. The Drosophila ATM homologue Mei-41 has an essential checkpoint function at the midblastula transition. *Curr. Biol*. **9**, 302–312 (1999).

Smitherman, M., Lee, K., Swanger, J., Kapur, R., and Clurman, B. E. Characterization and targeted disruption of murine Nup50, a p27(Kip1)-interacting component of the nuclear pore complex. *Mol Cell Biol*. **20**, 5631-42 (2000).

Stade, K., Ford, C. S., Guthrie, C., and Weis, K. Exportin 1 (Crm1p) is an essential nuclear export factor. *Cell* **90**, 1041-1050 (1997).

Stumpff, J., Duncan, T., Homola, E., Campbell, S. D., Su, T.T. Drosophila Wee1 kinase regulates Cdk1 and mitotic entry during embryogenesis. *Curr. Biol*. **14**, 2143-8 (2004).

Stuurman, N. Identification of a conserved phosphorylation site modulating nuclear lamin polymerization. *FEBS Lett*. **401**, 171-174 (1997).

Stüven, T., Hartmann, E., and Görlich D. Exportin 6: a novel nuclear export receptor that is specific for profilin-actin complexes. *EMBO J*. **22**, 5928-5940 (2003).

Thomas, B. J., Zavitz, K. H., Dong, X., Lane, M. E., Weigmann, K., Finley, R. L. Jr., Brent, R., Lehner, C.F., and Zipursky, S. L. roughex down-regulates G2 cyclins in G1. *Genes dev*. **11**, 1289-1298 (1997).

Toyoshima, H., and Hunter, T. p27 a novel inhibitor of G1 cyclin-cdk protein kinase activity, is related to p21. *Cell* **78**, 67-74 (1994).

Toyoshima, F., Moriguchi, T., Wada, A., Fukuda, M., and Nishida, E. Nuclear export of cyclin B1 and its possible role in the DNA damage-induced G2 checkpoint. *EMBO J.* **17**, 2728-2735 (1998).

Verma, R., Annan, R. S., Huddleston, M. J., Carr, S. A., Reynard, G. and Deshaies, R. J. Phosphorylation of Sic1 by G1 Cdk required for its degradation and entry into S phase. *Science* **278**, 455-460 (1997).

Vidwans, S. J., Di Gregorio, P. J., Shermoen, A. W., Foat, B., Iwasa, J., Yakubovich, N., and O'Farrell, P.H. (2002). Sister chromatids fail to separate during an induced endoreplication cycle in Drosophila embryos. *Curr. Biol*. **12**, 829-833.

Vlach, J., Hennecke, S., and Amati, B. Phosphorylation-dependent degradation of the cyclin-dependent kinase inhibitor p27. *EMBO J*. **16**, 5334-5344 (1997).

Weigmann, K., Cohen, S.M., and Lehner, C.F. Cell cycle progression, growth and patterning in imaginal discs despite inhibition of cell division after inactivation of Drosophila Cdc2 kinase. *Development* **124**, 3555-3563 (1997).

Weis, K., Ryder, U., and Lamond, A. I. The conserved amino-terminal domain of hSRP1 alpha is essential for nuclear protein import. *EMBO J.* **15**, 1818-1825 (1996).

Yamashita, M., Yoshikuni, M., Hirai, T., Fukada, S., and Nagahama, Y. A monoclonal antibody against PSTAIR sequence of $p34^{cdc2}$, catalytic subunit of maturation promoting factor and key regulator of the cell cycle. *Dev. Growth Differ*. **33**, 617-624 (1991).

Yang, J., Bardes, E. S. G., Moore, J. D., Brennan, J., Powers, M. A., and Kornbluth, S. Control of Cyclin B1 localization through regulated binding of the nuclear export factor CRM1. *Genes Dev*. **12**, 2131-2143 (1998).

Yu, K. R., Saint, R. B., and Sullivan, W. The grapes checkpoint coordinates nuclear envelope breakdown and chromosome condensation. *Nat. Cell Biol*. **2**, 609–615 (2000).

Zhu, L., Harlow, E., and Dynlacht, B. D. p107 uses a $p21^{CIP1}$-related domain to bind cyclin/cdk2 and regulate interactions with E2F. Genes Dev. 9, 1740-1752 (1995).

List of figures

Introduction

Methods

Results

Discussion

Appendix

List of tables

Materials

Results

Appendix

Appendix 1

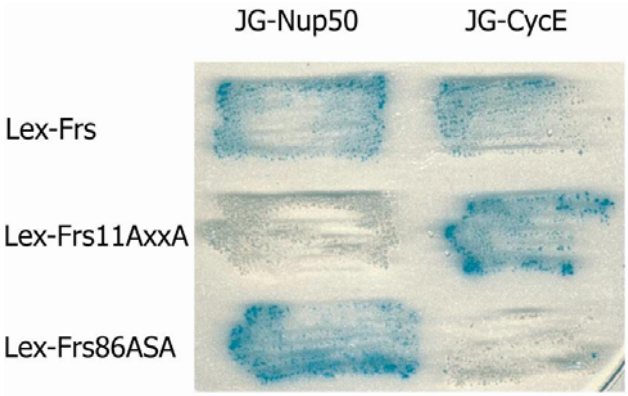

Appendix 1. Interaction test of Lex-Frs, Lex-Frs11AxxA and Lex-Frs86ASA alleles with JG-Nup50 and JG-CycE proteins in Yeast-Two-Hybrid assay. Alanine substitutions in the KxL motif (Frs86ASA) and in the putative NES motif (Frs11AxxA) strongly compromise the interaction of Frs with CycE (CycEΔN319) and Nup50 (full-length) respectively. Blue staining of the lacZ reporter gene indicates interaction (Großhans J.).

Appendix 2

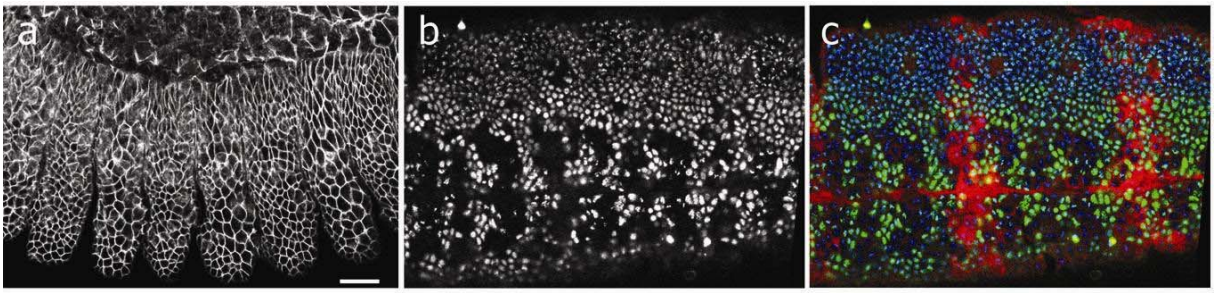

Appendix 2. *Drosophila* paired-Gal4/UAS-frs[H] embryos. *frs* inhibits M but not S phase. **a**) Cell number in the epidermis in segments with *frs* expression was half the number compared to neighboring segments (38±3 versus 20±3 cells per 34 µm2, *n*=10). Cell borders were labelled by staining with Dlg antibody. **b**, **c**) Progression through S phase was marked by BrdU incorporation (25 min pulse), BrdU - white/green; Frs - red; DNA - blue. Scale bar 20 µm (Großhans J.).

Appendix 3

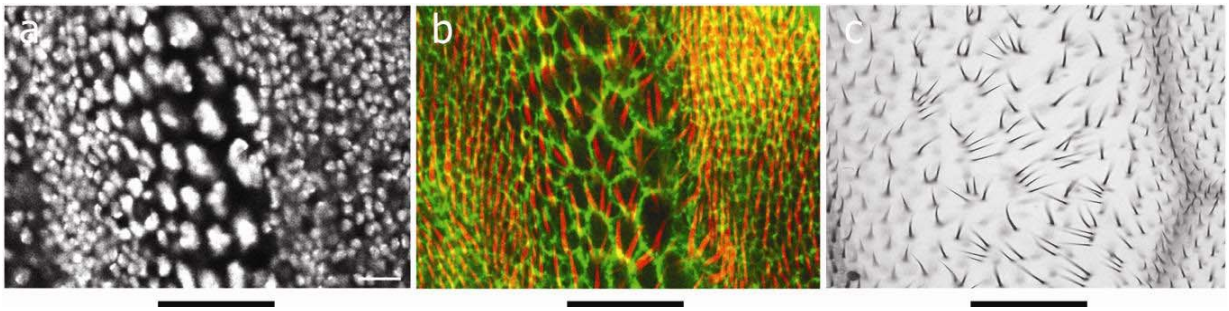

Appendix 3. *frs* expressed in a stripe (indicated by the black bar) in pupal wing imaginal discs of w;patched-Gal4, UAS-frs[J] flies. **a**, **b**) Pupal discs fixed and stained with Phalloidin (green - cell borders, red - higher optical section showing the trichomes) and DAPI (white). **c**) Section of a differentiated wing. Scale bar 20 µm (Großhans J.).

Appendix 4

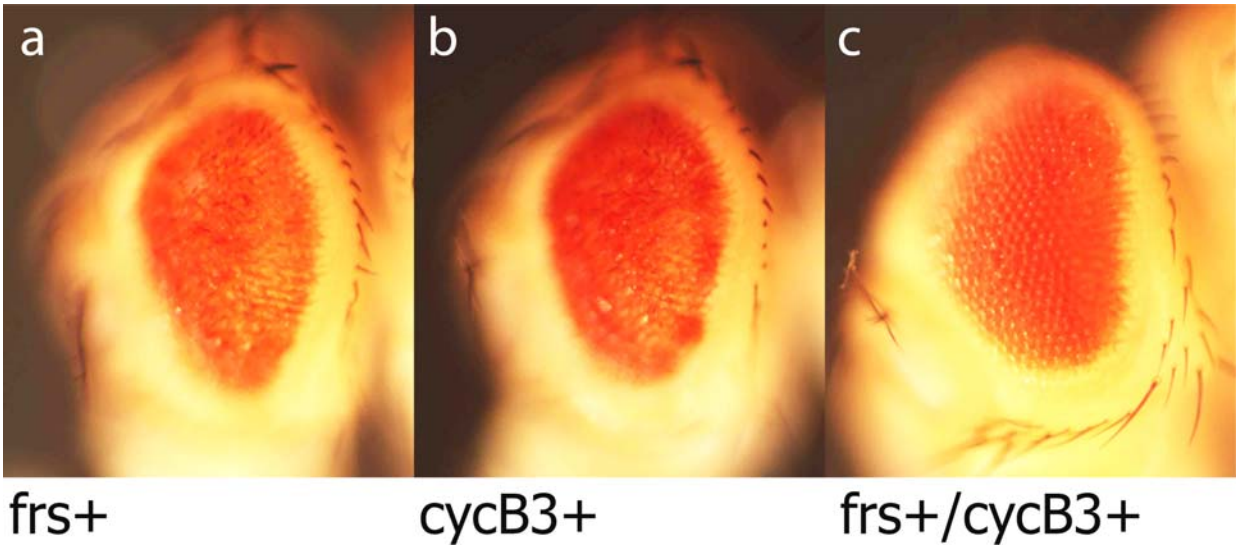

Appendix 4. The pictures present ectopically expressed *frühstart* in the *Drosophila* eyes without and with co-expressed *cyclinB3*. Over-expression of CycB3 together with *frühstart* in the *Drosophila* eyes rescued the rough eye phenotype, what means that *frühstart* genetically interacts with CycB3 in the *Drosophila* eyes. Genotypes: **a**) w;Sp/CyO;GMR-Gal4, UAS-frs[I]/TM3,hb-lacZ. **b**) yw;+/CyO;GMR-Gal4;+/+. **c**) w;UAS-cycB3/CyO;GMR-Gal4, UAS-frs[I]/TM3,hb-lacZ (Bartoszewski S.).